

# UC San Diego

## UC San Diego Electronic Theses and Dissertations

### Title

The role of caveolin-3 in cardiac protection and hypertrophy

### Permalink

<https://escholarship.org/uc/item/8z38s11m>

### Author

Horikawa, Yousuke Takashi

### Publication Date

2009

Peer reviewed|Thesis/dissertation

UNIVERSITY OF CALIFORNIA, SAN DIEGO

The Role of Caveolin-3 in Cardiac Protection and Hypertrophy

A dissertation submitted in partial satisfaction of the requirements for the degree

Doctor of Philosophy

in

Biomedical Sciences

by

Yousuke Takashi Horikawa

Committee in charge:

Professor David M. Roth, Chair  
Professor Paul A. Insel, Co-Chair  
Professor Ju Chen  
Professor Robert S. Ross  
Professor Francisco J. Villarreal

2009

Copyright

Yousuke Takashi Horikawa, 2009

All rights reserved.

The Dissertation of Yousuke Takashi Horikawa is approved, and is acceptable in quality and form for publication on microfilm and electronically:

---

---

---

---

Co-Chair

---

Chair

University of California, San Diego

2009

## DEDICATION

I dedicate my thesis to my grandfather, Takashi Horikawa who has continued to inspire, guide, and support me throughout all of my endeavors. I miss you greatly and hope that you are proud of me.

## TABLE OF CONTENTS

Signature Page.....	iii
Dedication.....	iv
Table of Contents.....	v
List of Abbreviations.....	viii
List of Figures.....	x
List of Tables.....	xiii
Acknowledgements.....	xiv
Vita.....	xvi
Abstract of the dissertation.....	xix
Chapter 1: Introduction .....	1
1.1 Scope of the Problem: Prevalence of cardiac heart failure .....	2
1.2 Understanding heart failure .....	3
1.3 Molecular signaling involved in heart failure .....	3
1.4 Caveolae and caveolins in heart failure .....	6
1.5 Role for caveolins in preconditioning against ischemia/reperfusion (I/R) injury.....	7
1.6 Caveolins in cardiac hypertrophy .....	9
1.7 How does Cav-3 protect the heart from failure? .....	11
1.8 Dissertation objectives and hypothesis .....	13
1.9 References.....	16
Chapter 2: Methods and Protocols.....	21
2.1 <i>in vivo</i> methods.....	22

2.2	<i>in vitro</i> methods.....	25
2.3	Molecular, Biochemical, Histological, and Electron Microscopy methods.....	27
2.4	References.....	33
Chapter 3:	Caveolin-3 expression and caveolae are required for isoflurane-induced cardiac protection from hypoxia and ischemia/reperfusion injury.....	34
3.1	Abstract.....	35
3.2	Introduction.....	35
3.3	Results.....	37
3.4	Discussion.....	39
3.5	Acknowledgements.....	42
3.6	References.....	49
Chapter 4:	Cardiac-specific overexpression of caveolin-3 induces endogenous cardiac protection by mimicking ischemic preconditioning.....	53
4.1	Abstract.....	54
4.2	Introduction.....	54
4.3	Results.....	56
4.4	Discussion.....	60
4.5	Acknowledgements.....	65
4.6	References.....	78
Chapter 5:	Cardiac-specific overexpression of caveolin-3 increases ANP production and attenuates cardiac hypertrophy.....	83
5.1	Abstract.....	84
5.2	Introduction.....	85

5.3	Results.....	86
5.4	Discussion.....	91
5.5	Acknowledgements.....	94
5.6	References.....	107
Chapter 6:	Discussion and Conclusions.....	111
6.1	Major Findings of the dissertation.....	112
6.2	Discussion of major dissertation issues.....	114
6.3	Future directions.....	116
6.4	Conclusions.....	117
6.5	References.....	119

## LIST OF ABBREVIATIONS

- Adult cardiac myocyte, (ACM or CM)
- Anesthetic preconditioning, (APC)
- Area at risk, (AAR)
- Atrial natriuretic peptide, (ANP)
- Body weight, (BW)
- B-type natriuretic peptide (BNP)
- Calcium ( $\text{Ca}^{2+}$ )/calmodulin-dependent kinase II, (CAMKII)
- Cardiac-specific caveolin-3 overexpressing mouse, (Cav-3 OE)
- Caveolin, (Cav)
- Caveolin-3 knockout mice (Cav-3 KO or Cav-3<sup>-/-</sup>)
- Colchicine (Colch)
- Cyclic-adenosine monophosphate-dependent protein kinase, (PKA)
- Electron microscopy, (EM)
- Extracellular regulated kinase, (Erk)
- GATA binding protein 4, (GATA4)
- G-protein coupled receptors, (GPCR)
- Infarct size, (IS)
- Ischemia/Reperfusion, (I/R)
- Ischemic preconditioning, (IPC)
- Isoflurane, (Iso)
- Left ventricle, (LV)

Methyl- $\beta$ -cyclodextrin, (M $\beta$ CD)

Mitogen activated protein kinase, (MAPK)

Myocardial infarction, (MI)

Myocyte enhancer factor 2, (MEF2)

Natriuretic peptide, (NP)

Natriuretic peptide receptor-A, and -B (NPR-A, NPR-B)

Nuclear factor of activated T cells, (NFAT)

Phenylephrine, (PE)

Phospho-inositol-3-kinase, (PI3K)

Polymerase chain reaction, (PCR)

Preconditioning, (PC)

Protein kinase B, (Akt)

Protein kinase C, (PKC)

Protein kinase D, (PKD)

Reaction oxygen species, (ROS)

Real time PCR, (RT-PCR)

Receptor tyrosine kinase, (RTK)

Renin-angiotensin-aldosterone system, (RAAS)

Src kinase, (Src)

Tibia length, (TL)

Transverse aortic constriction, (TAC)

Wheat germ agglutinin, (WGA)

$\beta$ -adrenergic receptor, ( $\beta$ -AR)

## LIST OF FIGURES

Figure 1-1: Pathophysiological mechanisms involved in heart failure .....	2
Figure 1-2: Schematic depicting various signaling molecules interacting with caveolae and caveolin scaffolding domain (CSD).....	5
Figure 1-3: Electron microscopy of a caveolae located on the plasma membrane in rat adult cardiac myocyte (ACM). Scale bar 0.05 $\mu\text{m}$ .....	6
Figure 1-4: Schematic of the biphasic protection involved in preconditioning...	8
Figure 1-5: Proposed mechanism of Cav-1 in cardiac protection.....	9
Figure 1-6: Molecular structure of atrial natriuretic peptide (ANP). ANP has a 17 amino acid core structure with a cysteine bond.....	11
Figure 1-7: Schematic of the effect ANP has on endothelial cells and cardiac myocytes. ANP signals via the natriuretic peptide receptor-A (NPR-A), aka the guanyl cyclase A receptor, to have numerous cardioprotective effects.....	12
Figure 1-8: Flow diagram of our proposed hypothesis.....	15
Figure 3-1: Stimulated ischemia/reperfusion (I/R) model.....	43
Figure 3-2: Effect of isoflurane on simulated ischemia/reperfusion (SI/R) of adult cardiac myocytes (CM).....	44
Figure 3-3: Impact of M $\beta$ CD and colchicine on expression by cardiac myocytes (CM) of caveolae, caveolin-3 and phosphocaveolin-1 and on response to isoflurane.....	45
Figure 3-4: Cardiac protection by isoflurane in the presence and absence of caveolae disruption.....	46
Figure 3-5: Absence of isoflurane-induced cardiac protection in caveolin-3 knockout mice.....	47
Figure 4-1: IPC increases the expression of caveolae and the enrichment of protein and cholesterol in buoyant fractions.....	66
Figure 4-2: Cav-3 adenovirus increases caveolae expression in adult cardiac myocytes (ACM).....	67

Figure 4-3: Cardiac myocyte-specific Cav-3 OE mice: caveolin, caveolae and NOS expression.....	68
Figure 4-4: NOS expression and activity.....	69
Figure 4-5: Cardiac protection in Cav-3 OE mice.....	70
Figure 4-6: Role of survival kinases in protection of Cav-3 OE mice.....	71
Figure 4-7: Electron micrograph of area at risk from the hearts of TG <sub>neg</sub> and Cav-3 OE mice following ischemia-reperfusion.....	72
Figure 4-8: Cardiac function and cell death in mice 24 h after ischemic injury....	73
Supplementary Figure 4-1: Generation of a cardiac myocyte specific caveolin-3 (Cav-3) transgenic mouse.....	74
Supplementary Figure 4-2: Area at risk (AAR) as a percent of the left ventricle (LV) was no different among the groups.....	75
Figure 5-1: Caveolin-3 (Cav-3) and caveolae alter atrial natriuretic peptide (ANP) expression and protein kinase B phosphorylation (pAkt)...	96
Figure 5-2: Akt phosphorylation and ANP expression are prevented by Wortmannin.....	97
Figure 5-3: Cardiac myocyte-specific caveolin-3 overexpressing (Cav-3 OE) mice have increased caveolae and ANP.....	98
Figure 5-4: ANP co-localizes with Cav-3 and inhibits nuclear factor of T-cells (NFATc3).....	99
Figure 5-5: Cav-3 overexpression inhibits pressure-induced cardiac hypertrophy and fibrosis.....	100
Figure 5-6: Real-time polymerase chain reaction following 48 hours of TAC.....	101
Figure 5-7: Caveolin-3 overexpression maintains cardiac function.....	102
Supplementary Figure 5-1: Cav-3 overexpression inhibits phenylephrine (PE) induced Erk phosphorylation.....	103
Supplementary Figure 5-2: Cav-3 and pErk levels increase with TAC.....	104

Figure 6-1: HEK-293 cells expressing Lac-Z or Cav-3. Cav-3 overexpression induced dramatic cellular death over 48 hours..... 115

Figure 6-2: Erk phosphorylation increases in Cav-3 OE when induced with epidermal growth factor, whereas PE induction results in a decrease in Erk phosphorylation..... 117

## LIST OF TABLES

Table 4-1: Hemodynamics.....	76
Table 4-2: Morphology, echocardiography, and hemodynamics.....	77
Table 5-1: Echocardiography measurements.....	105
Table 5-2: Hemodynamic data.....	106

## ACKNOWLEDGEMENTS

I would like to acknowledge and thank the numerous people who have made this work possible. I would like to thank my mentor Dr. David M. Roth for all of his guidance in all aspects of my research and clinical endeavors. I am grateful for his continued support and commitment to bettering me into a physician scientist. I would also like to thank my co-mentor Dr. Paul A. Insel who first introduced me to the Medical Scientist Training program and has continued to help mold, guide, and support me throughout the program. Additionally, I would like to thank the rest of my committee members: Dr. Ju Chen, Dr. Robert S. Ross, and Dr. Francisco J. Villarreal for their continued advice and support. I especially would like to acknowledge and thank Dr. Hemal H. Patel who has tirelessly helped teach, guide, support, and inspire me into becoming a better scientist.

I would also like to thank the entire Roth/Patel lab for all their technical and moral support including but not limited to Dr. Brian Head, Dr. Yasuo Tsutsumi, and Ingrid Niesman. I have greatly enjoyed my years in the lab and will forever remember them.

I would like to acknowledge and thank my family who have always encouraged and supported my endeavors, especially my grandfather. Finally, I would like to thank Tina Udaka for all of her love and support throughout my years of graduate school.

Chapter 3, in full, is a reprint of the material as it appears in *Journal of Molecular and Cellular Cardiology* 2008. Horikawa, Y; Patel, H; Tsutsumi, Y; Jennings, M; Kidd, M; Hagiwara, Y; Ishikawa, Y; Insel, P; and Roth, D, Elsevier

Journals, 2008. The dissertation author was the primary investigator and author for this manuscript.

Chapter 4, in full, is a reprint of the material as it appears in *Circulation* 2008. Tsutsumi, Y; Horikawa, Y; Jennings, M; Kidd, M; Niesman, I; Yokoyama, U; Head, B; Hagiwara, Y; Ishikawa, Y; Miyanohara, A; Patel, P; Insel, P; Patel, H; and Roth, D, American Heart Association, inc 2008. The dissertation author was the primary co-investigator and co-author of this material and played a pivotal role in all aspects of the manuscript, including the formulation and testing of the experiments and in the writing and editing of the manuscript.

Chapter 5, in full is currently being prepared for submission for publication of the material. The dissertation author was the primary investigator and author for this material.

## VITA

1999-2000	Research Assistant University of California, Irvine
2003	Bachelor of Science in Neurobiology University of California, Irvine
2007	Teaching Assistant, Department of Pathology University of California, San Diego
2009	Doctor of Philosophy University of California, San Diego
2011 (anticipated)	Doctor of Medicine University of California, San Diego

## RESEARCH FELLOWSHIPS AND AWARDS

2009	Japanese American Medical Association Scholarship Award
2009	Graduate Student Abstract Award ASPET, Experimental Biology 2009
2008	Cardiovascular Scholarship Award University of California, San Diego
2008-2009	Hypertension Training Grant Fellow University of California, San Diego
2006-2008	Pre-doctoral Fellowship American Heart Association

## PUBLICATIONS

**Horikawa YT**, Tsutsumi YM, Insel PA, Patel HH, and Roth DM. Cardiac specific overexpression of caveolin-3 attenuates cardiac hypertrophy. In preparation.

Tsutsumi YM, **Horikawa YT**, Kawaraguchi Y, Niesman IR, Kidd MW, Chin-Lee B, Head BP, Patel PM, Roth DM, and Patel HH. Role of caveolin-3 and GLUT-4 in isoflurane-induced delayed cardiac protection. Submitted to *Anesthesiology*.

Tsutsumi YM, **Horikawa YT**, Jennings MW, Kidd MW, Niesman IR, Yokoyama U, Head BP, Hagiwara Y, Ishikawa Y, Miyanohara A, Patel PM, Insel PA, Patel HH, and Roth DM. Cardiac-specific Overexpression of Caveolin-3 induces endogenous cardiac protection by mimicking ischemic preconditioning. *Circulation*. 2008; 118:1979-1988.

**Horikawa YT**, Patel HH, Tsutsumi YM, Jennings MM, Kidd MW, Hagiwara Y, Ishikawa Y, Insel PA, Roth DM. Caveolin-3 expression and caveolae are required for volatile anesthetic-induced cardiac protection from hypoxia and ischemia/reperfusion injury. *J Mol Cell Cardiol*. 2008. Jan;44(1):123-30.

Go K, **Horikawa Y**, Garcia R, Villarreal FJ. Fluorescent method for detection of cleaved collagens using O-phthaldialdehyde (OPA). *J Biochem Biophys Methods*. 2008. 70:878-82.

Tsutsumi YM, Yokoyama T, **Horikawa Y**, Roth DM, Patel HH. Reactive oxygen species trigger ischemic and pharmacological postconditioning: *in vivo* and *in vitro* characterization. *Life Sci*. 2007 Sep 22;81(15):1223-7

Patel HH, Tsutsumi YM, Head BP, Niesman IR, Jennings M, **Horikawa Y**, Huang D, Moreno AL, Patel PM, Insel PA, Roth DM. Mechanisms of cardiac protection from ischemia/reperfusion injury: a role for caveolae and caveolin-1. *FASEB J*. 2007 May;21(7):1565-74

Jimenez JC, Tyson DR, Dhar S, Nguyen T, **Hamai Y**, Bradshaw RA, and Evans GRD. Human Embryonic Kidney Cells (HEK-293): Characterization and Dose Response for Modulated Release of NGF for Nerve Regeneration. *Plast Reconstr Surg*. 2004 Feb;113(2):605-10.

Tyson DR, Larkin S, **Hamai Y**, Bradshaw RA. PC12 cell activation by epidermal growth factor receptor: role of autophosphorylation sites. *Int J Dev Neurosci*. 2003 21: 63-74.

## Published Abstracts

**Horikawa Y.T.**, Tsutsumi Y.M., Patel H.H., Roth D.M. Cardiac myocyte-specific overexpression modulates ANP production and attenuates cardiac hypertrophy *in vivo*. *FASEB J*, 23, #576.1, 2009.

Kawaraguchi Y., **Horikawa Y.T.**, Tsutsumi Y.M., Yokoyama T., Panneerselvam M., Villarreal F.J., Patel, P.M., Roth D.M., and Patel H.H. Epicatechin-induced cardiac protection is opioid receptor dependent. *FASEB J*, 23, #763.8, 2009.

Tsutsumi Y.M., **Horikawa Y.T.**, Roth D.M., and Patel H.H. Opioid-induced preconditioning is dependent on caveolin-3 expression. *FASEB J*, 23, #938.8, 2009.  
**Horikawa YT**, Tsutsumi YM, Patel HH, Insel PA, and Roth DM. Cardiac myocyte-specific Caveolin-3 overexpression modulates ERK/EGFR signaling and attenuates cardiac hypertrophy. *Circulation* 118:18, #3433, 2008.

**Horikawa YT**, Patel HH, Tsutsumi YM, Insel PA, and Roth DM. Essential role for caveolar microdomains and microtubules in cardiac protection. *Circulation* 116:II-100, #557, 2007.

**Horikawa YT**, Patel HH, Tsutsumi YM, Patel PM, and Roth DM. 2007. Intact caveolae are essential to isoflurane-induced cardiac protection. *Anesthesiology* 107:A1662, 2007.

**Horikawa YT**, Patel HH, Tsutsumi YM, Jennings M, Hagiwara Y, Ishikawa Y, Insel PA, and Roth DM. Caveolae formation and caveolin-3 expression is essential for cardiac protection. *American Heart Association Young Investigators Forum*: P38, 2007.

**Horikawa Y.T.**, Patel H.H., Tsutsumi Y.M., Yokoyama U., Insel P.A., Roth D.M. Cardiac-specific overexpression of caveolin-3 enhances Akt phosphorylation. *FASEB J*, 21(6), #723.8, 2007.

ABSTRACT OF THE DISSERTATION

The Role of Caveolin-3 in Cardiac Protection and Hypertrophy

By

Yousuke Takashi Horikawa

Doctor of Philosophy in Biomedical Sciences

University of California, San Diego, 2009

Professor David M. Roth, Chair  
Professor Paul A. Insel, Co-Chair

Heart failure occurs when the heart is unable to maintain sufficient blood flow to the body. In response the body retains salt and water, secretes neuro-hormones, and activates a variety of signaling cascades within the heart to increase cardiac function. However, these temporary changes ultimately add to the growing problem facing the myocardium. Unfortunately, the signaling involved in heart failure is highly complex, involving a vast variety of receptors, mediators, and end effectors. Rather than focusing on a unique isolated pathway, it may be preferable to understand the

temporal and spatial organization and localization of these proteins and how this affects signaling involved in heart failure.

Caveolae are small flask like invaginations of the plasma membrane. Their constituents include cholesterol, glycosphingolipids, caveolins (Cav), and numerous other proteins including signaling molecules involved in the prevention and progression of heart failure. Cav, the structural proteins that are responsible for caveolae formation have also been implicated in numerous signaling cascades involved in heart failure. I hypothesized that Cav-3 is essential for temporal and spatial organization of specific protective molecules and protects against heart failure and that modulation of Cav-3 can induce cardiac protection and inhibit hypertrophy possibly by the increased expression of atrial natriuretic peptide (ANP: a cardioprotective, anti-fibrotic, and anti-hypertrophic protein).

This dissertation utilized various *in vivo* (Cav-3 overexpressing and knockout mice) and *in vitro* (adult cardiac myocytes) techniques along with molecular (Cav-3 adenovirus), biochemical, and histological analysis to understand the importance of Cav-3 in cardiac protection and cardiac hypertrophy.

The results reveal that Cav-3 was not only essential to induce cardiac protection, but also that myocyte-specific overexpression of Cav-3 (Cav-3 OE) protects the heart from lethal ischemia/reperfusion (I/R) injury and pressure-induced cardiac hypertrophy. Interestingly, as Cav-3 expression increased, ANP expression also increased. These results suggest that modulating Cav-3 expression alters caveolae formation and increases ANP expression, as a mechanism that protects the myocardium from lethal I/R injury and cardiac hypertrophy.

# **Chapter 1:**

## **Introduction**

### 1.1 Scope of the problem: Prevalence of heart failure.

Cardiovascular diseases are the leading cause of mortality and morbidity in the Western world. There is approximately one death every 37 seconds attributed to cardiovascular disease(1). Of the numerous cardiovascular diseases, heart failure is mentioned on one out of eight death certificates and approximately 5 million Americans have been diagnosed with heart failure. Out of these 5 million people approximately half will die from this disease within five years(1).

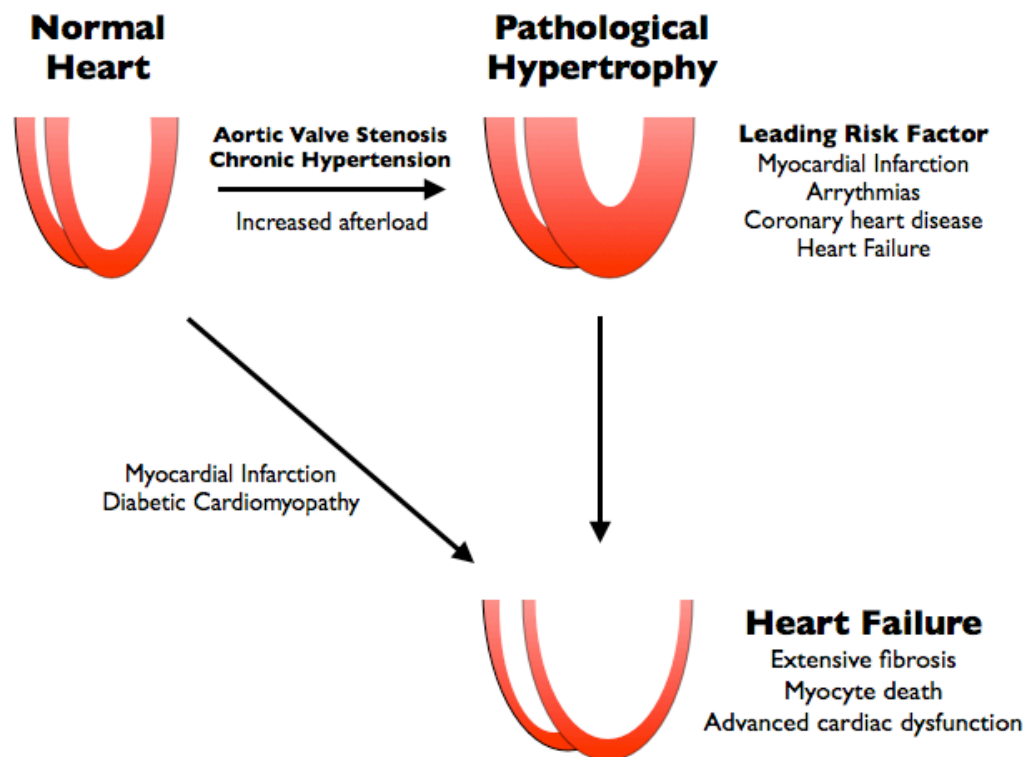


**Figure 1- 1:** Pathophysiological mechanisms involved in heart failure.

In heart failure, the heart dilates and displays extensive fibrosis, myocyte death, and advanced cardiac dysfunction. The leading causes of heart failure are a consequence of prolonged cardiac hypertrophy (via, for example, chronic hypertension

or aortic valve stenosis), myocardial infarction, or diabetic cardiomyopathy (Figure 1-1)(2). As a result, understanding the mechanisms for heart failure that accompany myocardial infarction and cardiac hypertrophy is vital to understanding the progression of the underlying disease.

### **1.2 Understanding heart failure.**

Heart failure occurs when the heart is unable to supply adequate blood flow and pressure to the body's changing demands. Heart failure can occur, for example, when the heart is physically damaged via ischemic disease or from cardiac hypertrophy. In order to compensate for the weakening heart, various physiological changes occur: these include salt and water retention from the kidneys, stimulation of neurohormones, and activation of intracellular signaling cascades in the heart (3). Although initially compensatory, these adaptations can ultimately further damage the heart. As a result, many current therapies focus on these neurohumoral changes by decreasing cardiac workload (e.g.  $\beta$ -blockers, diuretics, angiotensin converting enzyme inhibitors, angiotensin receptor blocker, and left ventricular assist devices) or increasing cardiac contractility (e.g. digoxin). However, these treatments are limited in their effectiveness and as a result, new therapies focus on specific signaling cascades involved in heart failure so as to prevent these detrimental changes.

### **1.3 Molecular signaling involved in heart failure.**

The pathophysiology of heart failure is highly complex and involves numerous signaling pathways. Myocardial infarction (MI) traditionally results in severe tissue

necrosis and ventricular remodeling, which includes wall thinning and myocardial fibrosis. These changes can induce activation of the renin-angiotensin-aldosterone system (RAAS) and epinephrine secretion (4). Stimulation of the RAAS and epinephrine secretion can induce an inflammatory response and cardiac hypertrophy in the surviving myocardium. Reperfusion of the infarcted area can also introduce reactive oxygen species (ROS), which can further induce myocyte apoptosis and subsequent heart failure (5).

Hypertrophy-induced heart failure has been associated with mechanisms similar to those found in MI-induced heart failure. Cardiac myocyte surface receptors such as G-protein coupled receptors (GPCR), receptor tyrosine kinases (RTK), and cytokine receptors have all been implicated in cardiac hypertrophy. Activation of these receptors can lead to a subsequent “stress response” of protein kinases and phosphatases, which include cyclic-adenosine 3',5' monophosphate (cAMP)-dependent protein kinase (PKA), protein kinase C (PKC), protein kinase D (PKD), mitogen activated protein kinases (MAPK), calcium ( $\text{Ca}^{2+}$ )/calmodulin-dependent kinase II (CAMKII) and calcineurin(3). These mediators in turn activate transcription factors such as GATA binding protein 4 (GATA4), myocyte enhancer factor 2 (MEF2), and nuclear factor of activated T cells (NFAT), which induce changes to the myocardium that include cardiac hypertrophy and fibrosis (3). Persistent stimulation of these pathways eventually results in decompensation and heart failure.

The molecular maze of signaling molecules involved in heart failure is one that continues to change and about which there is considerable debate. There is crosstalk between the various molecules, especially between GPCRs and RTKs. Originally,

inhibition of this transactivation was believed to inhibit pressure-induced hypertrophy(6); more recently it has been identified that  $\beta$ -adrenergic receptor ( $\beta$ -AR) transactivation of RTKs is protective against hypertrophy(7). Furthermore, there has been much debate on whether extracellular regulated kinase (Erk), once believed to be a hallmark molecule involved in hypertrophy, is required for hypertrophic growth as recent studies show that Erk knockout mice can still undergo hypertrophy(8).

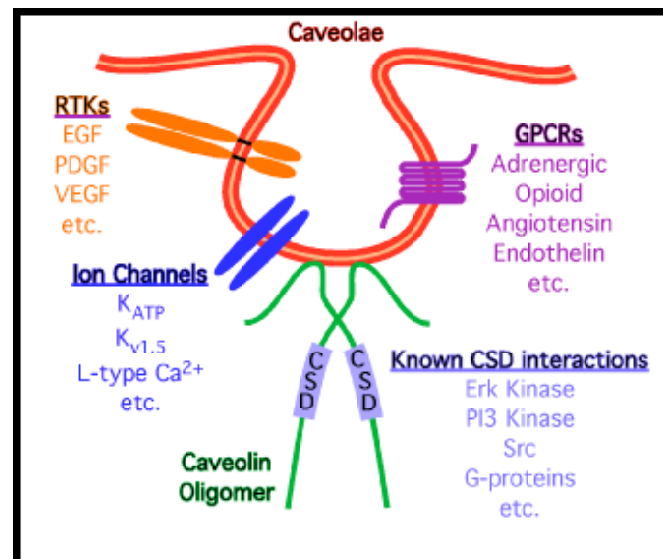


**Figure 1-2:** Schematic depicting various signaling molecules interacting with caveolae and the caveolin scaffolding domain (CSD).

Even though efforts increase that seek to understand individual signaling molecules involved in hypertrophy, the impact of spatial and temporal organization of various signaling molecules has been largely overlooked. Recently, there has been a growing interest in the compartmentalization of these molecules. Small flask-like invaginations of the plasma membrane called caveolae (“little caves”), are enriched with cholesterol, glycosphingolipids, and a vast number of important signaling

molecules that include adrenergic receptors, G-proteins, RTKs, GPCRs, and ion channels (Figure 1.2)(9).

#### 1.4 Caveolae and caveolins in heart failure.

Caveolae are approximately 50-100 nm in diameter and are anchored to the actin cytoskeleton (Figure 1-3)(10, 11). Due to their unique composition caveolae are detergent-insoluble and can be isolated from the rest of the plasma membrane via density gradients(12). Furthermore, there are a variety of compounds that can disrupt morphological caveolae from the plasma membrane; these include methyl- $\beta$ -cyclodextrin (M $\beta$ CD, which depletes cholesterol) and colchicine (Colch, which disrupts microtubules)(13).

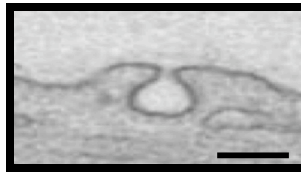


**Figure 2-3:** Electron microscopy of a caveolae located on the plasma membrane in rat adult cardiac myocyte (ACM). Scale bar 0.05  $\mu$ m.

Caveolins are the structural scaffolding proteins that are essential to caveolae formation. There are three known isoforms of caveolins: caveolin-1, -2, and -3 (Cav-1, Cav-2, and Cav-3, respectively). Traditionally, it is believed that Cav-1 and Cav-2 are ubiquitous, whereas Cav-3 is predominantly found in skeletal and cardiac muscle(14). All three isoforms of Cav are expressed in cardiac myocytes(15). All Cav isoforms have unique sequence motifs found within the caveolin scaffolding domain  $\phi$ X $\phi$ XXXX $\phi$ XX $\phi$ ,  $\phi$ X $\phi$ XXXX $\phi$ , or  $\phi$ XXXX $\phi$ XX $\phi$

( $\phi$ =aromatic residue and X is any amino acid; CSD on Figure 1-2)(16). This motif is conserved across numerous species and essential for the ability of Cav to regulate and interact with numerous signaling molecules, including Erk, phosphoinositide 3-kinase (PI3K), GPCR, and G-proteins (Figure 1-2) (16).

Caveolins were first associated with heart failure by evidence showing that pacing-induced heart failure was associated with a dramatic increase in caveolae formation and Cav-3 expression (17). Subsequent data indicated that disruption of Cav-1 can cause severe systolic and diastolic heart failure (18). In humans, Cav expression increases in response to mechanical loading in failing hearts (19). These results suggest a relationship between caveolins and the progression of heart failure and imply a compensatory role for caveolins in this setting.

### **1.5 Role for caveolins in preconditioning against ischemia/reperfusion (I/R) injury.**

Myocardial infarction is a major cause of heart failure and death. Although certain advances have led to increases in survival, prognosis remains poor particularly in early ischemia-reperfusion injury. The most beneficial experimental intervention in preventing subsequent MI is termed ischemic preconditioning (IPC). IPC occurs when the myocardium is exposed to *brief non-lethal* ischemic insults that result in protection from subsequent *prolonged lethal* ischemic insults(20-23). Since the original discovery of IPC, numerous agents have been identified that are able to induce protection: including volatile anesthetics (such as isoflurane) (24) (25), opioids (26), and adenosine (27, 28). Preconditioning (PC), is a biphasic event (Figure 1-4).

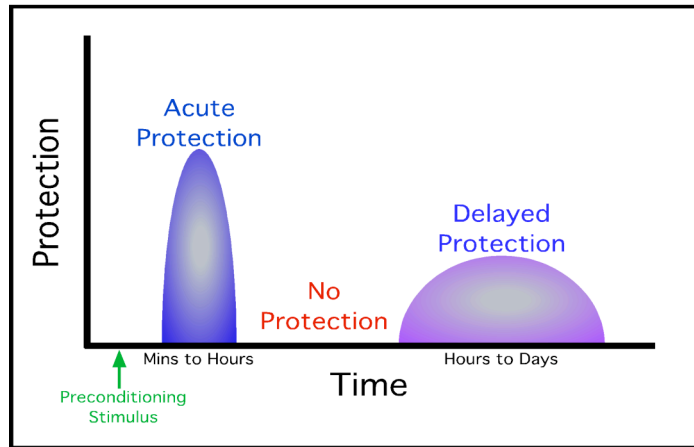


**Figure 1- 4:** Schematic of the biphasic protection involved in preconditioning.

Initially, there is a rapid response to the protective stimulus, however, this protection only lasts from minutes to hours and is a result of translocation and phosphorylation events(29). Approximately, 24 hours later there is another protective window, which lasts much longer and is believed to be a result of de novo synthesis of proteins(29).

The signal transduction pathways described for IPC are diverse and complex. What has emerged since the original description of IPC is a plethora of knowledge that organizes the mechanism of cardiac protection into putative triggers (e.g., GPCR-dependent or -independent mechanisms), mediators (e.g., PKC)(30, 31), and effectors (e.g., generation of ROS, reactive oxygen species(32-34) or activation of ATP-dependent mitochondrial  $K^+$  channels(33, 35)). The current belief is that these components of signal transduction co-exist, interact, and function in a lipid-rich environment (caveolae) that fosters protein-protein interaction among particular signaling molecules and thereby produces cardiac protection.

Numerous mechanisms for cardiac protection have been hypothesized, however, none have considered the possible role of signaling microdomains in the cell

membrane such as caveolae. Recently, we have shown that caveolin-1 is essential in facilitating temporal organization and phosphorylation of downstream mediators such as Src kinase (Src) and protein kinase B (Akt) and contributes to isoflurane-induced cardiac protection (Figure 1-5) (15). Taken together these results suggest that caveolae and other caveolins may be essential to cardiac protection and preconditioning mechanisms.

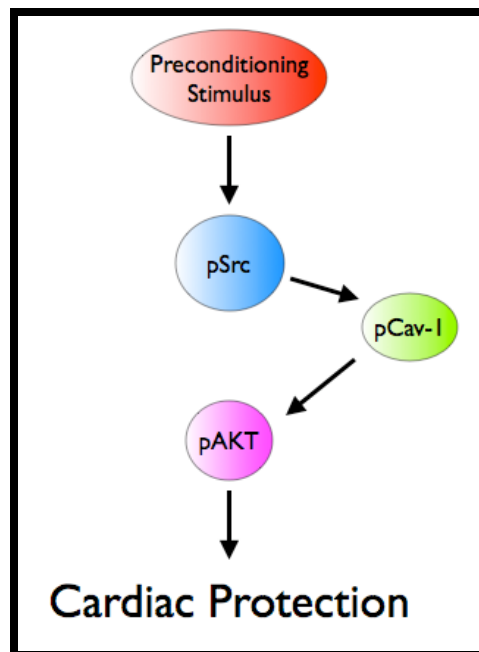


**Figure 1- 5:** Proposed mechanism of Cav-1 in cardiac protection.

### 1.6 Caveolins in cardiac hypertrophy.

The Center for Disease Control has stated that nearly 30% of all US adults older than 18 years of age have hypertension or are being treated for hypertension. As a result, understanding the mechanism of cardiac hypertrophy is vital to understanding the progression involved in heart failure. Hypertrophy is commonly caused by stressors (i.e. exercise, myocardial infarction [MI], or hypertension) that create an

increased demand on the heart. In order to compensate for such stress, the cardiac myocyte increases in size, thereby leading to changes in the diameter and geometry of the heart(36, 37). In certain situations the heart can completely compensate for the increase in demand, such as in exercise (physiological hypertrophy), however, following MI or chronic hypertension the initial compensatory hypertrophic response (pathological hypertrophy) is unable to maintain optimal function and can result in detrimental changes in size and function and ultimately in heart failure(2, 37, 38).

The signaling mechanisms involved in cardiac hypertrophy are complex and involve numerous pathways(2, 3, 37). Interestingly, many of the key components involved in hypertrophic signaling have been identified within caveolae and can interact with caveolins(16, 39). Although, the exact implications of Cav-3 (cardiac-specific) interactions are unknown, overexpression of Cav-3 in neonatal cardiac myocytes results in the inability of adrenergic agonists (e.g.,phenylephrine [PE]) and endothelin-1 to induce myocyte hypertrophy(40). Furthermore, other studies have described that caveolae and caveolin-3 levels are increased with cardiac hypertrophy, suggesting a potentially protective/reparative role for caveolin-3 in hypertrophy(41).

Suppression of cardiac caveolin-3 results in a cardiomyopathy and increased phosphorylation of Erk1/2(42). Non-specific global overexpression of Cav-3 leads to a cardiomyopathy-like phenotype(43). However, because Cav-3 is normally only expressed in skeletal and cardiac myocytes the observed cardiomyopathy may be a result of a vasculopathy and not necessarily to Cav-3 overexpression.

### 1.7 How does Cav-3 protect the heart from failure?

Although caveolins have been implicated in preconditioning pathways against I/R and in cardiac hypertrophy, how do caveolins produce such effects? Previous data have suggested that caveolins regulate key signaling molecules vital to the preconditioning and hypertrophic pathways. Nevertheless, how does a structural protein, such as Cav-3, cause such profound effects? Because Cav-3 expression directly correlates with caveolae formation and both increase following preconditioning(15) and during cardiac hypertrophy(41), formation of caveolae may have a protective role. One or more components within caveolae may thus compensate for the detrimental changes associated with heart failure. One such molecule that is found within caveolae is atrial natriuretic peptide (ANP).

ANP is an endogenous hormone and is part of a larger family of natriuretic peptides (NPs) that include: B-type (BNP) , C-type, *Dendroaspis* natriuretic peptides, and urodilatin (44). All five peptides have a similar 17 amino acid core ring structure with a cystine bridge (Figure 1-6) (44).

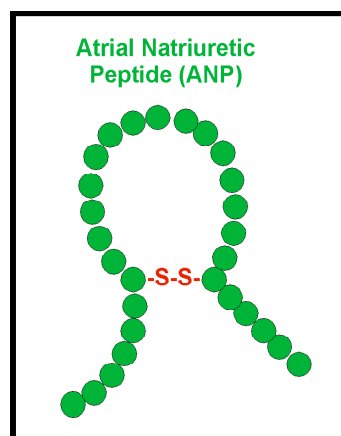


**Figure 1- 6:** Molecular structure of atrial natriuretic peptide (ANP). ANP has a 17 amino acid core structure with a cystine bond.

Of the five NPs only ANP and BNP are produced and secreted from myocardial cells. Traditionally, it is believed that ANP and BNP are secreted in response to wall stretch, which is elevated during cardiac hypertrophy and heart failure(45). ANP has vasodilatory, natriuretic, anti-fibrotic (46) and anti-hypertrophic (39) properties via the natriuretic peptide receptor-A, and –B (NPR-A, NPR-B, respectively: Figure 1-7) (45). Due to its protective cardiac effects, ANP has been investigated as a potential treatment for heart failure. A 6-year prospective open-label registry study of 3777

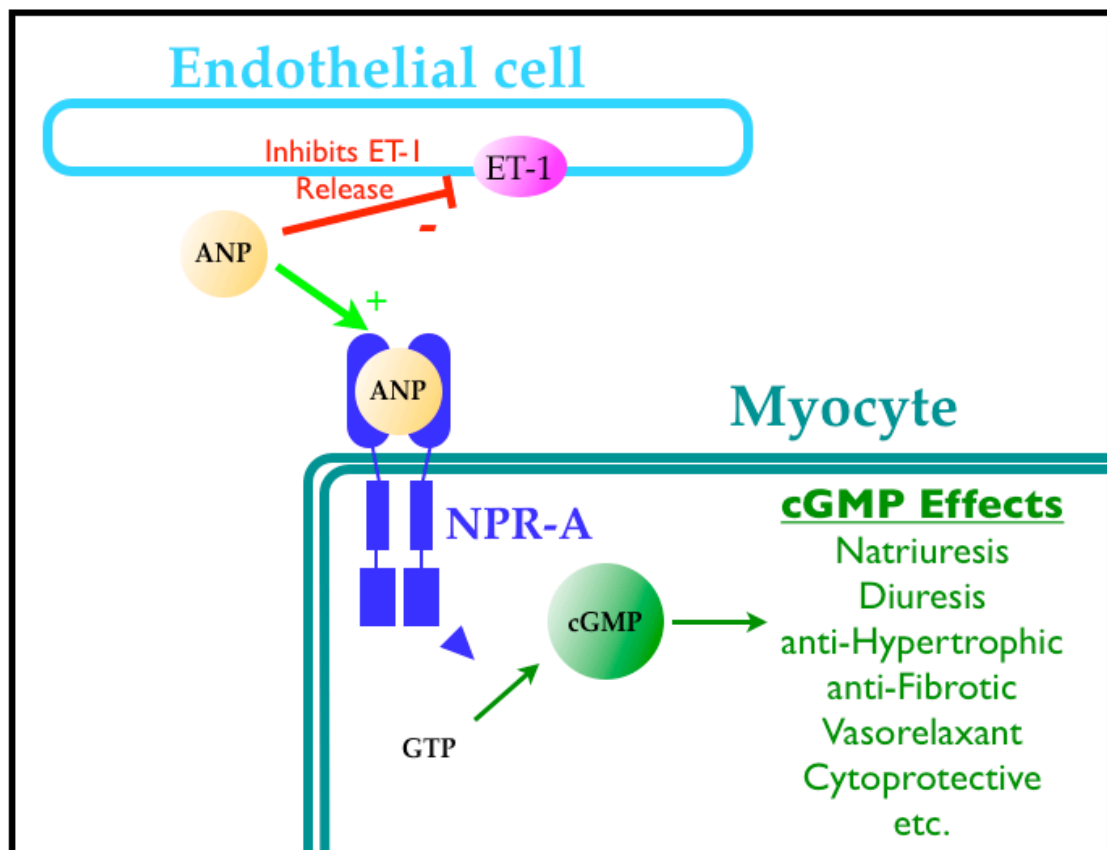


**Figure 1- 7:** Schematic of the effect ANP has on endothelial cells and cardiac myocytes. ANP signals via the natriuretic peptide receptor-A (NPR-A), aka the guanyl cyclase A receptor, to have numerous cardioprotective effects.

patients with acute heart failure treated with recombinant ANP indicated that 82% of the patients showed clinical improvement(47).

Interestingly, the history between ANP and caveolae/caveolins began nearly two decades ago when ANP was first localized within caveolae via immunoEM(48). A few years later, ANP receptors were found to co-localize with Cav-3, suggesting that ANP was not only stored within caveolae but also that it signaled within caveolae(49). However, since these early discoveries there have been few further investigations regarding caveolae and ANP. As a result, in this dissertation I sought to advance understanding of the effect that Cav-3 had on caveolae formation, hypothesizing that Cav-3 expression is essential to caveolae formation and the subsequent effects on cardiac protection and cardiac hypertrophy, in particular allowing for greater ANP storage and increased autocrine effects that would protect the myocyte against I/R injury and cardiac hypertrophy.

## **1.8 Dissertation Objectives and Hypothesis**

The major objective of this dissertation was to identify the importance of a structural protein, Cav-3, and its impact on cardiac failure by defining its role in cardiac protection from I/R injury and cardiac hypertrophy. As cardiac disease is one of the leading causes of death in the Western world, it is vital to understand the impact of Cav-3 on the normal and diseased myocardium; such understanding may facilitate the development of new therapeutics. I hypothesized that expression of Cav-3 is critical for the protection against heart failure and that modulation of Cav-3 can induce

cardiac protection and inhibit hypertrophy, possibly by the increased expression of pAkt and ANP. This hypothesis will be investigated in *Chapters 3-5*.

The objective of *Chapter 3* was to test the hypothesis that Cav-3 and caveolae are essential to isoflurane-induced cardiac protection. Within this chapter both *in vivo* and *in vitro* models of cardiac protection were used and the role of caveolin-3 and caveolae was determined. Methyl- $\beta$ -cyclodextrin (M $\beta$ CD), and colchicine (Colch), agents known to remove caveolae, were utilized to assess the role of caveolae on cardiac protection. Furthermore, Cav-3 knockout (Cav-3 KO) mice, which lack cardiac caveolae, were used to test whether such animals are protected against ischemia/reperfusion injury.

The objective of *Chapter 4* was to test the hypothesis that cardiac-specific overexpression of Cav-3 could produce a preconditioned phenotype in the absence of a preconditioning stimulus. Cardiac myocyte-specific caveolin-3-overexpressing transgenic mice (Cav-3 OE) were developed in order to test this hypothesis. Various biochemical, histological, and surgical techniques were utilized to determine the impact of increasing caveolin-3 expression in the cardiac myocyte.

The objective of *Chapter 5* was to test the hypothesis that cardiac-specific overexpression of Cav-3 modulates cardiac hypertrophy. Based on a possible relationship between caveolae, caveolins, and ANP (50), I investigated the impact of Cav-3 expression on ANP production and cardiac hypertrophy in Cav-3 OE mice and adult cardiac myocytes infected with Cav-3 adenovirus.

In *Chapter 6* I discuss the current results and future directions to better understand the role of caveolins, caveolae, and ANP in cardiac failure.

# Hypothesis

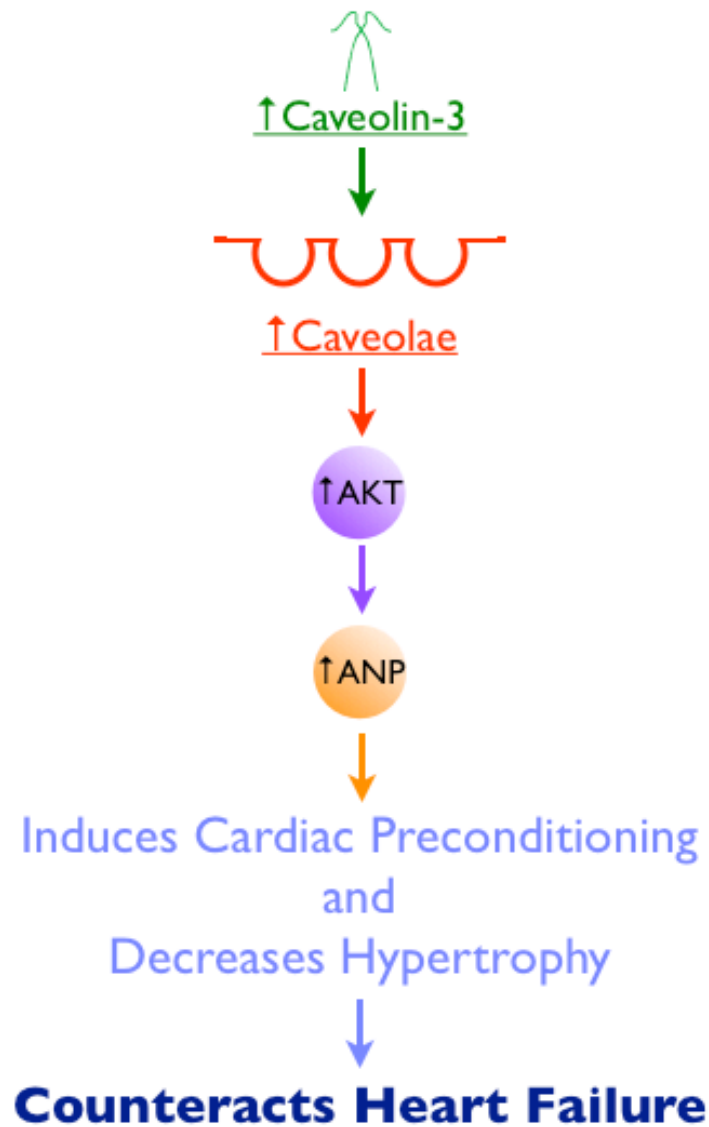


**Figure 1- 8:** Flow diagram of our proposed hypotheses. The working hypothesis is that overexpression of caveolin-3 will increase caveolae formation and ANP expression. These changes will then protect the myocardium from ischemia/reperfusion (I/R) injury and transverse aortic constriction (TAC) and prevent the development of heart failure.

## 1.9 References

1. Rosamond, W., Flegal, K., Furie, K., Go, A., Greenlund, K., Haase, N., Hailpern, S.M., Ho, M., Howard, V., Kissela, B., et al. 2008. Heart disease and stroke statistics--2008 update: a report from the American Heart Association Statistics Committee and Stroke Statistics Subcommittee. *Circulation* 117:e25-146.
2. Heineke, J., and Molkenin, J.D. 2006. Regulation of cardiac hypertrophy by intracellular signalling pathways. *Nat Rev Mol Cell Biol* 7:589-600.
3. Mudd, J.O., and Kass, D.A. 2008. Tackling heart failure in the twenty-first century. *Nature* 451:919-928.
4. Dorn, G.W., 2nd. 2009. Novel pharmacotherapies to abrogate postinfarction ventricular remodeling. *Nat Rev Cardiol* 6:283-291.
5. Foo, R.S., Mani, K., and Kitsis, R.N. 2005. Death begets failure in the heart. *J Clin Invest* 115:565-571.
6. Asakura, M., Kitakaze, M., Takashima, S., Liao, Y., Ishikura, F., Yoshinaka, T., Ohmoto, H., Node, K., Yoshino, K., Ishiguro, H., et al. 2002. Cardiac hypertrophy is inhibited by antagonism of ADAM12 processing of HB-EGF: metalloproteinase inhibitors as a new therapy. *Nat Med* 8:35-40.
7. Noma, T., Lemaire, A., Naga Prasad, S.V., Barki-Harrington, L., Tilley, D.G., Chen, J., Le Corvoisier, P., Violin, J.D., Wei, H., Lefkowitz, R.J., et al. 2007. Beta-arrestin-mediated beta1-adrenergic receptor transactivation of the EGFR confers cardioprotection. *J Clin Invest* 117:2445-2458.
8. Purcell, N.H., Wilkins, B.J., York, A., Saba-El-Leil, M.K., Meloche, S., Robbins, J., and Molkenin, J.D. 2007. Genetic inhibition of cardiac ERK1/2 promotes stress-induced apoptosis and heart failure but has no effect on hypertrophy in vivo. *Proc Natl Acad Sci U S A* 104:14074-14079.
9. Fujita, T., Toya, Y., Iwatsubo, K., Onda, T., Kimura, K., Umemura, S., and Ishikawa, Y. 2001. Accumulation of molecules involved in alpha1-adrenergic signal within caveolae: caveolin expression and the development of cardiac hypertrophy. *Cardiovasc Res* 51:709-716.
10. Palade, G. 1953. Fine structure of blood capillaries. *Journal of Applied Physics* 24:1424.
11. Yamada, E. 1955. The fine structure of the gall bladder epithelium of the mouse. *J Biophys Biochem Cytol* 1:445-458.

12. Song, K.S., Li, S., Okamoto, T., Quilliam, L.A., Sargiacomo, M., and Lisanti, M.P. 1996. Co-purification and direct interaction of Ras with caveolin, an integral membrane protein of caveolae microdomains. Detergent-free purification of caveolae microdomains. *J Biol Chem* 271:9690-9697.
13. Head, B.P., Patel, H.H., Roth, D.M., Murray, F., Swaney, J.S., Niesman, I.R., Farquhar, M.G., and Insel, P.A. 2006. Microtubules and actin microfilaments regulate lipid raft/caveolae localization of adenylyl cyclase signaling components. *J Biol Chem* 281:26391-26399.
14. Song, K.S., Scherer, P.E., Tang, Z., Okamoto, T., Li, S., Chafel, M., Chu, C., Kohtz, D.S., and Lisanti, M.P. 1996. Expression of caveolin-3 in skeletal, cardiac, and smooth muscle cells. Caveolin-3 is a component of the sarcolemma and co-fractionates with dystrophin and dystrophin-associated glycoproteins. *Journal of Biological Chemistry* 271:15160-15165.
15. Patel, H.H., Tsutsumi, Y.M., Head, B.P., Niesman, I.R., Jennings, M., Horikawa, Y., Huang, D., Moreno, A.L., Patel, P.M., Insel, P.A., et al. 2007. Mechanisms of cardiac protection from ischemia/reperfusion injury: a role for caveolae and caveolin-1. *FASEB J* 21:1565-1574.
16. Razani, B., Woodman, S.E., and Lisanti, M.P. 2002. Caveolae: from cell biology to animal physiology. *Pharmacol Rev* 54:431-467.
17. Hare, J.M., Lofthouse, R.A., Juang, G.J., Colman, L., Ricker, K.M., Kim, B., Senzaki, H., Cao, S., Tunin, R.S., and Kass, D.A. 2000. Contribution of caveolin protein abundance to augmented nitric oxide signaling in conscious dogs with pacing-induced heart failure. *Circ Res* 86:1085-1092.
18. Wunderlich, C., Schober, K., Lange, S.A., Drab, M., Braun-Dullaeus, R.C., Kasper, M., Schwencke, C., Schmeisser, A., and Strasser, R.H. 2006. Disruption of caveolin-1 leads to enhanced nitrosative stress and severe systolic and diastolic heart failure. *Biochem Biophys Res Commun* 340:702-708.
19. Uray, I.P., Connelly, J.H., Frazier, O.H., Taegtmeier, H., and Davies, P.J. 2003. Mechanical unloading increases caveolin expression in the failing human heart. *Cardiovasc Res* 59:57-66.
20. Murry, C.E., Jennings, R.B., and Reimer, K.A. 1986. Preconditioning with ischemia: a delay of lethal cell injury in ischemic myocardium. *Circulation* 74:1124-1136.
21. Li, G.C., Vasquez, J.A., Gallagher, K.P., and Lucchesi, B.R. 1990. Myocardial protection with preconditioning. *Circulation* 82:609-619.

22. Schott, R.J., Rohmann, S., Braun, E.R., and Schaper, W. 1990. Ischemic preconditioning reduces infarct size in swine myocardium. *Circ Res* 66:1133-1142.
23. Liu, G.S., Thornton, J., Van Winkle, D.M., Stanley, A.W., Olsson, R.A., and Downey, J.M. 1991. Protection against infarction afforded by preconditioning is mediated by A1 adenosine receptors in rabbit heart. *Circulation* 84:350-356.
24. Kersten, J.R., Schmeling, T.J., Hettrick, D.A., Pagel, P.S., Gross, G.J., and Warltier, D.C. 1996. Mechanism of myocardial protection by isoflurane: role of adenosine triphosphate-regulated potassium ( $K_{ATP}$ ) channels. *Anesthesiology* 85:794-807.
25. Kersten, J.R., Schmeling, T.J., Pagel, P.S., Gross, G.J., and Warltier, D.C. 1997. Isoflurane mimics ischemic preconditioning via activation of KATP channels: Reduction of myocardial infarct size with an acute memory phase. *Anesthesiology* 87:361-370.
26. Schultz, J.E.J., Hsu, A.K., and Gross, G.J. 1996. Morphine mimics the cardioprotective effect of ischemic preconditioning via a glibenclamide-sensitive mechanism in the rat heart. *Circulation Research* 78:1100-1104.
27. Ganote, C.E., Armstrong, S., and Downey, J.M. 1993. Adenosine and A1 selective agonists offer minimal protection against ischaemic injury in isolated rat cardaomyocytes. *Cardiovasc Res* 27:1670-1676.
28. Armstrong, S., Downey, J.M., and Ganote, C.E. 1994. Preconditioning of isolated rabbit cardiomyocytes: induction by metabolic stress and blockade by the adenosine antagonist SPT and calphostin C, a protein kinase C inhibitor. *Cardiovasc Res* 28:72-77.
29. Bienengraeber, M.W., Weihrauch, D., Kersten, J.R., Pagel, P.S., and Warltier, D.C. 2005. Cardioprotection by volatile anesthetics. *Vascul Pharmacol* 42:243-252.
30. Ytrehus, K., Liu, Y., and Downey, J.M. 1994. Preconditioning protects ischemic rabbit heart by protein kinase C activation. *Am J Physiol* 266:H1145-1152.
31. Liu, Y., Ytrehus, K., and Downey, J.M. 1994. Evidence that translocation of protein kinase C is a key event during ischemic preconditioning of rabbit myocardium. *J Mol Cell Cardiol* 26:661-668.

32. Nishida, M., Maruyama, Y., Tanaka, R., Kontani, K., Nagao, T., and Kurose, H. 2000. G alpha(i) and G alpha(o) are target proteins of reactive oxygen species. *Nature* 408:492-495.
33. Tokube, K., Kiyosue, T., and Arita, M. 1996. Openings of cardiac K<sub>ATP</sub> channel by oxygen free radicals produced by xanthine oxidase reaction. *Am J Physiol Heart Circ Physiol* 271:H478-H489.
34. Das, D.K., Maulik, N., Sato, M., and Ray, P.S. 1999. Reactive oxygen species function as second messenger during ischemic preconditioning of heart. *Mol Cell Biochem* 196:59-67.
35. Grover, G.J., Sleph, P.G., and Dzwonczyk, S. 1992. Role of myocardial ATP-sensitive potassium channels in mediating preconditioning in the dog heart and their possible interaction with adenosine A<sub>1</sub>-receptors. *Circulation* 86:1310-1316.
36. Abraham, J., Abreu, P., Aglietta, M., Aguirre, C., Allard, D., Allekotte, I., Allen, J., Allison, P., Alvarez-Muniz, J., Ambrosio, M., et al. 2008. Upper limit on the diffuse flux of ultrahigh energy tau neutrinos from the Pierre Auger Observatory. *Phys Rev Lett* 100:211101.
37. Catalucci, D., Latronico, M.V., Ellingsen, O., and Condorelli, G. 2008. Physiological myocardial hypertrophy: how and why? *Front Biosci* 13:312-324.
38. Patel, H.H., Murray, F., and Insel, P.A. 2008. Caveolae as organizers of pharmacologically relevant signal transduction molecules. *Annu Rev Pharmacol Toxicol* 48:359-391.
39. Horio, T., Nishikimi, T., Yoshihara, F., Matsuo, H., Takishita, S., and Kangawa, K. 2000. Inhibitory regulation of hypertrophy by endogenous atrial natriuretic peptide in cultured cardiac myocytes. *Hypertension* 35:19-24.
40. Koga, A., Oka, N., Kikuchi, T., Miyazaki, H., Kato, S., and Imaizumi, T. 2003. Adenovirus-Mediated Overexpression of Caveolin-3 Inhibits Rat Cardiomyocyte Hypertrophy. *Hypertension* 42:213-219.
41. Kikuchi, T., Oka, N., Koga, A., Miyazaki, H., Ohmura, H., and Imaizumi, T. 2005. Behavior of caveolae and caveolin-3 during the development of myocyte hypertrophy. *J Cardiovasc Pharmacol* 45:204-210.
42. Woodman, S.E., Park, D.S., Cohen, A.W., Cheung, M.W., Chandra, M., Shirani, J., Tang, B., Jelicks, L.A., Kitsis, R.N., Christ, G.J., et al. 2002.

- Caveolin-3 knock-out mice develop a progressive cardiomyopathy and show hyperactivation of the p42/44 MAPK cascade. *J Biol Chem* 277:38988-38997.
43. Aravamudan, B., Volonte, D., Ramani, R., Gursoy, E., Lisanti, M.P., London, B., and Galbiati, F. 2003. Transgenic overexpression of caveolin-3 in the heart induces a cardiomyopathic phenotype. *Hum. Mol. Genet.* 12:2777-2788.
  44. Lee, C.Y., and Burnett, J.C., Jr. 2007. Natriuretic peptides and therapeutic applications. *Heart Fail Rev* 12:131-142.
  45. Rubattu, S., Sciarretta, S., Valenti, V., Stanzione, R., and Volpe, M. 2008. Natriuretic peptides: an update on bioactivity, potential therapeutic use, and implication in cardiovascular diseases. *Am J Hypertens* 21:733-741.
  46. Maki, T., Horio, T., Yoshihara, F., Suga, S., Takeo, S., Matsuo, H., and Kangawa, K. 2000. Effect of neutral endopeptidase inhibitor on endogenous atrial natriuretic peptide as a paracrine factor in cultured cardiac fibroblasts. *Br J Pharmacol* 131:1204-1210.
  47. Suwa, M., Seino, Y., Nomachi, Y., Matsuki, S., and Funahashi, K. 2005. Multicenter prospective investigation on efficacy and safety of carperitide for acute heart failure in the 'real world' of therapy. *Circ J* 69:283-290.
  48. Page, E., Upshaw-Earley, J., and Goings, G.E. 1994. Localization of atrial natriuretic peptide in caveolae of in situ atrial myocytes. *Circ Res* 75:949-954.
  49. Doyle, D.D., Ambler, S.K., Upshaw-Earley, J., Bastawrous, A., Goings, G.E., and Page, E. 1997. Type B atrial natriuretic peptide receptor in cardiac myocyte caveolae. *Circ Res* 81:86-91.
  50. Page, E., Upshaw-Earley, J., and Goings, G.E. 1994. Localization of atrial natriuretic peptide in caveolae of in situ atrial myocytes. *Circulation Research* 75:949-954.

# **Chapter 2:**

## **Methods and Protocols**

## **2.1 *in vivo* methods**

### **Animals.**

All animals were treated in compliance with the Guide for the Care and Use of Laboratory Animals (National Academy of Science) and protocols were approved by the VA San Diego Healthcare System IACUC. All animals were kept on a 12 h light-dark cycle in a temperature-controlled room with *ad lib* access to food and water.

Cav-3 OE mice were on a C57BL/6 background. Full-length Cav-3 cDNA (455 bp) was cloned into a vector containing the  $\alpha$  myosin heavy chain promoter and was used for microinjection (UCSD Transgenic Core)(1). Cav-3 KO mice were created as reported previously (2).

### ***In vivo* ischemia-reperfusion experimental protocol.**

Pentobarbital (80mg/kg)-anesthetized mice were mechanically ventilated and ischemia was produced by occluding the left coronary artery with a 7-0 silk suture on a tapered BV-1 needle (Ethicon) for 30 min(3). After 30 min occlusion, the ligature was released and the heart was reperfused for 2 h. Reperfusion was confirmed by observing return of blood flow in the epicardial coronary arteries and via electrocardiography.

Ischemic preconditioning (IPC) was induced by occlusion of the left coronary artery for 5 min followed by 15 min reperfusion just prior to ischemia. Isoflurane (anesthetic)- induced preconditioning (APC) was administered by giving mice 1.4% isoflurane vol/vol in O<sub>2</sub>, which is equivalent to 1 minimum alveolar concentration (MAC)(4) for 30 min followed by a 15 min washout. Some Cav-3 OE mice were also

treated with 5-hydroxydecanoate (5-HD: 10 mg/kg i.v., Sigma) 10 min before myocardial ischemia.

The area at risk (AAR) was determined by staining with 1% Evans blue (1.0 ml, Sigma – St. Louis, MO). The heart was immediately excised and placed into 1% agarose and allowed to harden. Once hardened, the heart was cut into 1 mm slices (McIlwain tissue chopper; Brinkmann Instruments, Inc. – Westbury, NY). Each slice of left ventricle (LV) was counterstained with 3.0 ml of 1% 2,3,5-triphenyltetrazolium chloride (Sigma – St. Louis, MO) for 5 min at 37°C. After overnight storage in 10% formaldehyde, slices were weighed and visualized under a microscope (Leica Microsystems Inc. – Bannockburn, IL) equipped with a charge-coupled device camera (Cool SNAP-Pro, Media Cybernetics, Inc. – Silver Spring, MD). The images were analyzed (Image-Pro Plus Version 4.5, Media Cybernetics, Inc. – Silver Spring, MD) and infarct size was determined by planimetry. The AAR was expressed as a percentage of the LV (AAR/LV). Infarct size (IS) was expressed as a percentage of the AAR (IS/AAR)(3).

### ***In vivo* transverse aortic constriction (TAC).**

8-16 week old transgenic mice with cardiac myocyte-specific overexpression of Cav-3 (Cav-3 OE)(1) and transgene-negative mice (Control) underwent a modified version of transverse aortic constriction (TAC), as previously published(5). In brief, following echocardiography mice were briefly anesthetized with isoflurane, intubated, and mechanically ventilated. An incision was made in the second intercostal space and a 7-0 silk suture was carefully placed around the aorta and a 27g needle between

the innominate and left carotid artery. A double surgeon's knot was utilized and the needle was carefully removed resulting in approximately 0.41mm stenosis. Mice were allowed to recover at 34°C and 100% oxygen for one hr. Mice were euthanized after 48 hr or 4 wk of stenosis. Sham animals underwent all aspects of the surgery, except placement of the stenosis.

### **Detecting cardiac troponin I levels.**

Cardiac troponin levels, a second measure of cardiac injury, were determined from a subset of animals using a mouse cardiac Tn-I ELISA kit (Life Diagnostics – West Chester, PA). Serum was prepared from each test group and stored at -80°C. ELISA was run per the manufacturer's recommended protocol and absorbance was read at 405 nm using an Infinite M500 plate reader (Tecan – San Jose, CA).

### **Echocardiography**

Echocardiography was performed in a subset of Cav-3 OE and Control mice prior to TAC surgery and prior to euthanasia. Mice were anesthetized with isoflurane using an echocardiograph and L15/6-MHz transducer (Sonos 5500, Philips Medical Systems, Andover, Mass) as described previously. All mice were evaluated after two weeks for placement of the stenosis and had >3.5m/s gradient across the stenosis.

### **Cardiac function.**

Mice were anesthetized with pentobarbital (80mg/kg) and cardiac catheterization was performed using a high-fidelity 1.4F Mikro-tip pressure transducer

(SPR-671, Millar). The catheter was advanced via the right carotid artery into the LV after measuring mean arterial pressure (MAP). Parameters were determined by an algorithm from EMKA Technologies.

### **Conscious Blood Pressure.**

A subset of Cav-3 OE and Control mice were trained so that their blood pressure could be measured without anesthesia. Mice were trained for 3 days on the CODA noninvasive tail blood pressure system from Kent Scientific (Torrington, CT). Data were analyzed using the CODA v2.5 software.

## **2.2 *in vitro* methods**

### **Adult cardiac myocyte (ACM) isolation.**

ACM were isolated from adult Sprague-Dawley rats (Harlan – Indianapolis, IN; 250–300 g, male), adult Cav-3 OE mice, and transgene negative (Control) mice. Animals were heparinized (1,000U, intraperitoneally, IP) 5 min before being anesthetized with pentobarbital (80 mg/kg IP). The hearts were removed and placed in ice-cold cardioplegic (20 mM KCl) heart media solution (HM, in mmol/l: 112 NaCl, 5.4 KCl, 1 MgCl<sub>2</sub>, 9 NaH<sub>2</sub>PO<sub>4</sub>, and 11.1 D-glucose; supplemented with 10 HEPES, 30 taurine, 2 DL-carnitine, and 2 creatine, pH 7.4) and then retrograde-perfused on a Langendorff apparatus with Ca<sup>2+</sup>-free HM for 5 min at 5 ml/min at 37°C, followed by perfusion with Ca<sup>2+</sup>-free HM containing collagenase II (210 U/mg; Worthington – Lakewood, NJ) for 20 min. After perfusion, both ventricles were removed and minced in collagenase II-containing HM for 2 mins. Minced ventricles were then triturated for

6 min at 37 °C. The cell solution was then washed several times with wash buffer (1% BSA in 199 medium) to remove collagenase II and re-exposed to 1.2 mM Ca<sup>2+</sup> over 25 min to produce Ca<sup>2+</sup>-tolerant CM. Myocytes were then plated in 4% FBS on laminin (2 µg/cm<sup>2</sup>)-coated plates for 1 hr. Plating/maintenance media was changed to serum-free medium [1% bovine serum albumin (BSA)+0.1% penicillin/streptomycin in 199 medium (Invitrogen – Carlsbad, CA)] to remove all non-myocytes, and CM were incubated at 37°C in 5% CO<sub>2</sub> for 24 hr.

### **Simulated ischemia/reperfusion (SI/R) in isolated CM.**

CM were plated on laminin-coated 12-well plates, allowed to incubate for 24 hr, and then subjected to various experimental conditions at 37°C. Simulated ischemia was induced by replacing the air with a 95% N<sub>2</sub> and 5% CO<sub>2</sub> gas mixture at 2 L/min in a metabolic chamber (Columbus Instruments – Columbus, OH) and by replacing the serum free media with glucose-free media (glucose-free DMEM, Invitrogen – Carlsbad, CA) for 60 min. This treatment was then followed by 60 min of “reperfusion” by replacing the media with normal maintenance media and by incubating the cells with 21% O<sub>2</sub> and 5% CO<sub>2</sub>. CM were exposed to isoflurane for 30-min prior to SI/R. Isoflurane concentrations were verified continuously by sampling exhaust gas with a Datex Capnomac (SOMA Technology Inc. – Cheshire, CT). Concentrations of isoflurane (0.7%, 1.4%, and 2.8% vol/vol in air) were chosen based on the minimum alveolar concentrations (MAC) in rodents (where 1.4% vol/vol is equivalent to 1 MAC). Cell death was quantified by counting trypan blue-stained cells with results expressed as a percentage of total cells counted. To determine the impact

of caveolae on cardiac protection, M $\beta$ CD and colchicines were used to disrupt caveolae (6). CM were incubated under maintenance media (control conditions) or in the presence of M $\beta$ CD (1 mM) or colchicine (30 $\mu$ M) for 1 hr before SI/R or isoflurane + SI/R.

### **2.3 Molecular, Biochemical, Histological, and Electron Microscopy methods**

#### **Plasmid and recombinant adenovirus production.**

A mouse Cav-3 cDNA (455bp) was generated, cloned, and co-transfected with pJM170 (containing E1 region deletion). Plaques were expanded in HEK293 cells transformed with adenovirus (Adv) E1. Adv containing LacZ (Adv.LacZ) served as control. CM were treated with Adv.LacZ or Adv.Cav-3 for 16-24 h.

#### **Sucrose density membrane fractionation.**

ACM were fractionated to isolate caveolae-rich domains using a detergent-free method(7). Cells from a 10-cm<sup>2</sup> plate were washed twice in ice-cold PBS, scraped into 3 ml of 150 mM Na<sub>2</sub>CO<sub>3</sub> with 1 mM EDTA (pH 11.0), homogenized with a tissue grinder with three 10-sec bursts, and then sonicated with three cycles of 20-sec bursts interspersed with 1 min of incubation on ice. Whole cell lysates were normalized to GAPDH expression. 1 ml of homogenate was mixed with 1 ml of 80% sucrose in MES-buffered saline (MBS: 25 mM MES, 150 mM NaCl, 2 mM EDTA-MBS, pH 6.5) to form 40% sucrose and loaded at the bottom of an ultracentrifuge tube. A discontinuous sucrose gradient was generated by layering 6 ml of 35% sucrose prepared in MBS and then 4 ml of 5% sucrose in MBS. The gradient was centrifuged

at 175,000 *g* using a SW41Ti rotor (Beckman Instruments – Fullerton, CA) for 3 hr at 4°C. Samples were removed in 1 ml aliquots to yield 12 fractions, which were analyzed for protein content. We defined fractions 4-6 as buoyant membrane fractions (BF) enriched in caveolae and proteins associated with caveolae. Fractions 9-12 were defined as non-buoyant fractions.

### **Immunoblot Analysis.**

Proteins in individual fractions, whole cell lysates, and whole tissue lysates were separated by SDS-PAGE using 10% polyacrylamide precast gels (Invitrogen – Carlsbad, CA) and transferred to a polyvinylidene difluoride (Millipore – Billerica, MA) membrane by electroelution. Membranes were blocked in 20 mM TBS-Tween (1%) containing 1.5% nonfat dry milk and incubated with primary antibody overnight (Caveolin-1 and Caveolin-3, Abcam – Cambridge, MA; GAPDH, Imgenex – San Diego, CA; p-Caveolin-1 Y14, Chemicon – Temecula, CA; ANP, Santa Cruz biotechnology – Santa Cruz, CA) at 4°C. Bound primary antibodies were visualized using secondary antibodies conjugated to horseradish peroxidase (Santa Cruz Biotechnology – Santa Cruz, CA) and enhanced chemiluminescence reagent (GE Healthcare/Amersham – Piscataway, NJ). All displayed bands migrated at the appropriate size, as determined by comparison with molecular weight standards (Santa Cruz Biotechnology – Santa Cruz, CA).

**Nitric oxide synthase (NOS) activity and cholesterol assay.**

Basal NOS activity was determined in TG<sub>neg</sub> and Cav-3 OE mice.

Homogenized tissues were prepared and measured using a Nitric Oxide Synthase Assay Kit, Colorimetric (EMD Biosciences) as described by the manufacturer.

Cholesterol in fractions was measured using the Amplex Red Cholesterol Assay Kit (Invitrogen) as described by the manufacturer.

**Immunofluorescence.**

CMs or cryostat embedded ventricular slices were fixed with paraformaldehyde, incubated with 100 mM glycine, permeabilized in 0.1% buffered Triton X-100, blocked with 1% BSA, PBS, and 0.05% Tween. Samples were then incubated with primary antibody (1:100) in 1% BSA, PBS, and 0.05% Tween for 24 h. Excess antibody was removed, and samples were incubated with fluorescein Alexa-conjugated secondary antibodies (1:250) for 1 h. To remove excess secondary antibody, samples were washed with PBS/0.1% Tween and incubated for 20 min with the nuclear stain 4',6-diamidino-2-phenylindole (1:5000) diluted in PBS. Samples were mounted in gelvatol for microscopy imaging and images were captured with a DeltaVision deconvolution microscope system (Applied Precision, Inc., Issaquah, WA, USA). The system includes a Photometrics charge-coupled device mounted on a Nikon TE-200 inverted epifluorescence microscope. Twenty optical sections spaced 0.2 mm were taken. Exposure times were set such that the camera response was in the linear range for each fluorophore. Images were taken at 400x magnification and were deconvolved and analyzed using SoftWorx software (Applied Precision, Inc) on a

Silicon Graphics Octane workstation. Colocalization of pixels was assessed quantitatively by CoLocalizer Pro 1.0 software (<http://www.homepage.mac.com/colocalizerpro/>). All images were normalized to a background threshold value of 30.

### **Histology.**

Left ventricles from Cav-3 OE and Control mice that underwent sham and TAC surgery were fixed in 10% neutral-buffered formalin and paraffin embedded. Sections were stained with wheat germ agglutinin (WGA) to determine myocyte cross sectional area, and Masson's Trichrome staining to determine fibrosis.

### **Apoptosis.**

For TUNEL assays, AAR was removed from the mice after 24 h of reperfusion. The tissue was cut, fixed in 3.7% formalin and sections (5  $\mu$ m) were used for TUNEL assays using the Apoptosis Detection Kit (R&D Systems), according to the manufacturer's instructions. Real-time PCR analysis of gene expression of pro- and anti-apoptotic genes was performed on total RNA isolated from the heart after 24 h of reperfusion using a RNeasy Mini Kit (Qiagen Inc) as described previously.

### **Electron microscopy (EM).**

Whole hearts or cells were fixed with 2.5% glutaraldehyde in 0.1 M cacodylate buffer for 2 h, post-fixed in 1% OsO<sub>4</sub> in 0.1 M cacodylate buffer (1 h) and embedded as monolayers in LX-112 (Ladd Research). Sections were stained in uranyl acetate and

lead citrate and observed with an electron microscope (JEOL 1200 EX-II, JEOL USA or Philips CM-10, Philips Electronic Instruments). Random sections were taken by an EM technician blinded to the treatments.

### **Quantitative Real-Time PCR analysis.**

Total RNA was isolated from ACM using a RNeasy Mini Kit (Qiagen, Valencia, CA, USA). First strand cDNA synthesis (iScript cDNA synthesis kit; Bio-Rad, Hercules, CA, USA) was performed using random hexamers on 1–2  $\mu\text{g}$  of total RNA. The concentration of cDNA was determined and adjusted to 50 ng/ $\mu\text{L}$  for real-time PCR analysis, which was performed on a MJ Research Opticon 2 (Bio-Rad, Hercules, CA, USA) in triplicate using the IQ SYBR Green Supermix (Bio-Rad, Hercules, CA, USA) with 100 ng cDNA and 0.5  $\mu\text{M}$  forward/reverse primer mix in 20  $\mu\text{L}$  final reaction volume. ANP, BNP, and  $\alpha\text{MHC}$  primers were QuantiTect Primers (Qiagen, Valencia, CA, USA). Primer sequences for  $\alpha\text{-sk-actin}$  forward: GTGTCACCCACAACGTGC, reverse: AGGGCCACATAGCACAGC;  $\beta\text{-MHC}$  forward: GCTGAAAGCAGAAAGAGATTATC, reverse: TGGAGTTCTTCTTCTGGAG. Thermal cycle conditions were as follows: 94°C-10 min (1 cycle); 94°C-20 s, 55°C-20 s, and 72°C-30 s (40 cycles). Resulting PCR products were confirmed by melt curve analysis. Analysis of cycle threshold (Ct) was performed using Opticon 2 analysis software (Bio-Rad); normalized values were obtained for each group by subtracting matched glyceraldehyde-3-phosphate dehydrogenase (GAPDH) Ct values.

**Statistical Analysis.**

Data analysis was performed by observers blinded to experimental groups. Group size to determine the primary outcome variable of infarct size was determined by power analysis. Statistical analysis was performed with Prism 4.0 (GraphPad) by the unpaired Student's *t*-test or one-way ANOVA followed by post-hoc test with Bonferroni correction for multiple comparisons. All data are expressed as mean  $\pm$  SEM. Statistical significance was defined as  $P < 0.05$ .

## 2.4 References

1. Tsutsumi, Y.M., Horikawa, Y.T., Jennings, M.M., Kidd, M.W., Niesman, I.R., Yokoyama, U., Head, B.P., Hagiwara, Y., Ishikawa, Y., Miyanohara, A., et al. 2008. Cardiac-specific overexpression of caveolin-3 induces endogenous cardiac protection by mimicking ischemic preconditioning. *Circulation* 118:1979-1988.
2. Hagiwara, Y., Sasaoka, T., Araishi, K., Imamura, M., Yorifuji, H., Nonaka, I., Ozawa, E., and Kikuchi, T. 2000. Caveolin-3 deficiency causes muscle degeneration in mice. *Hum Mol Genet* 9:3047-3054.
3. Tsutsumi, Y.M., Patel, H.H., Lai, N.C., Takahashi, T., Head, B.P., and Roth, D.M. 2006. Isoflurane produces sustained cardiac protection after ischemia-reperfusion injury in mice. *Anesthesiology* 104:495-502.
4. Deady, J.E., Koblin, D.D., Eger, E.I., Heavner, J.E., and D'Aoust, B. 1981. Anesthetic potencies and the unitary theory of narcosis. *Anesth Analg* 60:380-384.
5. Rockman, H.A., Ross, R.S., Harris, A.N., Knowlton, K.U., Steinhilper, M.E., Field, L.J., Ross, J., Jr., and Chien, K.R. 1991. Segregation of atrial-specific and inducible expression of an atrial natriuretic factor transgene in an in vivo murine model of cardiac hypertrophy. *Proc Natl Acad Sci U S A* 88:8277-8281.
6. Head, B.P., Patel, H.H., Roth, D.M., Murray, F., Swaney, J.S., Niesman, I.R., Farquhar, M.G., and Insel, P.A. 2006. Microtubules and actin microfilaments regulate lipid raft/caveolae localization of adenylyl cyclase signaling components. *J Biol Chem* 281:26391-26399.
7. Song, K.S., Li, S., Okamoto, T., Quilliam, L.A., Sargiacomo, M., and Lisanti, M.P. 1996. Co-purification and direct interaction of Ras with caveolin, an integral membrane protein of caveolae microdomains. Detergent-free purification of caveolae microdomains. *J Biol Chem* 271:9690-9697.

## **Chapter 3:**

**Caveolin-3 expression and caveolae are required for volatile anesthetic-induced cardiac protection from hypoxia and ischemia/reperfusion injury**

### 3.1 Abstract

**Volatile anesthetics protect the heart from ischemia/reperfusion injury but the mechanisms for this protection are poorly understood. Caveolae, sarcolemmal invaginations, and caveolins, scaffolding proteins in caveolae, localize molecules involved in cardiac protection. We tested the hypothesis that caveolae and caveolins are essential for volatile anesthetic-induced cardiac protection using cardiac myocytes (CM) from adult rats and *in vivo* studies in caveolin-3 knockout mice (*Cav-3<sup>-/-</sup>*). We incubated CM with methyl- $\beta$ -cyclodextrin (M $\beta$ CD) or colchicine to disrupt caveolae formation, and then exposed the myocytes to the volatile anesthetic isoflurane (30 min, 1.4%), followed by simulated ischemia/reperfusion (SI/R). Isoflurane protected CM from SI/R [23.2 $\pm$ 1.6% vs. 71.0 $\pm$ 5.8% cell death (assessed by trypan blue exclusion),  $P$ <0.001] but this protection was abolished by M $\beta$ CD or colchicine (84.9 $\pm$ 5.5% and 64.5 $\pm$ 6.1% cell death,  $P$ <0.001). Membrane fractionation by sucrose density gradient centrifugation of CM treated with M $\beta$ CD or colchicine revealed that buoyant (caveolae-enriched) fractions had decreased phosphocaveolin-1 and caveolin-3 compared to control CM. Cardiac protection *in vivo* was assessed by measurement of infarct size relative to the area at risk and cardiac troponin levels. Isoflurane-induced a reduction in infarct size and cardiac troponin relative to control (infarct size: 26.5% $\pm$ 2.6% vs. 45.3% $\pm$ 5.4%,  $P$ <0.01; troponin: 27.7 $\pm$ 4.4 vs. 77.7 $\pm$ 11.8 ng/mL,  $P$ <0.05). Isoflurane induced cardiac protection was abolished in *Cav-3<sup>-/-</sup>* mice (infarct size: 53.4% $\pm$ 6.1% vs. 53.2% $\pm$ 3.5%,  $P$ <0.01; troponin: 102.1 $\pm$ 22.3 vs. 105.9 $\pm$ 8.2 ng/mL,  $P$ <0.01). Isoflurane-induced cardiac protection is thus dependent on the presence of caveolae and the expression of caveolin-3. We conclude that caveolae and caveolin-3 are critical for volatile anesthetic-induced protection of the heart from ischemia/reperfusion injury.**

### 3.2 Introduction

Protection of the heart from ischemia/reperfusion injury can be induced by multiple stimuli (e.g., ischemia (1), opioids (2) and volatile anesthetics (3, 4)). Though many volatile anesthetics, including isoflurane (3, 4), sevoflurane (5, 6), and desflurane (6) show cardiac protection *in vivo*, the precise mechanism for volatile anesthetic-induced cardiac protection has not been elucidated.

Caveolae are small (~100nm diameter), flask-like invaginations (7) of the

plasma membrane that are enriched in particular lipids [e.g., cholesterol and glycosphingolipids (8)] and structural proteins, caveolins. There are three known isoforms of caveolin: caveolin-1, caveolin-2 and caveolin-3 (9), each of which has scaffolding domains that interact with signaling molecules (10, 11). Cardiac myocytes (CM) express the muscle-specific isoform caveolin-3 (12) while other cell types in the heart express caveolin-1 and -2. Recent studies have shown: 1) the presence and interaction of all three caveolin isoforms in adult cardiac myocytes (13, 14), 2) a signaling role for caveolin-1 in cardiac myocytes (15), and 3) that caveolins can scaffold proteins associated with cardiac protection (16, 17).

Caveolae can be disrupted using agents such as methyl- $\beta$ -cyclodextrin (M $\beta$ CD), which depletes membrane cholesterol (18, 19), or colchicine, which disrupts microtubules (20). Colchicine can abolish anesthetic-induced cardiac protection *in vivo* (21) although the molecular mechanism for this effect is not known. We have recently shown that M $\beta$ CD can disrupt caveolae and attenuate ischemic- and opioid-induced cardiac myocyte protection (19) but the role of caveolae expression and caveolin-3 in volatile anesthetic-induced cardiac protection is not known. Therefore, in the current study we used both *in vitro* and *in vivo* approaches to test the hypothesis that caveolae and the expression of caveolin-3 are essential for volatile anesthetic (e.g., isoflurane)-induced cardiac protection from ischemia/reperfusion injury. Our findings establish that caveolins and caveolae help mediate the action of a wide range of cardiac protective agents.

## Materials and Methods

Please see *Chapter 2* for detailed materials and methods.

### 3.3 Results

#### *Isoflurane induces cardiac protection in adult CM*

Adult CM were exposed to various concentrations of isoflurane and then to simulated ischemia/reperfusion (SI/R) (Figure 3-2). Exposure to 0.7% and 1.4% isoflurane before SI/R decreased cell death when compared to SI/R alone ( $37.4 \pm 5.0\%$ , and  $23.2 \pm 1.6\%$  vs.  $71.0 \pm 5.8\%$  cell death, respectively). However, at higher concentrations of isoflurane (2.8%), cardiac protection was not observed ( $64.4 \pm 9.8\%$  cell death).

#### *M $\beta$ CD and colchicine abolish caveolae formation and alter caveolin expression*

Treatment of CM with M $\beta$ CD or colchicine reduced the expression of caveolae (Figure 3-3A). The amount of phosphorylated caveolin-1 was significantly reduced in buoyant caveolar fractions (BF, Fractions 4-6) following sucrose density fractionation of M $\beta$ CD- or colchicine-treated cells (Figure 3-3B). Expression of caveolin-3 in BF was significantly reduced in M $\beta$ CD-treated cells and to a lesser extent in colchicine-treated cells after incubation with isoflurane (Figure 3-3B). Expression of caveolin-3 in non-buoyant fractions (Fractions 9-12) was not significantly altered among the experimental groups (data not shown).

*MβCD and colchicine abolish isoflurane-induced cardiac protection*

CM were incubated with 1% BSA + 0.1% penicillin/streptomycin (Control) media or in control media along with MβCD (1 mM), or colchicine (30 μM) and then exposed to 1.4% isoflurane (Figure 3-4A). The protective effect of isoflurane was abolished in CM incubated with MβCD or colchicine ( $84.9 \pm 5.5\%$  and  $64.5 \pm 6.1\%$  cell death, respectively). We observed no significant increase in basal cell death with the various treatments (Figure 3-4B).

*Caveolin-3 is required for isoflurane-induced cardiac protection*

Electron micrographs of caveolin-3<sup>-/-</sup> mouse hearts revealed the absence of caveolae in cardiac myocyte sarcolemmal membranes (Figure 3-5A). The absence of caveolin-3 protein in the hearts of caveolin-3<sup>-/-</sup> mice was verified by Western immunoblot analysis; these mice had normal levels of caveolin-1 (Figure 3-5B). To assess the role of caveolin-3 in the protection from ischemia/reperfusion injury, we treated C57BL/6 mice or caveolin-3<sup>-/-</sup> mice with 1.4% isoflurane for 30 min, followed by 15 min washout and then exposed the mice to ischemia/reperfusion (Figure 3-5C). The ability of isoflurane to protect from ischemia/reperfusion injury was abolished in caveolin-3<sup>-/-</sup> mice compared to control animals [ $45.3 \pm 5.4\%$  and  $26.5 \pm 2.6\%$  infarct size/area at risk (AAR)] even though there was a similar AAR in both groups of animals (Figure 3-5D;  $53.2 \pm 3.5\%$  vs.  $53.4 \pm 6.1\%$  AAR). Cardiac troponin I levels were significantly attenuated by isoflurane treatment in wild-type mice compared to control mice subjected to ischemia/reperfusion ( $27.7 \pm 4.4$  and  $77.7 \pm 11.8$  ng/mL); however, isoflurane failed to reduce cardiac troponin I levels in caveolin-3<sup>-/-</sup> mice, a

level similar to control caveolin-3<sup>-/-</sup> mice was observed ( $102.1 \pm 22.3$  and  $105.9 \pm 8.2$  ng/mL).

### 3.4 Discussion

The current data show that the presence of caveolae and the expression of caveolin-3 in CM are essential for isoflurane-induced cardiac protection from ischemia/reperfusion (I/R) injury. Treatment with M $\beta$ CD and colchicine, agents that decrease the number of caveolae and the amount of phosphorylated caveolin-1, attenuated isoflurane-induced protection in CM exposed to SI/R. Consistent with these findings, caveolin-3 knockout mice devoid of CM caveolae lack isoflurane-induced cardiac protection from I/R injury.

Volatile anesthetics are short chain halogenated alkanes and ethers that interact with cell membrane lipids and are thought to interact with membrane-bound proteins to produce cellular effects (22). Volatile anesthetics produce cardiac protection in a number of species, including man (5). It is not clear whether volatile anesthetics act via specific receptors or via “nonspecific” membrane effects to alter effector molecules that mediate cardiac protection. Isoflurane administration can activate opioid and adenosine receptors and blockade of these G-protein-coupled receptors can abolish cardiac protection produced by isoflurane (23). Volatile anesthetics affect several signaling pathways implicated in preconditioning, including Src tyrosine kinase, the phosphatidylinositol-3-kinase/protein kinase B/glycogen synthase kinase 3 beta pathway (24), protein kinase C (25, 26), and mitogen-activated protein kinases (MAPK), including extracellular signal-regulated kinase 1 and 2 (27) and p38 MAPK

(28). In addition, volatile anesthetics modulate ATP-sensitive potassium channel activity (25, 26), the generation of reactive oxygen species, and mitochondrial permeability transition pore opening (29). Of note, many of those signaling molecules and effector systems can either interact directly with the scaffolding domain of caveolin or are known to localize to caveolae (16, 17, 30).

Caveolae and caveolins organize signaling molecules and facilitate rapid, precise and coordinated signal transduction (31, 32). Isoflurane increases the phosphorylation of Src kinase and caveolin-1 is required for isoflurane-induced cardiac protection (15); isoflurane increases the phosphorylation of caveolin-1 in a Src-dependent manner and caveolin-1 knockout mice are not able to be protected from myocardial ischemia/reperfusion injury by isoflurane. Importantly, myocytes isolated from these animals have normal caveolae (unpublished observations). The current results confirm and extend those findings by showing that two different pharmacological approaches that disrupt caveolae and reduce caveolin-1 phosphorylation also attenuate isoflurane-induced protection of CM. In addition, the current data involving the use of caveolin-3<sup>-/-</sup> mice define a requirement for caveolin-3 in isoflurane-induced cardiac protection.

Caveolin-3, the predominant isoform in CM, mediates interactions with cytoskeletal elements (including  $\alpha$ -tubulin and filamin (14)) and is responsible for caveolae formation in these cells. A role for caveolin-3 in cardiac protection has not been investigated. Previous studies have shown that caveolin-3 overexpression prevents cardiac hypertrophy in isolated neonatal myocytes and may be beneficial in preventing pathological cardiac remodeling via the inhibition of Erk signaling (33).

Caveolin-3 co-localizes with opioid receptors, which can contribute to cardiac protection from ischemia (19). The current data indicate that a decreased number of myocardial caveolae are found in caveolin-3<sup>-/-</sup> mice even though caveolin-1 expression is normal and that such mice lose the ability to undergo isoflurane-induced cardiac protection from ischemia/reperfusion injury. Collectively, these and previous data implicate a role for both caveolin-1 and -3 and the presence of caveolae in cardiac protection from ischemia/reperfusion injury.

Our results showing the absence of cardiac protection at higher concentrations of isoflurane (2.8%) are in contrast to past studies in a dog model *in vivo* (34) and in an adult rat CM *in vitro* (35) in which a concentration-dependent increase in cardiac protection was observed with isoflurane. However, Kehl et al (34), who examined the cardiac protective effects of isoflurane in an *in vivo* dog model, only used a maximum concentration of isoflurane of 1.6%. Although Zaugg, et al (35), showed increased cardiac protection at 2.8% isoflurane compared to lower concentrations, those studies utilized different methods of isoflurane delivery (bubbling) and simulated ischemia (mineral oil layering), and did not investigate simulated reperfusion injury, which is believed to be a major contributor to cell death following myocardial ischemia (36).

Based on the current results, we conclude that caveolae and caveolin-3 are essential for the protection of the heart from ischemia/reperfusion injury and in particular, for volatile anesthetic-induced cardiac protection. The results thus suggest that treatments designed to enhance expression of caveolins and caveolae in CM have the potential to prevent ischemic damage in the heart and perhaps other tissues.

### 3.5 Acknowledgements

The studies conducted were supported by: American Heart Association Predoctoral Fellowship 06150217Y(YTH), American Heart Association Scientist Development Grant 060039N (HHP), American Heart Association Scientist Beginning Grant-in-Aid 0765076Y (YMT), Merit Award from the Department of Veterans Affairs (DMR), and NIHHL081400 (DMR), and HL66941 (DMR, PAI)

Chapter 3, in full, is a reprint of the material as it appears in *Journal of Molecular and Cellular Cardiology* 2008. Horikawa, Y; Patel, H; Tsutsumi, Y; Jennings, M; Kidd, M; Hagiwara, Y; Ishikawa, Y; Insel, P; and Roth, D, Elsevier Journals, 2008. The dissertation author was the primary investigator and author for this manuscript.

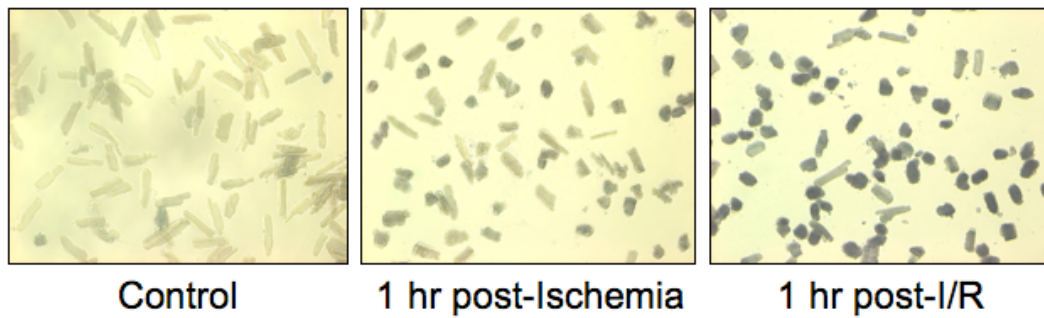


**Figure 3-1:** Simulated ischemia/reperfusion (I/R) model. Adult cardiac myocytes were rod-shaped and viable with oxygen exposure alone. Cell death increased with ischemia, however, maximal cell death was observed following reperfusion.

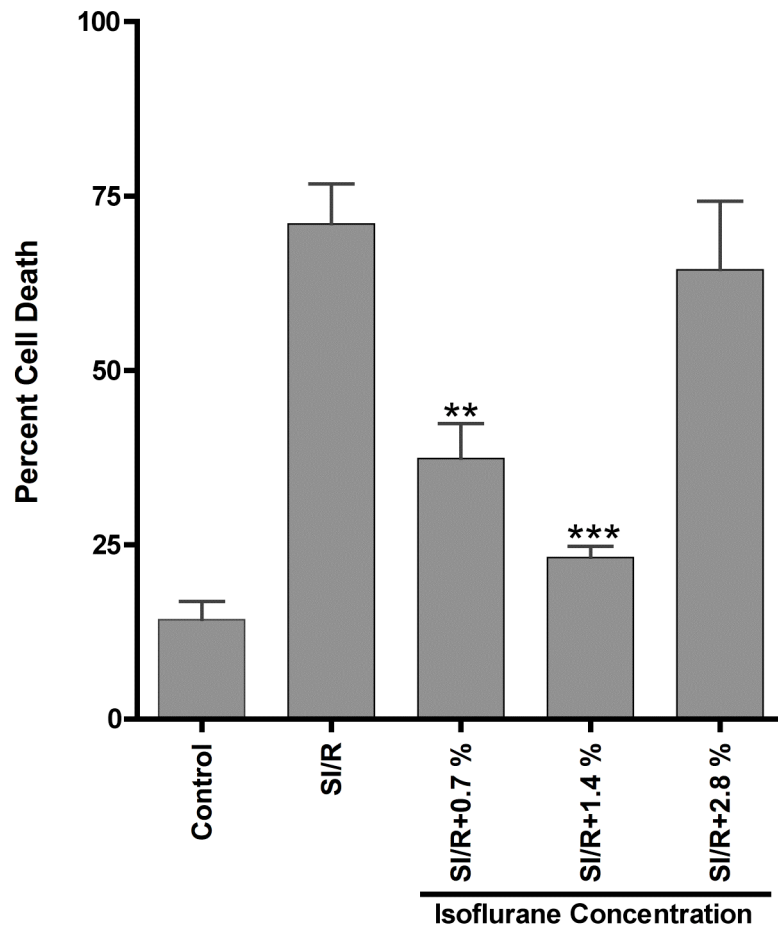


**Figure 3-2:** Effect of isoflurane on simulated ischemia/reperfusion (SI/R) of adult cardiac myocytes (CM). CM were plated and treated with various concentrations of isoflurane prior to exposure to SI/R. Cell death was determined by trypan blue staining. CM under control conditions had minimal cell death. Optimal protection was observed at 1.4% isoflurane. No protection was observed at 2.8%.  $n = 6$  for all groups. \*\*  $P < 0.01$  compared to SI/R, \*\*\*  $P < 0.001$  compared to SI/R..

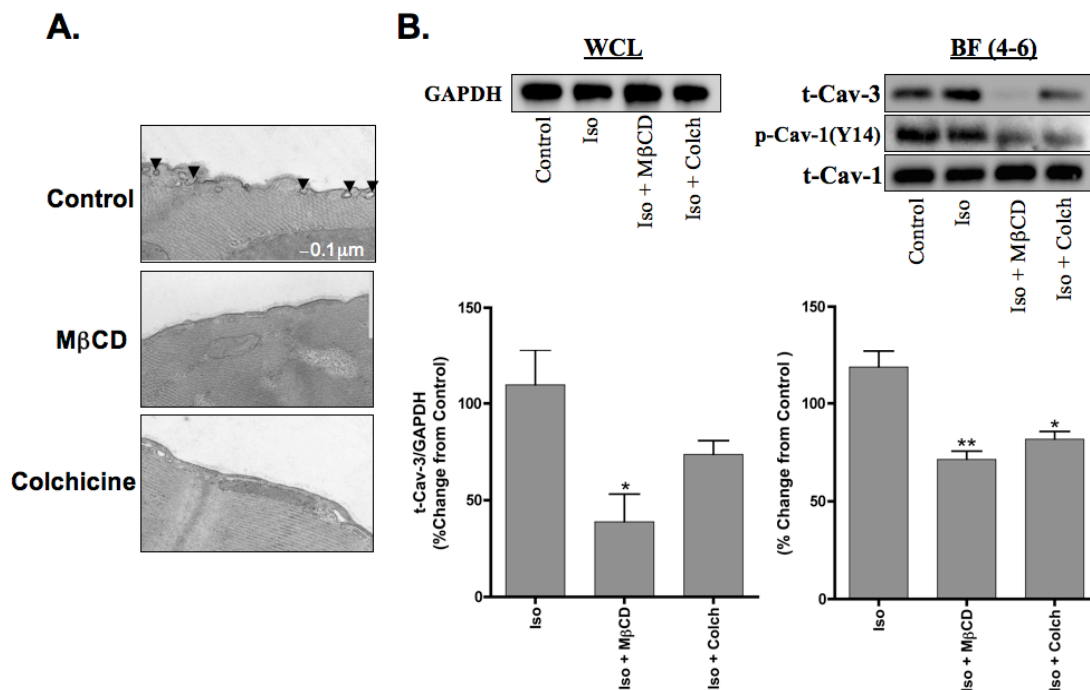


**Figure 3-3:** Impact of MβCD and colchicine on expression by cardiac myocytes (CM) of caveolae, caveolin-3 and phosphocaveolin-1 and on response to isoflurane. A. Electron micrographs of CM reveal caveolae at the surface of the plasma membrane in cells under control conditions (black arrows). MβCD- and colchicine-treated myocytes have no visible caveolae  $n = 2$  per group (magnification = 11,500x). B. Whole cell lysates (WCL) were normalized via expression of GAPDH prior to sucrose density fractionation. Sucrose gradient fractions of 1.4% isoflurane (Iso) exposed CM revealed decreased expression of pCaveolin-1 (p-Cav-1 Y14) and Caveolin-3 (t-Cav-3) in the buoyant fraction (BF = fractions 4-6) of MβCD- and colchicine (Colch)-treated cells. Densitometry revealed a significant decrease in p-Cav-1 Y14 in both MβCD- and colchicine-treated groups, whereas t-Cav-3 expression was only significantly decreased in the MβCD group.  $n = 3$  per group. \*  $P < 0.05$  compared to Iso, \*\*  $P < 0.01$  compared to Iso.

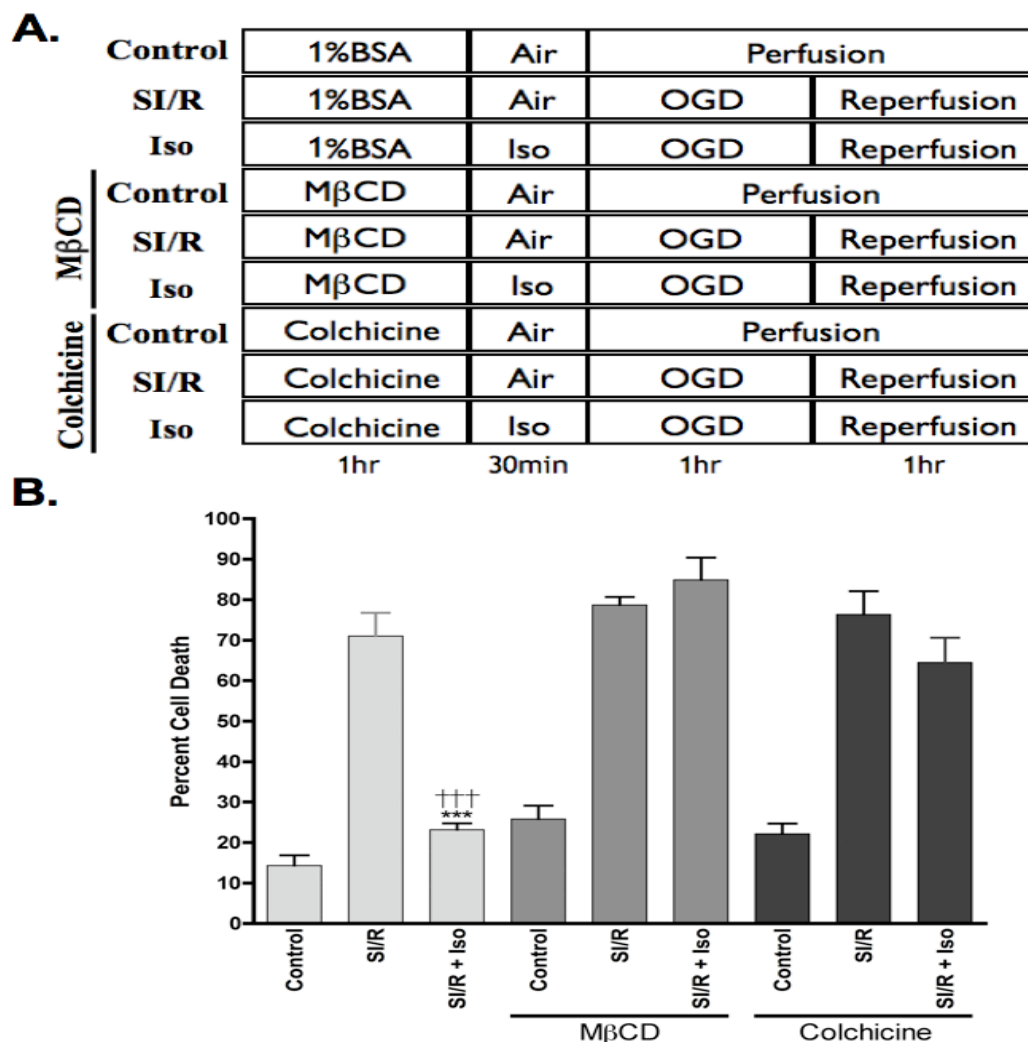
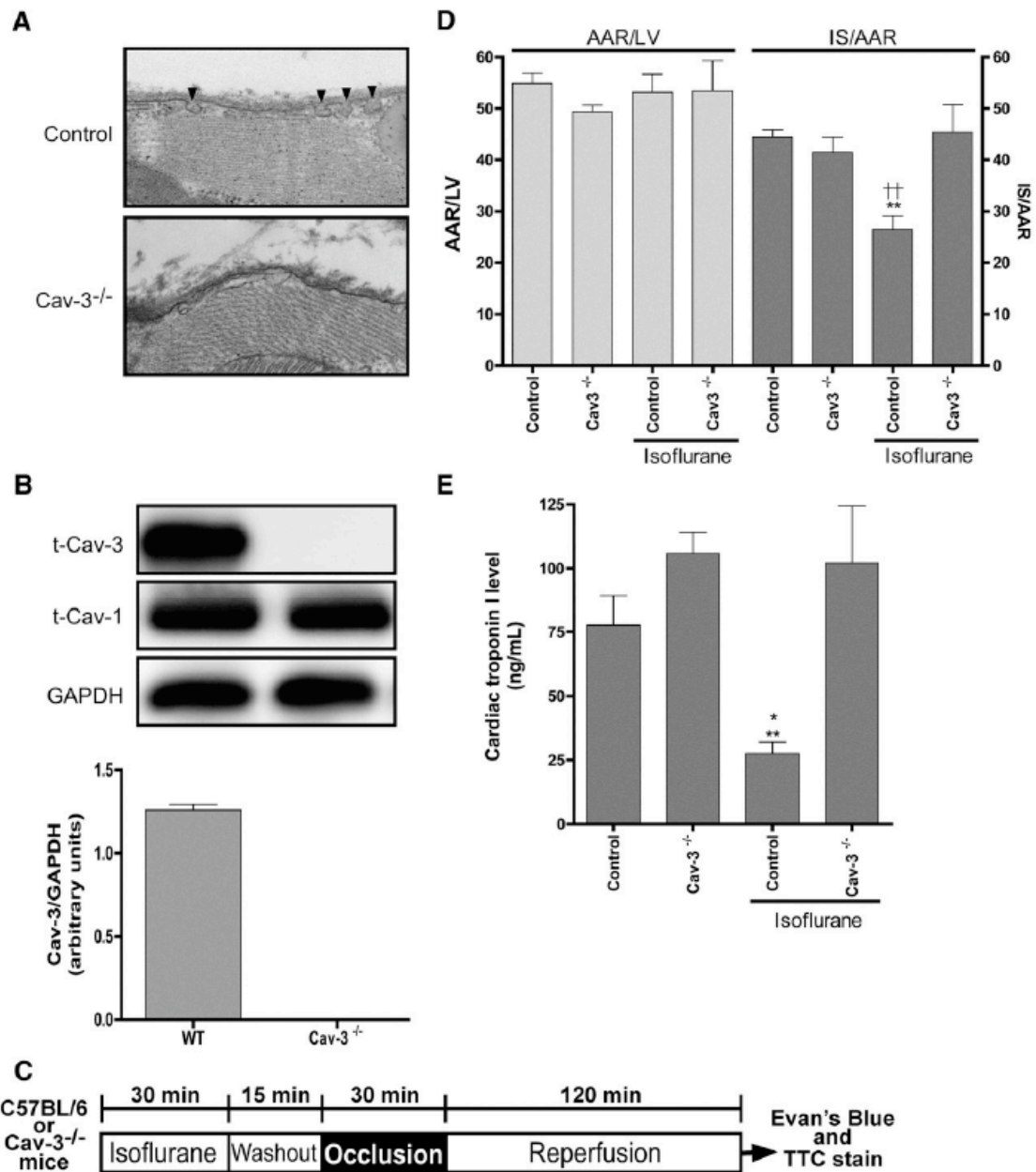


**Figure 3-4:** Cardiac protection by isoflurane in the presence and absence of caveolae disruption. A. Cardiac myocytes were exposed to control conditions, simulated ischemia/reperfusion (SI/R), or SI/R + isoflurane (Iso) in the presence or absence of M $\beta$ CD and colchicine. M $\beta$ CD- and colchicine (Colch)-treated groups were incubated with M $\beta$ CD (1 mM) or Colch (30  $\mu$ M) in maintenance media (1% BSA) for 1 hr, the latter of which was used for control cells. Cells were then incubated with air or 1.4% isoflurane for 30 min. SI/R was then produced by aerating a metabolic chamber with 95% N<sub>2</sub> + 5% CO<sub>2</sub> and changing to glucose-free media, which results in oxygen and glucose deprivation (OGD). This incubation was then followed by “reperfusion” by placement of cells in normal maintenance media at 21% O<sub>2</sub> and 5% CO<sub>2</sub> for 1 hr. All experiments were performed at 37°C. B. Isoflurane-induced cardiac protection was diminished in the presence of M $\beta$ CD or Colch. n = 6 in all groups. \*\*\*  $P < 0.001$  compared to SI/R + Iso + M $\beta$ CD, †††  $P < 0.001$  compared to SI/R + Iso + Colchicine.

**Figure 3-5:** Absence of isoflurane-induced cardiac protection in caveolin-3 knockout mice. A. Electron micrographs of cardiac tissue from caveolin-3 knockout ( $Cav-3^{-/-}$ ) mice reveal an absence of caveolae in the sarcolemmal membrane (8,900x). B. Western blot analysis confirmed the absence of caveolin-3 protein in the hearts of the  $Cav-3^{-/-}$  mice but with similar levels of caveolin-1 ( $Cav-1$ ),  $n = 6$  in all groups. C. *In vivo* anesthetic (isoflurane)-induced cardiac protection protocol. D. Isoflurane-induced cardiac protection was abolished in  $Cav-3^{-/-}$  mice, as shown by no significant decrease in infarct size (IS)/area at risk (AAR) when compared to control  $Cav-3^{-/-}$ ; however, a significant decrease in IS was noted between Control + Isoflurane vs. Control and  $Cav-3^{-/-}$  + Isoflurane,  $n = 6$  in all groups. \*\*  $P < 0.01$  compared to Control. ††  $P < 0.01$  compared to  $Cav-3^{-/-}$  + Isoflurane. E. Following ischemia/reperfusion injury cardiac troponin I levels in  $Cav-3^{-/-}$  mice were elevated when compared to control. In addition, no significant decrease in troponin I levels were observed in  $Cav-3^{-/-}$  mice following isoflurane-induced cardiac protection, whereas, a significant decrease was noted in control mice that received isoflurane. Troponin I was also decreased in Control + Isoflurane vs.  $Cav-3^{-/-}$  + Isoflurane,  $n = 4-6$  for all groups. \*  $P < 0.05$  compared to Control, \*\*  $P < 0.01$  compared to  $Cav-3^{-/-}$  + Isoflurane.



### 3.6 References

1. Murry, C.E., Jennings, R.B., and Reimer, K.A. 1986. Preconditioning with ischemia: a delay of lethal cell injury in ischemic myocardium. *Circulation* 74:1124-1136.
2. Schultz, J.E., Hsu, A.K., and Gross, G.J. 1996. Morphine mimics the cardioprotective effect of ischemic preconditioning via a glibenclamide-sensitive mechanism in the rat heart. *Circ Res* 78:1100-1104.
3. Cason, B.A., Gamperl, A.K., Slocum, R.E., and Hickey, R.F. 1997. Anesthetic-induced preconditioning: previous administration of isoflurane decreases myocardial infarct size in rabbits. *Anesthesiology* 87:1182-1190.
4. Kersten, J.R., Schmeling, T.J., Pagel, P.S., Gross, G.J., and Warltier, D.C. 1997. Isoflurane mimics ischemic preconditioning via activation of K(ATP) channels: reduction of myocardial infarct size with an acute memory phase. *Anesthesiology* 87:361-370.
5. Obal, D., Preckel, B., Scharbatke, H., Mullenheim, J., Hoterkes, F., Thamer, V., and Schlack, W. 2001. One MAC of sevoflurane provides protection against reperfusion injury in the rat heart in vivo. *Br J Anaesth* 87:905-911.
6. Preckel, B., Thamer, V., and Schlack, W. 1999. Beneficial effects of sevoflurane and desflurane against myocardial reperfusion injury after cardioplegic arrest. *Can J Anaesth* 46:1076-1081.
7. Palade, G. 1953. Fine structure of blood capillaries. *J Appl Physiol* 24:1424-1436.
8. Kurzchalia, T.V., and Parton, R.G. 1999. Membrane microdomains and caveolae. *Curr Opin Cell Biol* 11:424-431.
9. Williams, T.M., and Lisanti, M.P. 2004. The Caveolin genes: from cell biology to medicine. *Ann Med* 36:584-595.
10. Lisanti, M.P., Scherer, P.E., Tang, Z., and Sargiacomo, M. 1994. Caveolae, caveolin and caveolin-rich membrane domains: a signalling hypothesis. *Trends Cell Biol* 4:231-235.
11. Okamoto, T., Schlegel, A., Scherer, P.E., and Lisanti, M.P. 1998. Caveolins, a family of scaffolding proteins for organizing "preassembled signaling complexes" at the plasma membrane. *J Biol Chem* 273:5419-5422.

12. Song, K.S., Li, S., Okamoto, T., Quilliam, L.A., Sargiacomo, M., and Lisanti, M.P. 1996. Co-purification and direct interaction of Ras with caveolin, an integral membrane protein of caveolae microdomains. Detergent-free purification of caveolae microdomains. *J Biol Chem* 271:9690-9697.
13. Hagiwara, Y., Nishina, Y., Yorifuji, H., and Kikuchi, T. 2002. Immunolocalization of caveolin-1 and caveolin-3 in monkey skeletal, cardiac and uterine smooth muscles. *Cell Struct Funct* 27:375-382.
14. Head, B.P., Patel, H.H., Roth, D.M., Murray, F., Swaney, J.S., Niesman, I.R., Farquhar, M.G., and Insel, P.A. 2006. Microtubules and actin microfilaments regulate lipid raft/caveolae localization of adenylyl cyclase signaling components. *J Biol Chem* 281:26391-26399.
15. Patel, H.H., Tsutsumi, Y.M., Head, B.P., Niesman, I.R., Jennings, M., Horikawa, Y., Huang, D., Moreno, A.L., Patel, P.M., Insel, P.A., et al. 2007. Mechanisms of cardiac protection from ischemia/reperfusion injury: a role for caveolae and caveolin-1. *FASEB J* 21:1565-1574.
16. Krajewska, W.M., and Maslowska, I. 2004. Caveolins: structure and function in signal transduction. *Cell Mol Biol Lett* 9:195-220.
17. Siracusano, L., Girasole, V., Alvaro, S., and Chiavarino, N.D. 2006. Myocardial preconditioning and cardioprotection by volatile anaesthetics. *J Cardiovasc Med (Hagerstown)* 7:86-95.
18. Furuchi, T., and Anderson, R.G. 1998. Cholesterol depletion of caveolae causes hyperactivation of extracellular signal-related kinase (ERK). *J Biol Chem* 273:21099-21104.
19. Patel, H.H., Head, B.P., Petersen, H.N., Niesman, I.R., Huang, D., Gross, G.J., Insel, P.A., and Roth, D.M. 2006. Protection of adult rat cardiac myocytes from ischemic cell death: role of caveolar microdomains and delta-opioid receptors. *Am J Physiol Heart Circ Physiol* 291:H344-350.
20. Goldman, R.D. 1971. The role of three cytoplasmic fibers in BHK-21 cell motility. I. Microtubules and the effects of colchicine. *J Cell Biol* 51:752-762.
21. Ismaeil, M.S., Tkachenko, I., Hickey, R.F., and Cason, B.A. 1999. Colchicine inhibits isoflurane-induced preconditioning. *Anesthesiology* 91:1816-1822.
22. Keil, R.L., Wolfe, D., Reiner, T., Peterson, C.J., and Riley, J.L. 1996. Molecular genetic analysis of volatile-anesthetic action. *Mol Cell Biol* 16:3446-3453.

23. Toller, W.G., Kersten, J.R., Gross, E.R., Pagel, P.S., and Warltier, D.C. 2000. Isoflurane preconditions myocardium against infarction via activation of inhibitory guanine nucleotide binding proteins. *Anesthesiology* 92:1400-1407.
24. Feng, J., Fischer, G., Lucchinetti, E., Zhu, M., Bestmann, L., Jegger, D., Arras, M., Pasch, T., Perriard, J.C., Schaub, M.C., et al. 2006. Infarct-remodeled myocardium is receptive to protection by isoflurane postconditioning: role of protein kinase B/Akt signaling. *Anesthesiology* 104:1004-1014.
25. Marinovic, J., Bosnjak, Z.J., and Stadnicka, A. 2005. Preconditioning by isoflurane induces lasting sensitization of the cardiac sarcolemmal adenosine triphosphate-sensitive potassium channel by a protein kinase C-delta-mediated mechanism. *Anesthesiology* 103:540-547.
26. Ludwig, L.M., Weihrauch, D., Kersten, J.R., Pagel, P.S., and Warltier, D.C. 2004. Protein kinase C translocation and Src protein tyrosine kinase activation mediate isoflurane-induced preconditioning in vivo: potential downstream targets of mitochondrial adenosine triphosphate-sensitive potassium channels and reactive oxygen species. *Anesthesiology* 100:532-539.
27. Toma, O., Weber, N.C., Wolter, J.I., Obal, D., Preckel, B., and Schlack, W. 2004. Desflurane preconditioning induces time-dependent activation of protein kinase C epsilon and extracellular signal-regulated kinase 1 and 2 in the rat heart in vivo. *Anesthesiology* 101:1372-1380.
28. da Silva, R., Grampp, T., Pasch, T., Schaub, M.C., and Zaugg, M. 2004. Differential activation of mitogen-activated protein kinases in ischemic and anesthetic preconditioning. *Anesthesiology* 100:59-69.
29. Krolkowski, J.G., Bienengraeber, M., Weihrauch, D., Warltier, D.C., Kersten, J.R., and Pagel, P.S. 2005. Inhibition of mitochondrial permeability transition enhances isoflurane-induced cardioprotection during early reperfusion: the role of mitochondrial KATP channels. *Anesth Analg* 101:1590-1596.
30. Hausenloy, D.J., and Yellon, D.M. 2006. Survival kinases in ischemic preconditioning and postconditioning. *Cardiovasc Res* 70:240-253.
31. Shaul, P.W., and Anderson, R.G. 1998. Role of plasmalemmal caveolae in signal transduction. *Am J Physiol* 275:L843-851.
32. Ostrom, R.S., and Insel, P.A. 2004. The evolving role of lipid rafts and caveolae in G protein-coupled receptor signaling: implications for molecular pharmacology. *Br J Pharmacol* 143:235-245.

33. Koga, A., Oka, N., Kikuchi, T., Miyazaki, H., Kato, S., and Imaizumi, T. 2003. Adenovirus-mediated overexpression of caveolin-3 inhibits rat cardiomyocyte hypertrophy. *Hypertension* 42:213-219.
34. Kehl, F., Krolikowski, J.G., Mraovic, B., Pagel, P.S., Warltier, D.C., and Kersten, J.R. 2002. Is isoflurane-induced preconditioning dose related? *Anesthesiology* 96:675-680.
35. Zaugg, M., Lucchinetti, E., Spahn, D.R., Pasch, T., and Schaub, M.C. 2002. Volatile anesthetics mimic cardiac preconditioning by priming the activation of mitochondrial K(ATP) channels via multiple signaling pathways. *Anesthesiology* 97:4-14.
36. Gross, G.J., and Auchampach, J.A. 2007. Reperfusion injury: does it exist? *J Mol Cell Cardiol* 42:12-18.

## **Chapter 4:**

# **Cardiac-specific overexpression of caveolin-3 induces endogenous cardiac protection by mimicking ischemic preconditioning**

## 4.1 Abstract

**Background:** Caveolae, lipid-rich microdomains of the sarcolemma, localize and enrich cardiac protective signaling molecules. Caveolin-3 (Cav-3), the dominant isoform in cardiac myocytes, is a determinant of caveolae formation. We hypothesized that cardiac-specific overexpression of Cav-3 would enhance the formation of caveolae and augment cardiac protection *in vivo*.

**Methods and Results:** Ischemic preconditioning (IPC) *in vivo* increased formation of caveolae. Adenovirus for Cav-3 increased caveolar formation and phosphorylation of survival kinases in cardiac myocytes. A transgenic (TG) mouse with cardiac myocyte-specific overexpression of Cav-3 (Cav-3 OE) showed enhanced formation of caveolae on the sarcolemma. Cav-3 OE mice subjected to ischemia/reperfusion injury had a significantly reduced infarct size relative to TG<sub>neg</sub> mice. Endogenous cardiac protection in Cav-3 OE mice was similar to wild-type mice undergoing IPC; no increased protection was observed in preconditioned Cav-3 OE mice. Cav-3 knockout mice did not show endogenous protection and showed no protection in response to IPC. Cav-3 OE mouse hearts had increased basal Akt and GSK3 $\beta$  phosphorylation comparable to wild-time mice exposed to IPC. Wortmannin, a PI3K inhibitor, attenuated basal phosphorylation of Akt and GSK3 $\beta$  and blocked the endogenous cardiac protection in Cav-3 OE mice. Cav-3 OE mice had improved functional recovery and reduced apoptosis at 24 hours of reperfusion.

**Conclusion:** Expression of caveolae is both necessary and sufficient for cardiac protection, a conclusion that unites long-standing ultrastructural and molecular observations in the ischemic heart. The current results indicate that increased expression of caveolins has the potential to preserve tissue in the heart exposed to ischemia-reperfusion injury.

## 4.2 Introduction

The concept that an organ can develop tolerance to subsequent ischemic stress was initially suggested by studies of traumatic injury.(1) In 1986, Murry *et al*(2) found that non-lethal injury, termed ischemic preconditioning (IPC), could protect the heart from lethal injury. Subsequent work has shown that IPC is a highly effective way to protect multiple organs from ischemic injury. Many studies have evaluated individual signaling molecules and pathways in IPC(3) but no single, unifying intervention explains the temporal efficiency (*i.e.*, rapid coupling of plasma membrane to

intracellular signaling) and spatial 3-dimensionality (*i.e.*, simultaneous activation of numerous parallel pathways) of IPC. An emerging idea in signal transduction emphasizes the role of multi-protein complexes organized in discrete microenvironments in cell regulation and pathophysiology;(4, 5) such organization perhaps might explain the temporal/spatial conundrum of IPC.

Caveolae, cholesterol- and sphingolipid-enriched invaginations of the plasma membrane, a subset of lipid/membrane rafts, are one such microenvironment.(6-8) Caveolins, structural proteins essential for caveolae formation, are present in three isoforms:(9) caveolin-1 and -2 (Cav-1 and -2) are expressed in multiple cell types, while caveolin-3 (Cav-3) is found primarily in striated (skeletal and cardiac) muscle and certain smooth muscle cells.(10) Caveolins have scaffolding domains that anchor and regulate the function of proteins that modulate a variety of cellular processes(11) and signal transduction.(4, 5) Caveolins can function as scaffolds for multiple, interacting signaling molecules, thereby providing temporal and spatial regulation of cellular signal transduction.(5)

Disruption of caveolae attenuates protection of adult cardiac myocytes from ischemic damage(12) and Cav-3 knockout mice (Cav-3 KO), which lack cardiac myocyte caveolae, are resistant to pharmacological preconditioning.(13) Such findings imply that myocyte caveolae are a prerequisite for protection from ischemia-reperfusion injury. Because Cav-3 expression is essential for the formation of caveolae in cardiac myocytes,(14) we hypothesized and provide evidence that cardiac myocyte-specific overexpression of Cav-3 increases the formation of caveolae and enhances

protective signaling from ischemia, thus identifying cell-specific expression of caveolins and caveolae as a novel approach to achieve such protection.

### **4.3 Results**

#### **Ischemic preconditioning modulates membrane caveolae and Cav-3 expression.**

We assessed the effect of IPC on cardiac membrane caveolae by subjecting mice to IPC and performing electron microscopy (EM). Representative EM images show that IPC increases formation of caveolae (arrows in **Fig. 4-1A**). To verify these morphologic findings using biochemical techniques, hearts from IPC and control animals were fractionated on a discontinuous sucrose gradient and analyzed for protein and cholesterol content and for distribution of caveolin. IPC increases the total protein and cholesterol content in fractions 4-6 (buoyant fractions), which are enriched in caveolin(15) (**Fig. 4-1B,C**) and increases the amount of Cav-3, but not Cav-1, in buoyant fractions (**Fig. 4-1D,E**). These findings are consistent with evidence that formation of cardiac myocyte caveolae is dependent on Cav-3.(14, 16)

#### **Adenoviral overexpression of Cav-3 in adult cardiac myocytes *in vitro* increases caveolae formation and phosphorylation of survival kinases.**

Cardiac myocytes incubated with a Cav-3-adenovirus have increased expression of caveolae (**Fig. 4-2A**) and increased levels of phosphorylated protein kinase B (Akt) and glycogen synthase kinase 3 $\beta$  (GSK3 $\beta$ ), two enzymes associated with IPC-induced cardiac protection(3) (**Fig. 4-2B**).

**Cardiac myocyte-specific Cav-3 overexpressing mice have increased myocyte caveolae but unaltered nitric oxide synthase (NOS) expression and activity.**

Using an  $\alpha$ -myosin heavy chain promoter, we generated mice with cardiac myocyte-specific overexpression of Cav-3 (**Supplementary Fig. 4-1A**). Thirty-nine mouse lines were generated, 5 of which were positive for the transgene (TG)

(**Supplementary Fig. 4-1B**). Two of these 5 lines were propagated, one of which had an 8-fold elevation in Cav-3 mRNA expression compared to TG-negative (TG<sub>neg</sub>) animals (**Fig. 4-3A**). We developed and characterized this line and refer to it as the Cav-3 overexpressor (Cav-3 OE). Cav-3 OE mice have increased Cav-3 protein expression without a change in Cav-1 and Cav-2 expression (**Fig. 4-3B**). The increased protein expression in the Cav-3 OE mice localizes to cardiac myocyte membranes (red pixels, **Fig. 4-3C**) and results in an increased number of caveolae in cardiac myocytes (**Fig. 4-3D**); increased expression of Cav-3 was not observed in lung, brain, liver, kidney or skeletal muscle of these mice (data not shown).

Because caveolins negatively regulate activity of NOS isoforms,(11, 17) we quantitated basal NOS expression and activity in the Cav-3 OE mice. Given the well-known interaction of NOS with caveolins, we were surprised to find similar expression of NOS and phosphorylated endothelial NOS (eNOS) isoforms and similar NOS activity in the whole hearts of TG<sub>neg</sub> and Cav-3 OE mice (**Fig. 4-4A,B**). To determine if compartmented activity of NOS may be altered by cardiac specific caveolin-3 expression, we subjected TG<sub>neg</sub> and Cav-3 OE hearts to sucrose density fractionation and probed NOS activity in buoyant (BF, caveolae rich) and non-buoyant (non-BF, non-caveolar) fractions using a <sup>3</sup>H-arginine assay. No difference in NOS

activity was observed in BF and non-BF in TG<sub>neg</sub> vs. Cav-3 OE (**Fig. 4-4C**). Rat cerebellum homogenate was used as a positive control (<sup>3</sup>H-citrulline, 42000 CPM/ $\mu$ l sample).

### **Cav-3 OE mice are protected from ischemia-reperfusion injury.**

Cav-3 OE mice exposed to 30 min of cardiac ischemia and 2 h of reperfusion have a substantial reduction in infarct size compared to TG<sub>neg</sub> mice ( $23.4 \pm 3.0\%$  vs.  $43.0 \pm 3.9\%$  risk area,  $n = 11$ ,  $P < 0.001$ , **Fig. 4-5A**), even though these mice show no differences in pre-occlusion hemodynamics (heart rate, mean arterial pressure, and rate-pressure product; **Supplementary Table 1**) or in the cardiac area at risk (AAR) for ischemic damage (**Supplementary Fig. 2**). This “endogenous protection” in Cav-3 OE mice is similar to that produced in TG<sub>neg</sub> mice subjected to IPC ( $26.3 \pm 2.4\%$  risk area,  $n = 8$   $P < 0.05$ ) and was not enhanced by IPC ( $21.1 \pm 2.8\%$  risk area,  $n = 8$ ) but was attenuated by pretreatment with 5-HD, a mitochondrial ATP-sensitive potassium ( $K_{ATP}$ ) channel inhibitor ( $38.1 \pm 4.4\%$  risk area,  $n = 8$ ) (**Fig. 4-5A**). Akin to the results with 5-HD, IPC does not protect Cav-3 KO mice from ischemic damage (**Fig 4-5A**). Cardiac troponin I (cTnI) confirmed infarct size measurements (**Fig 4-5B**).

### **Role of survival kinases in endogenous protection.**

Hearts excised from Cav-3 OE mice had an ~3-fold increase in basal phosphorylation of Akt and in phosphorylation of GSK3 $\beta$  ( $P < 0.05$ ,  $n = 6$ , **Fig. 4-6A**), signaling molecules involved in cardiac protection.(18) The level of basal elevation in Akt and GSK3 $\beta$  in the hearts of Cav-3 OE mice were comparable to the elevation seen after

IPC *in vivo* (**Fig. 4-6A**). To determine the role of PI3K/Akt/GSK3 $\beta$  in this endogenous protection, Cav-3 OE mice were treated with wortmannin, a PI3K inhibitor, or DMSO (vehicle). Wortmannin reduced the endogenous phosphorylation of both Akt and GSK3 $\beta$ , which are activated by PI3K relative to vehicle control (**Fig. 4-6B**). Vehicle treated Cav-3 OE mice showed a cardiac protected phenotype as in Fig. 4-5A with reduced infarct size and cardiac troponin-I (**Fig. 4-6C,D**). Wortmannin attenuated the endogenous cardiac protection observed in Cav-3 OE mice (**Fig. 4-6C,D**)

**Cav-3 OE mice have preserved ultrastructure following ischemia-reperfusion injury.**

We also used EM analysis to examine the AAR after ischemia-reperfusion (30 min-2 h) in Cav-3 OE and TG<sub>neg</sub> mice (**Fig. 4-7**). Following injury, the ischemia-reperfusion TG<sub>neg</sub> groups displayed highly disorganized patterns of cardiac myocytes and their mitochondria. In addition, the sarcolemma exhibited evidence of damage, including disrupted Z-lines and myofibrillar stretching. Mitochondria were swollen and contained amorphous matrix densities, indicating that injury was in an irreversible phase(19) (**Fig. 4-7C**). By contrast, hearts of Cav-3 OE mice subjected to ischemia-reperfusion showed limited ultrastructural change relative to sham and in particular, no mitochondrial swelling, myofibril stretching, or Z-line deformation (**Figs. 4-7D**).

### **Cav-3 OE mice have preserved cardiac function and reduced apoptosis following ischemia-reperfusion.**

We assessed cardiac function of TG<sub>neg</sub> and Cav-3 OE mice during cardiac catheterization after 30 min ischemia and 24 h of reperfusion. Left ventricular systolic function ( $dP/dt$  max), was greater while cTnI levels were significantly lower in the Cav-3 OE mice (**Fig. 4-8A,B**).

Cav-3 OE mice also had reduced apoptosis, assayed by terminal deoxynucleotidyl transferase-mediated deoxyuridine triphosphate nick end labeling (TUNEL)-positive cells (arrows in **Fig 4-8C, left panel**), as the percent of total nuclei after 24 h of reperfusion (**Fig. 4-8C, right panel**). Hearts of Cav-3 OE animals also tended to have decreased pro-apoptotic and increased anti-apoptotic gene expression (**Fig. 4-8D**) and protein expression (**Fig. 4-8E**).

Total body overexpression of Cav-3 results in cardiomyopathy in 6 month old mice.(20) Accordingly, we assessed morphology, echocardiography and hemodynamics in 6-9 month old cardiac myocyte-specific Cav-3 OE mice. We found that heart weight to tibia length were similar in Cav-3 OE and age-matched TG<sub>neg</sub> mice (**Supplementary Table 2**). In addition, echocardiographic parameters, heart rate, mean arterial pressure and rate-pressure product were similar between Cav-3 OE and TG<sub>neg</sub> mice (**Supplementary Table 2**).

#### **4.4 Discussion**

Numerous mechanisms have been proposed to explain the ability of an organ to develop tolerance to subsequent lethal ischemia-reperfusion injury.(21) IPC, an

intervention that was first shown over 20 years ago to prevent such injury, has lacked a unifying hypothesis to account for the diverse pathways by which it impacts on the heart and other organs. We show here that IPC alters the morphology and function of the plasma membrane of cardiac myocytes, increasing the number of caveolae.

Moreover, we find that the protein Cav-3 is both necessary and sufficient to protect the heart from ischemia-reperfusion injury. Spatial organization of signaling molecules within caveolar microdomains and the interaction of signaling molecules with caveolins thus help determine the protection of the heart from ischemia-reperfusion injury. The current data imply that expression of Cav-3 and caveolae represent a unifying mechanism for IPC.

Caveolae were first identified by electron microscopy in the 1950's by Palade and Yamada(6, 7) in endothelium and epithelium, respectively, and in the sarcolemma of cardiac myocytes in 1975 by McNutt.(22) Early research on myocardial ischemia focused on ischemia-induced changes in the sarcolemma(23, 24) and provided evidence that caveolae in cardiac myocytes can be rapidly affected by perturbation of oxygen tension and tonicity.(25, 26) In spite of such results, a role for caveolae and caveolins in the setting of ischemic preconditioning has not been explored.

An emerging concept emphasizes the organization of signaling molecules in multiprotein complexes, "signalosomes," that form and dissociate under basal and stimulated conditions.(11) Caveolins play an integral role in the dynamics of these multiprotein complexes in caveolae, by interacting with a wide range of signaling molecules that include multiple G-protein coupled receptors,  $G\alpha$  subunits of heterotrimeric G-proteins, Src kinases, PI3K, eNOS, protein kinase C (PKC) isoforms,

extracellular signal-regulated kinase 1 and 2 (ERK 1/2), and superoxide dismutase. Many of these proteins can bind to the scaffolding domain of caveolin (CSD) and be regulated by caveolin.(27) A number of proteins that bind caveolin have been overexpressed in cardiac myocytes and shown to produce tolerance to myocardial ischemia-reperfusion injury; these include adenosine receptors,(28) alpha 1 adrenergic receptors,(29) PKC isoforms,(30) mitogen activated protein kinases,(31) eNOS,(32, 33) and proteins involved in the scavenging of free radicals.(34) Overexpression of heat shock proteins (HSP:  $\alpha$ B crystallin, HSP60-10 complex, and H11 kinase(35-37)) also confers protection from ischemic damage and conceivably caveolins contribute to such interactions.(38) *In silico* analysis of the protein sequence of  $\alpha$ B crystallin reveals a putative caveolin binding motif (aa167wvcyqypgy), suggesting future avenues of investigation.

Caveolar microdomains are enriched in cholesterol. We show that IPC increases caveolar microdomains and total cholesterol primarily in the buoyant fractions. The mechanism by which IPC increases total cholesterol is not known. Studies show that class B scavenger receptors (CD36) localize to caveolae and regulate cholesterol homeostasis.(39) Co-expression of CD36 and caveolin has been shown to enhance the uptake of cholesterol.(40) It is possible that the increase in cholesterol may drive caveolae formation or on the other hand an increase in caveolae formation may drive the influx of cholesterol. Defining this important distinction remains an interesting avenue for future investigations.

Of particular importance for ischemia is the evidence that Cav-3 is an activator of PI3K/Akt/ GSK3 $\beta$  signaling,(41) a pro-survival pathway that can contribute to

cardiac ischemic preconditioning.(3, 21) Such ideas are pertinent to the current data indicating that adenoviral Cav-3-mediated overexpression in myocytes and Cav-3 OE mice show increased Cav-3 expression, formation of caveolae and phosphorylation of Akt and GSK3 $\beta$ . In addition, our results show that mice engineered to overexpress Cav-3 in cardiac myocytes are protected from ischemia-reperfusion injury to an extent comparable to that induced by IPC and in a manner that depends on mitochondrial K<sub>ATP</sub> channel and PI3K activity, putative effectors of cardiac protection from ischemia-reperfusion injury.(21, 42) Cav-3 OE mice also showed a preserved sarcomeric ultrastructure following ischemia-reperfusion injury suggesting that Cav-3 OE mice are resistant to membrane rupture. Whether this preserved ultrastructure is a result of reduced injury or due to caveolin-3 overexpression remains to be determined.

The precise molecular mechanism by which Cav-3 in myocytes protects the heart and its myocytes from ischemia-reperfusion injury remains to be determined. Caveolins can inhibit activity of signaling proteins, such as eNOS and ERK1/2,(43, 44) by interaction of the CSD with the binding motif of such partners. In addition, caveolins can promote signaling *via* enhanced receptor-effector coupling or enhanced receptor affinity.(11, 45) Based on data showing that infusion of a peptide with the CSD sequence can protect the heart from ischemia-reperfusion injury, Young *et al*(46) proposed that the CSD peptide produces ischemic tolerance by enhancing release of endothelium-derived nitric oxide.(46) Additional studies show that ischemia-reperfusion injury activates a redistribution of Cav-3 and a down-regulation of Cav-1 association with ERK(47) while IPC leads to a translocation of eNOS to caveolae.(48) The current results, in which overexpressed Cav-3 in cardiac myocytes yields no

change in basal expression of NOS isoforms or in nitric oxide (NO) generation, lead us to conclude that the ischemic tolerance produced by Cav-3 expression does not result from changes in NO production and that cardiac myocyte eNOS is not a major source of cardiac NO. The latter idea is supported by results indicating that re-expression of Cav-1 exclusively within the endothelium of Cav-1 knockout mice rescues cardiac defects.(49)

The phenotype of cardiac myocyte-specific Cav-3 OE mice is strikingly different from that of mice that have a total body overexpression of Cav-3 in brain, fat, liver, lung and spleen as well as smooth, skeletal and cardiac muscle.(50) Such mice develop a muscular dystrophy phenotype at 3-4 weeks of age and after 6 months of age show cardiac degeneration, fibrosis and reduced cardiac NOS activity and cardiac function.(20) In contrast, cardiac myocyte-specific overexpression of Cav-3 does not result in cardiomyopathy in 6-8 month old mice or a reduction in NOS activity. We conclude that increased cardiac myocyte expression of Cav-3 is not responsible for the late-appearing cardiac changes observed in the total body Cav-3 OE mice.

In conclusion, the current results show that IPC increases the number of plasma membrane caveolae in cardiac myocytes and that mice with cardiac myocyte-specific Cav-3 overexpression are protected from ischemic injury in a manner that mimics the cardiac protection produced by IPC. The ability to recapitulate or block the alterations of the plasma membrane produced by IPC via the respective overexpression or knockout of Cav-3 implies that Cav-3 is necessary and sufficient for IPC-induced cardiac protection. Our results also define a molecular mechanism to explain aspects of sarcolemmal ultrastructure, caveolae, and ischemic preconditioning

that have been poorly understood for many years. Cardiac myocyte targeted overexpression of Cav-3 may provide a novel means to protect the heart from ischemia-reperfusion injury. More generally, our results imply that cell type-selective expression of caveolins may offer a means to augment mechanisms of preservation of the heart and perhaps other organs.

#### **4.5 Acknowledgements**

Supported by American Heart Association Beginning Grant in Aid 0765076Y (YMT), American Heart Association Predoctoral Fellowship 06150217Y (YTH), American Heart Association Scientist Development Grant 0630039N (HHP), NIH 1PO1 HL66941 (PAI and DMR), Senior Scholar Award from Ellison Foundation (PAI), Merit Award from the Department of Veterans Affairs (DMR), and NIH RO1 HL081400 (DMR).

The text of Chapter Four is a reprint of the material as it appears in *Circulation* 2008. Tsutsumi, Y; Horikawa, Y; Jennings, M; Kidd, M; Niesman, I; Yokoyama, U; Head, B; Hagiwara, Y; Ishikawa, Y; Miyanohara, A; Patel, P; Insel, P; Patel, H; and Roth, D, American Heart Association, inc 2008. The dissertation author was the primary co-investigator and co-author of this material and played a pivotal role in all aspects of the manuscript, including the formulation and testing of the experiments and in the writing and editing of the manuscript.

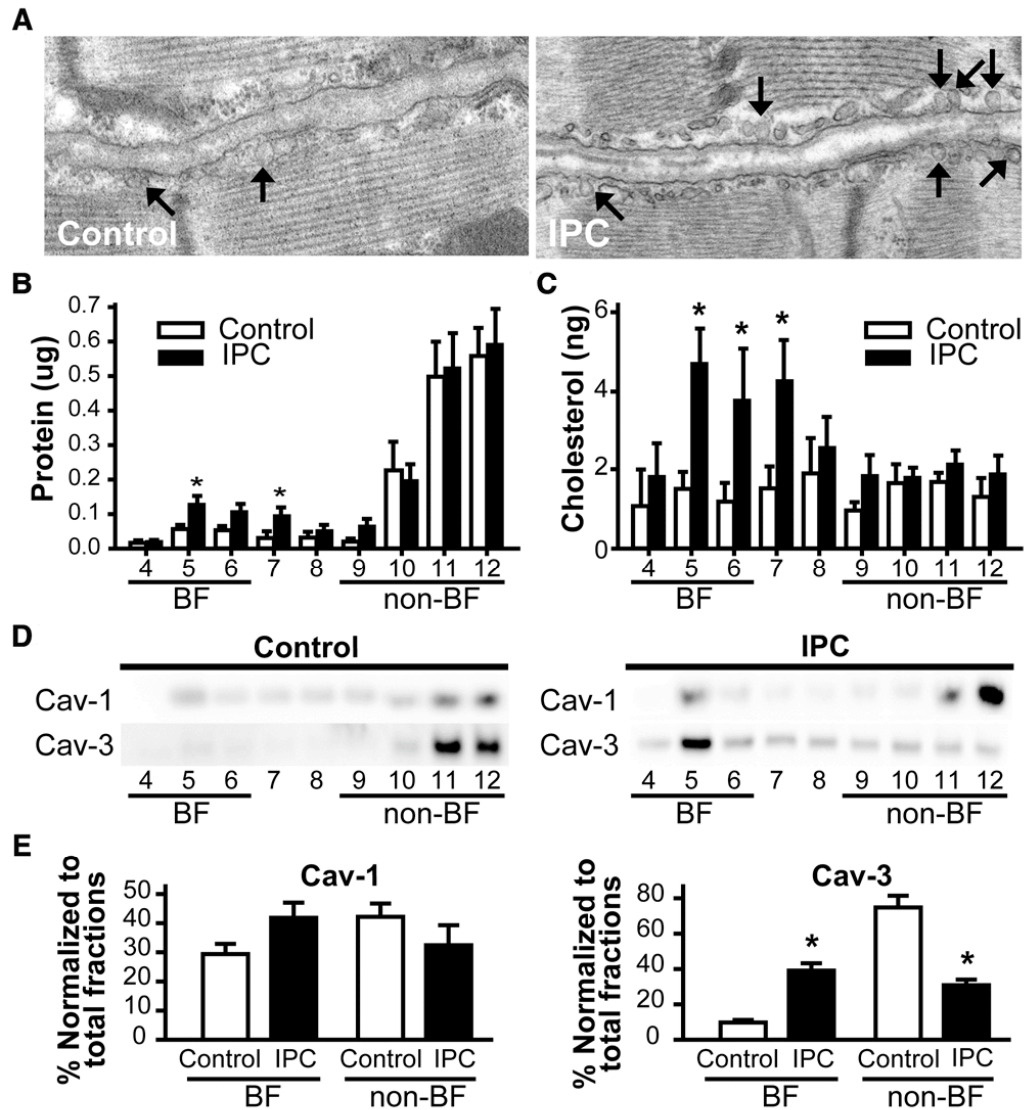


**Figure 4-1:** IPC increases the expression of caveolae and the enrichment of protein and cholesterol in buoyant fractions. Hearts were subjected to a 5 min IPC stimulus. Control wild-type animals underwent no treatment. (A) Electron microscopy showed an increase in number of caveolae compared to control hearts (arrow). (B) and (C) Excised control and hearts subjected to IPC underwent sucrose density fractionation. Protein and cholesterol assays showed increased protein and cholesterol in buoyant fractions (BF) after IPC (\*P < 0.05). (D) and (E) Fractions were probed for Cav-1 and Cav-3. Cav-3, but not Cav-1, was increased in buoyant fractions after IPC (representative immunoblots are shown) and confirmed by densitometry normalized to total fraction amounts (E). \*P < 0.05 relative to respective control. Summary data are from 6 mice per group.

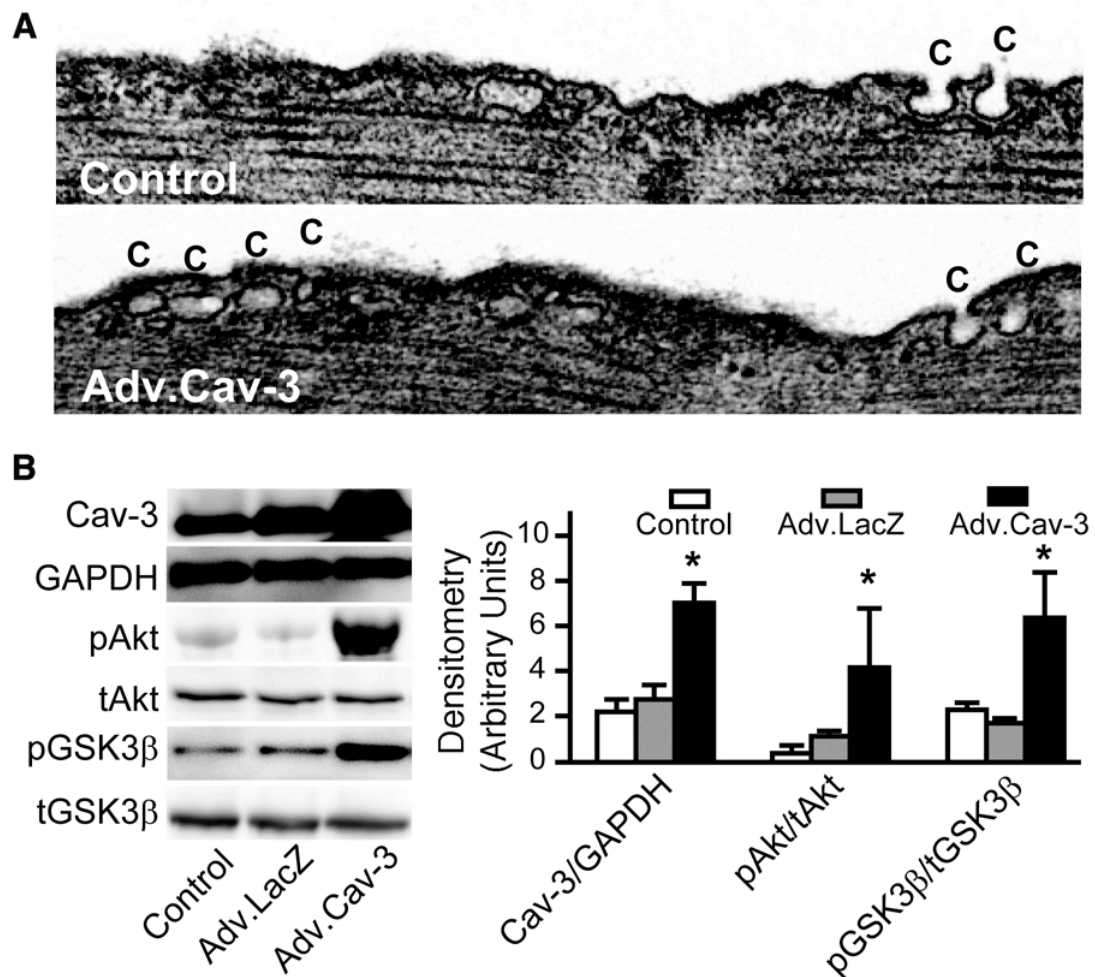


**Figure 4-2:** *Cav-3* adenovirus increases caveolae expression in adult cardiac myocytes (ACM). (A) ACM incubated with an adenovirus (Adv) encoding full-length mouse *Cav-3* (Adv.Cav-3) for 72 h increased caveolae (C) number. (B) ACM exposed to no virus, Adv.LacZ or Adv.Cav-3 for 72 h. were lysed and immunoblotted (left panel). Adv.Cav-3-treated ACM have increased expression of *Cav-3* protein as well as increased phosphorylated phospho Akt and GSK3 $\beta$  compared to control or LacZ-treated ACM (n = 4-6) (right panel). \* $P < 0.05$  vs. Adv.LacZ.

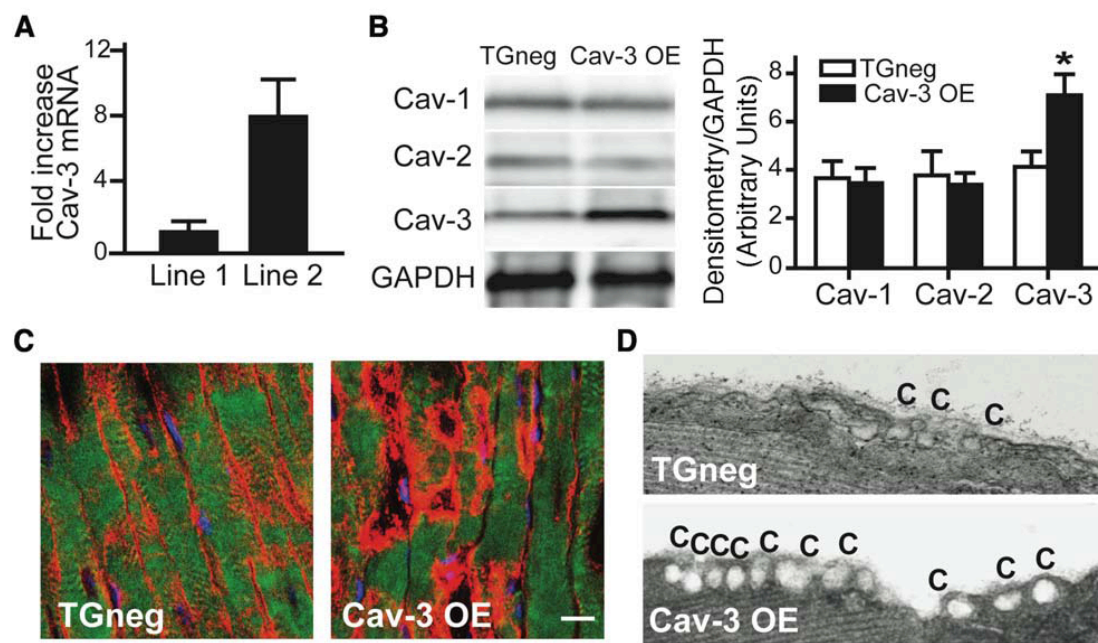


**Figure 4-3:** Cardiac myocyte-specific Cav-3 OE mice: caveolin, caveolae and NOS expression. **(A)** Real-time PCR of Cav-3 mRNA expression in two founder lines. Line 2 had 8-fold increased Cav-3 mRNA expression compared to Line 1. Data are represented relative to TG<sub>neg</sub> and normalized to GAPDH expression (n = 4). **(B)** Immunoblot of Cav-1, -2, and -3 in whole heart homogenates from Cav-3 OE and TG<sub>neg</sub> mice (left panel). Densitometry was normalized to expression of GAPDH and showed a significant increase in Cav-3 protein in whole heart homogenates (right panel; \*P = 0.011, 7-9 mice in each group). **(C)** Immunohistochemistry showed increased Cav-3 (red pixels) in sarcolemma of cardiac myocytes from Cav-3 OE vs. TG<sub>neg</sub> mice. The bar donates 10  $\mu$ m. **(D)** Electron microscopy shows increased caveolae (C) in cardiac myocytes from Cav-3 OE vs. TG<sub>neg</sub> mice. **(E)** Immunoblot analysis of basal expression of NOS and phosphorylated eNOS in TG<sub>neg</sub> and Cav-3 OE mice (left panel). Densitometry was normalized to GAPDH (right panel). No differences were observed in expression of any NOS isoforms. Summary data are from 5 mice per group. **(F)** Basal NOS activity was measured in TG<sub>neg</sub> and Cav-3 OE murine hearts. We detected no differences between groups.

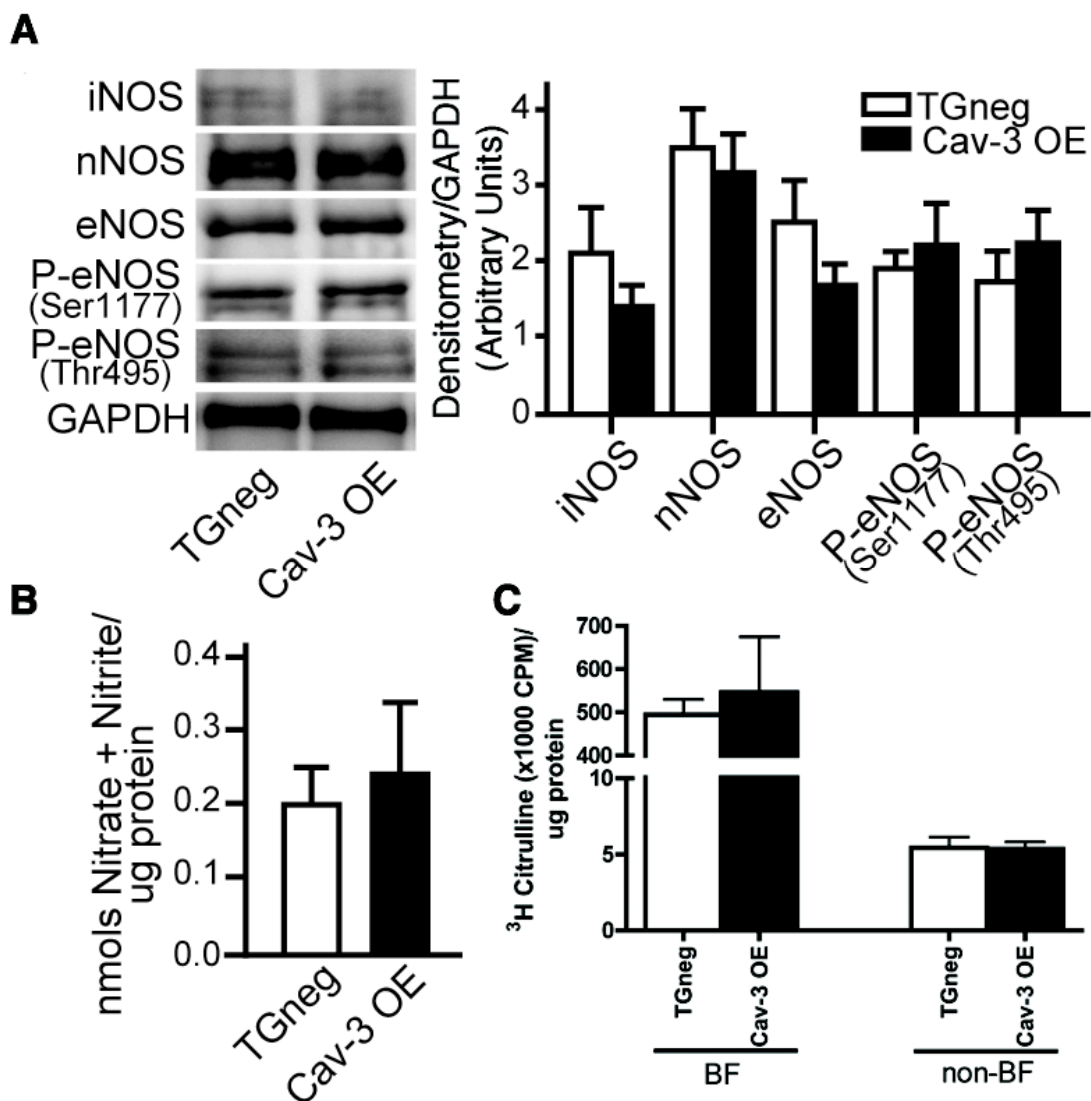


**Figure 4-4:** NOS expression and activity. (A) Immunoblot analysis of basal expression of NOS and phosphorylated eNOS in TG<sub>neg</sub> and Cav-3 OE mice (left panel). Densitometry was normalized to GAPDH (right panel). No differences were observed in expression of any NOS isoforms. Summary data are from 5 mice per group. (B) Basal NOS activity was measured in TG<sub>neg</sub> and Cav-3 OE murine whole heart homogenates. No differences in basal NOS activity was observed between groups. (C) Hearts from TG<sub>neg</sub> and Cav-3 OE mice were homogenized in triton-X and fractionated on a discontinuous sucrose density gradient to separate buoyant (caveolae) and non-buoyant (non-caveolar membrane) fractions (BF and non-BF, respectively). NOS activity was measured in BF and non-BF using a <sup>3</sup>H-arginine assay. No difference in NOS activity was observed in the two separate fractions in TG<sub>neg</sub> vs. Cav-3 OE mice.

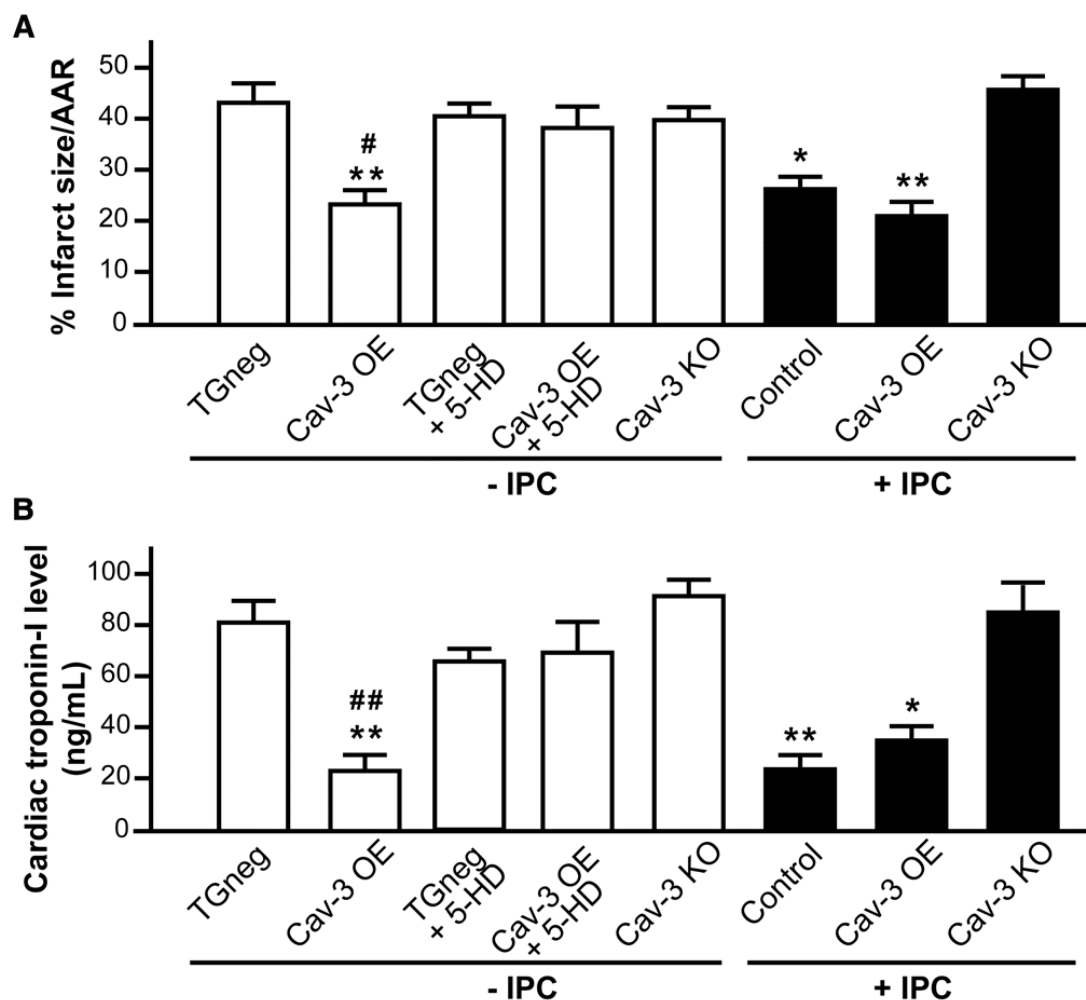


**Figure 4-5:** Cardiac protection in Cav-3 OE mice. Mice were subjected to ischemia-reperfusion injury. **(A)** Infarct size (percent of AAR) was reduced by IPC in control animals; however, Cav-3 OE mice were protected to similar levels with and without IPC. Cav-3 KO mice could not be protected with IPC. Treatment of Cav-3 OE mice with 5-hydroxydecanoate (5-HD; 10 mg/kg i.v.), a mitochondrial  $K_{ATP}$  channel inhibitor, abolished protection. TG<sub>neg</sub> treated with 5-HD had similar infarct size to controls. \* $P < 0.05$ , \*\* $P < 0.001$  vs. TG<sub>neg</sub> mice, and # $P < 0.05$  vs. Cav-3 OE + 5-HD. **(B)** Serum cardiac troponin-I, a marker of cardiac myocyte damage, was measured following 2 h of reperfusion ( $n = 8-11$ , mean  $\pm$  s.e.m.). \* $P < 0.05$ , \*\* $P < 0.001$  vs. TG<sub>neg</sub> mice, and ## $P < 0.01$  vs. Cav-3 OE + 5-HD.

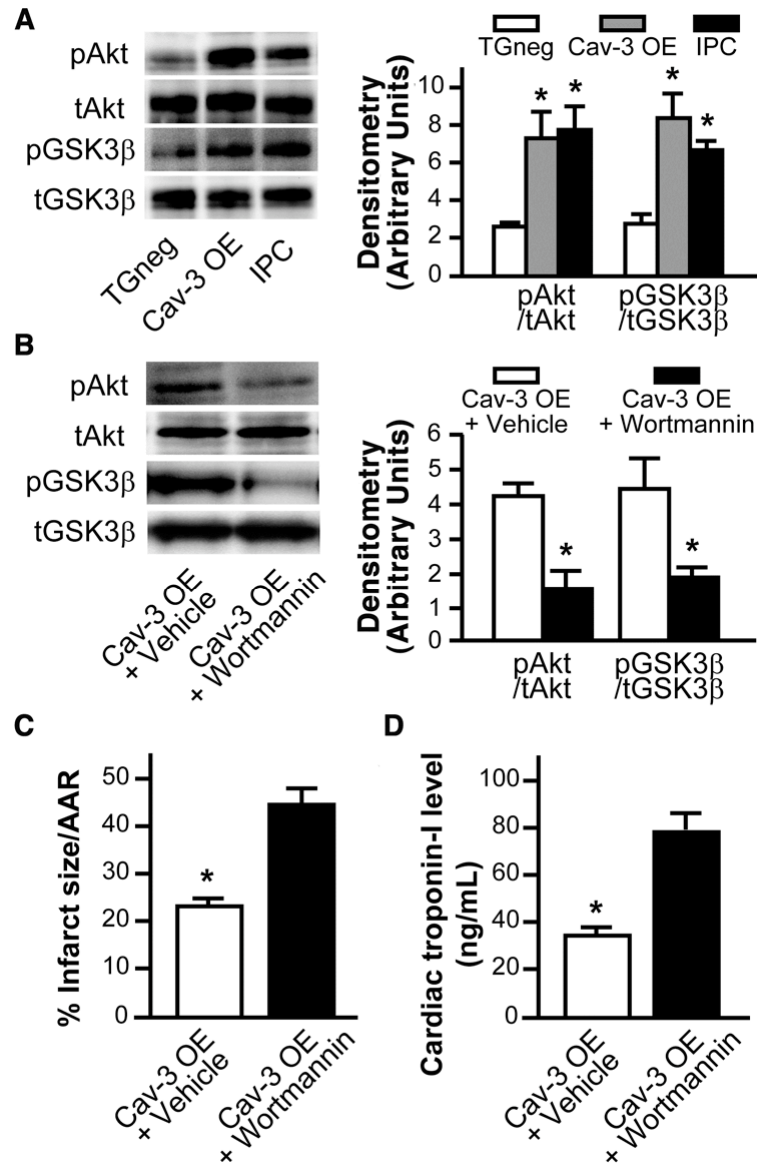


**Figure 4-6:** Role of survival kinases in protection of Cav-3 OE mice. (A) Whole heart homogenates showed elevated phosphorylation of Akt and GSK3 $\beta$  in IPC-treated mice and Cav-3 OE mice when compared to TG<sub>neg</sub> mice (n = 6-10). Total Akt or GSK3 $\beta$  was used to assess protein loading. \* P < 0.05 vs. TG<sub>neg</sub> mice. (B-D) To determine the role of PI3K/Akt/ GSK3 $\beta$  in the endogenous protection, Cav-3 OE mice were treated with a PI3K inhibitor, wortmannin (15 $\mu$ g/kg), 15 minutes prior to index ischemia-reperfusion. DMSO vehicle treated Cav-3 OE served as controls (n=7). Wortmannin treatment resulted in decreased basal phosphorylation of Akt and GSK3 $\beta$  (B). Additionally, wortmannin treatment attenuated the endogenous protection seen in vehicle treated Cav-3 OE mice with respect to infarct size (C) and cardiac troponin-I (D).

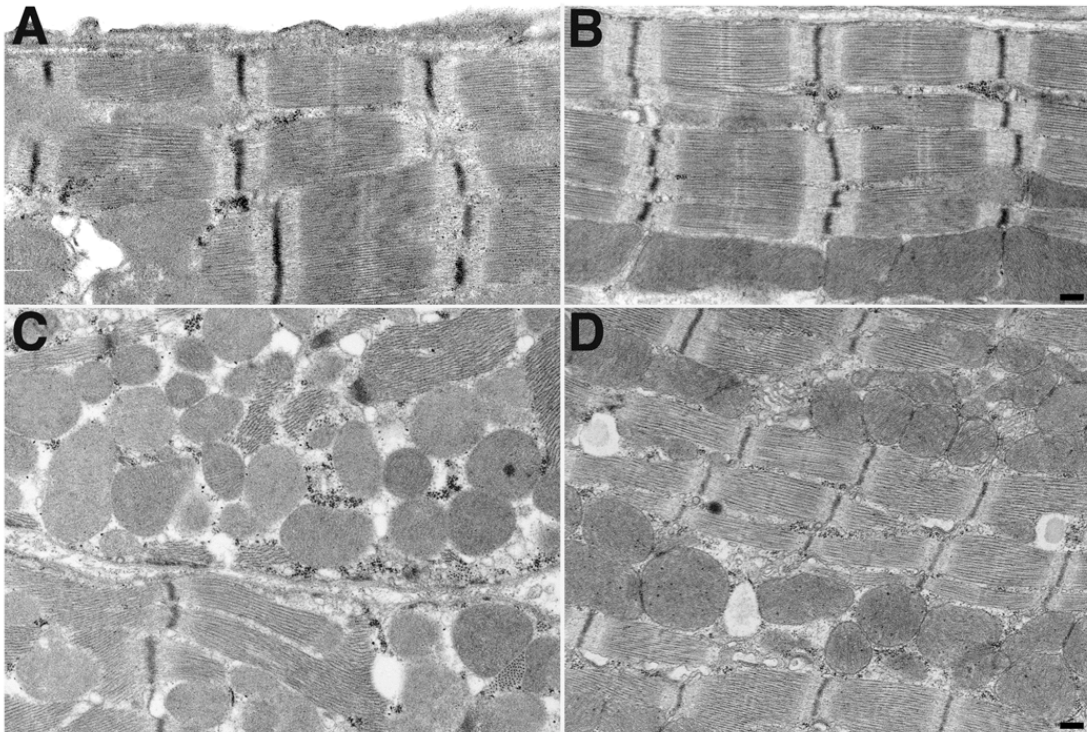


**Figure 4-7:** Electron micrograph of area at risk from the hearts of TG<sub>neg</sub> and Cav-3 OE mice following ischemia-reperfusion. **(A)** and **(B)** No tissue swelling or structural change were seen in sham groups from TG<sub>neg</sub> and Cav-3 OE mice. **(C)** After ischemia-reperfusion in TG<sub>neg</sub> mice, myofibrils were distended, Z-lines were irregular and unclear, and mitochondria were swollen and contained amorphous matrix densities. **(D)** Cav-3 OE mice had fewer damaged myocytes after ischemia-reperfusion: Myofibrils had well-arranged Z-lines and organized mitochondria.

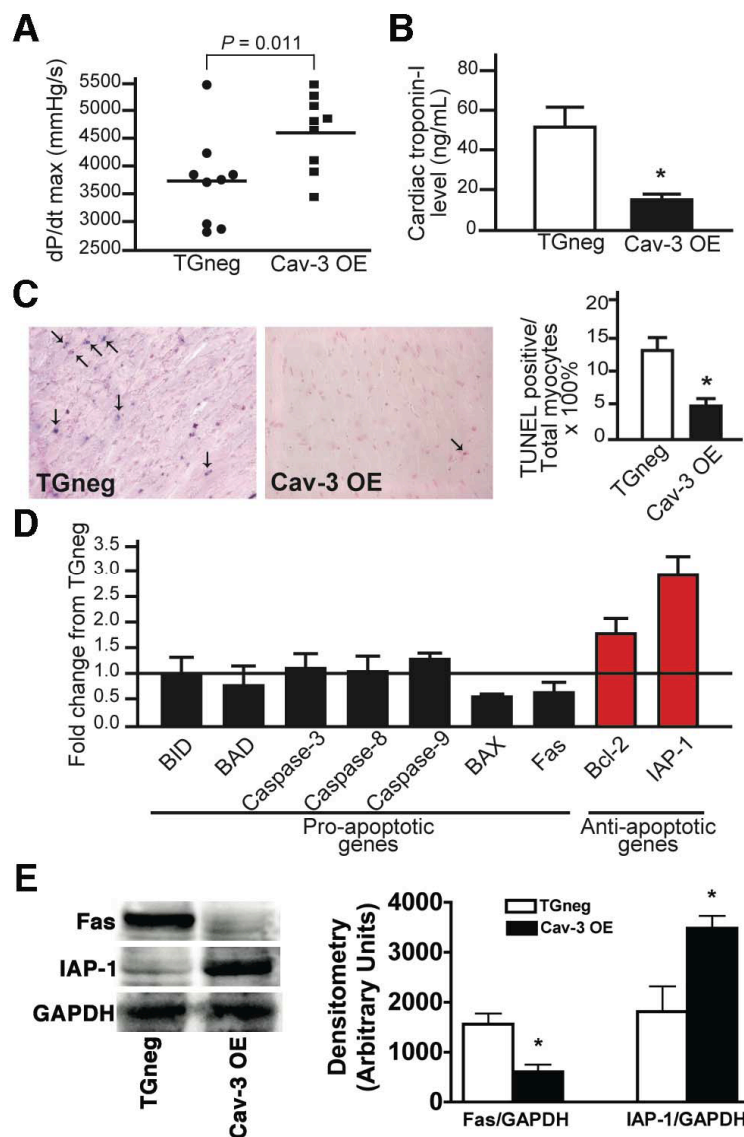
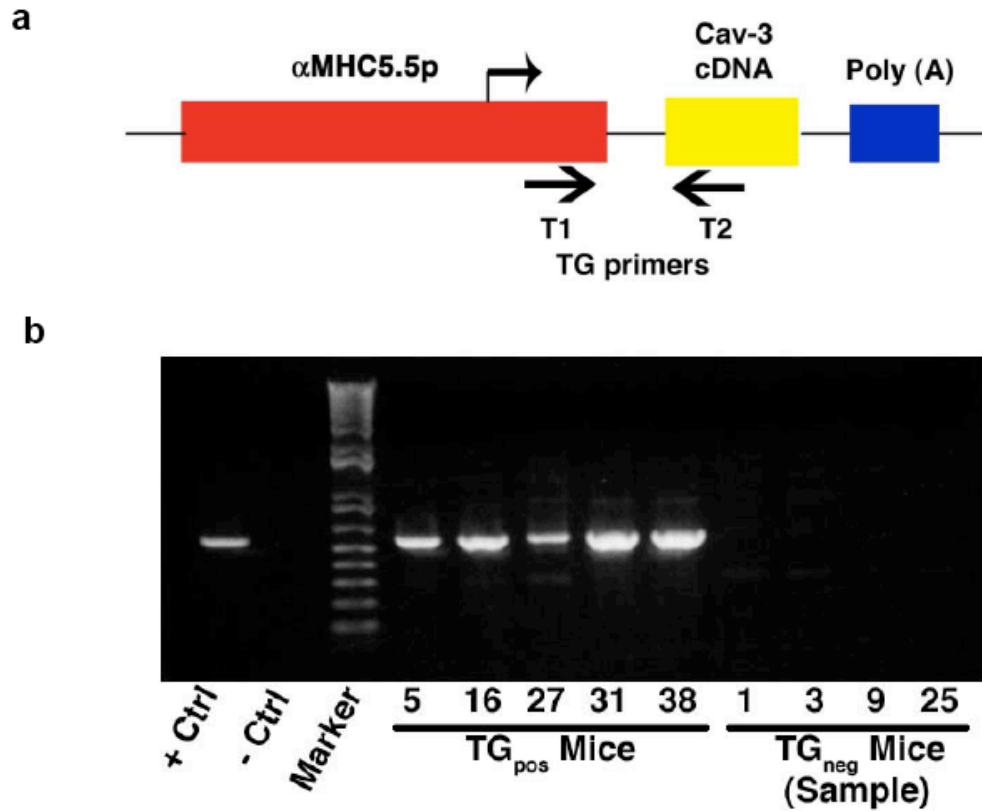
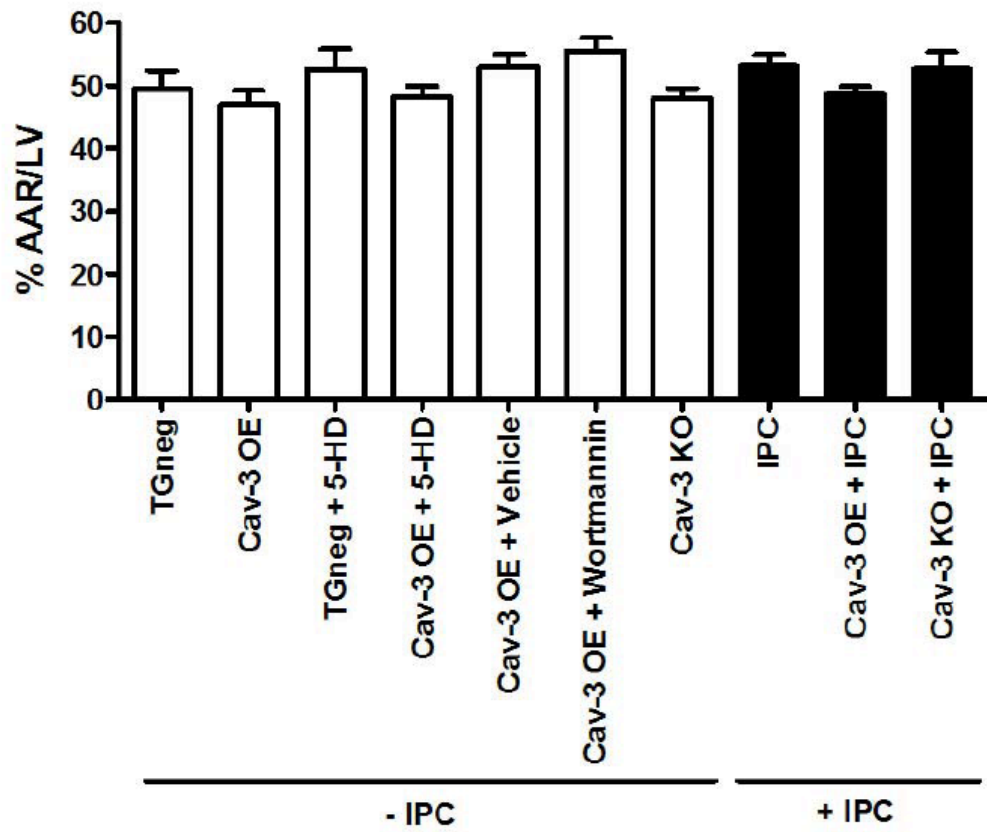


**Figure 4-8:** Cardiac function and cell death in mice 24 h after ischemic injury. Following 30 min of ischemia, mice were allowed to recover for 24 h. **(A)** Cav-3OE mice displayed better cardiac function, as measured by dP/dt max ( $4619 \pm 226$  vs.  $3717 \pm 275$  mmHg/s,  $n = 9$ ,  $P = 0.011$ ). **(B)** Cardiac troponin-I levels were significantly decreased in Cav-3 OE mice ( $n = 7-8$ ,  $*P = 0.002$  vs. TG<sub>neg</sub>). **(C)** Apoptosis in the AAR, determined using TUNEL staining, in 24 h reperfused hearts (arrow, representative images). Nuclei staining positive for TUNEL, quantified as a percent of total nuclei, were significantly decreased in hearts from Cav-3 OE vs. TG<sub>neg</sub> mice (right panel). The data shown are representative of 4-5 independent experiments.  $*P = 0.003$  vs. TG<sub>neg</sub> mice. **(D)** Real-time PCR analysis of pro- and anti-apoptotic gene expression in AAR 24 h after reperfusion of Cav-3 OE mice and TG<sub>neg</sub> mice ( $n=5$ ). **(E)** Immunoblot analysis shows decreased Fas (pro-apoptotic) and increased IAP-1 (anti-apoptotic) protein expression in agreement with mRNA data presented in **(D)** ( $n=4$ ).



**Supplementary Figure 4-1:** Generation of a cardiac myocyte specific caveolin-3 (Cav-3) transgenic mouse. (a) Schematic of Cav-3 construct. Full-length cDNA for mouse Cav-3 (~489bp) was cloned into a vector containing the  $\alpha$ -myosin heavy chain promoter ( $\alpha$ MHC) to facilitate cardiac myocyte-specific expression of Cav-3. (b) PCR products using transgenic (TG) primers (from (a)) for positive control vector DNA, negative control, and tail snip genomic DNA of TG-positive and TG-negative (TGneg) mice were run on an agarose gel. Five mice were Cav-3 TG positive (Cav-3 OE).



**Supplementary Figure 4-2:** Area at risk (AAR) as a percent of the left ventricle (LV) was no different among the groups

**Table 4-1: Hemodynamics**

	Baseline	Pre-occlusion	Ischemia 30 min	Reperfusion 120 min
<b>Heart rate, beats · min<sup>-1</sup></b>				
TGneg	457 ± 7	453 ± 8	431 ± 17	430 ± 19
Cav-3 OE	440 ± 7	442 ± 9	429 ± 12	440 ± 11
TGneg + 5-HD	439 ± 13	427 ± 10	424 ± 18	416 ± 10
Cav-3 OE + 5-HD	465 ± 11	439 ± 12	425 ± 10*	413 ± 11*
Cav-3 OE + Wortmannin	435 ± 7	441 ± 9	427 ± 10	418 ± 11
Cav-3 OE + Vehicle	448 ± 12	442 ± 12	428 ± 14	426 ± 12
Cav-3 KO	438 ± 7	428 ± 12	414 ± 13	406 ± 14
IPC	452 ± 13	444 ± 15	430 ± 12	428 ± 15
Cav-3 OE + IPC	443 ± 20	428 ± 15	441 ± 23	425 ± 13
Cav-3 KO + IPC	450 ± 21	422 ± 20	412 ± 23	417 ± 13
<b>Mean arterial pressure, mmHg</b>				
TGneg	74 ± 2	71 ± 2	67 ± 3	59 ± 2*§
Cav-3 OE	75 ± 2	72 ± 2	67 ± 2*	69 ± 2
TGneg + 5-HD	72 ± 2	69 ± 2	61 ± 1*†	57 ± 1*§
Cav-3 OE + 5-HD	73 ± 2	71 ± 2	62 ± 2*	58 ± 2*§
Cav-3 OE + Wortmannin	75 ± 2	73 ± 2	62 ± 2*	59 ± 2*§
Cav-3 OE + Vehicle	72 ± 2	71 ± 2	69 ± 1	66 ± 2
Cav-3 KO	75 ± 2	73 ± 2	61 ± 3*†	58 ± 3*§
IPC	71 ± 1	69 ± 1	71 ± 1	66 ± 1*
Cav-3 OE + IPC	72 ± 3	70 ± 3	65 ± 2	66 ± 2
Cav-3 KO + IPC	73 ± 2	69 ± 3	63 ± 1*	56 ± 1*§†
<b>Rate-pressure product, beats · min<sup>-1</sup> · mmHg · 10<sup>3</sup></b>				
TGneg	33.7 ± 1.1	32.4 ± 1.5	28.8 ± 1.9	25.3 ± 1.8*
Cav-3 OE	33.0 ± 1.0	31.7 ± 0.7	28.8 ± 0.8*	30.3 ± 0.8
TGneg + 5-HD	31.8 ± 1.5	29.4 ± 1.1	26.0 ± 1.2*	23.9 ± 0.9*§
Cav-3 OE + 5-HD	33.9 ± 1.3	31.3 ± 1.5	26.5 ± 1.1*	23.8 ± 1.0*§
Cav-3 OE + Wortmannin	32.4 ± 1.0	32.1 ± 1.1	26.5 ± 0.9*	24.7 ± 1.2*
Cav-3 OE + Vehicle	32.1 ± 1.0	31.3 ± 0.8	29.6 ± 1.0	28.0 ± 0.9*
Cav-3 KO	32.9 ± 0.9	31.3 ± 1.3	25.2 ± 1.0*	23.7 ± 1.4*§
IPC	32.0 ± 1.1	30.7 ± 1.3	30.4 ± 0.8	28.3 ± 1.2
Cav-3 OE + IPC	32.0 ± 2.1	30.0 ± 1.9	28.8 ± 1.7	27.9 ± 1.3
Cav-3 KO + IPC	32.7 ± 1.7	27.5 ± 1.8	25.7 ± 1.2*	23.5 ± 0.6*§

Data are mean ± SEM. n=6-11 per group. Abbreviations are: TGneg, transgenic-negative; Cav-3 OE, caveolin-3 overexpression; 5-HD, 5-hydroxydecanoate; Cav-3 KO, caveolin-3 knockout; IPC, ischemic preconditioning. \* Significantly ( $p < 0.05$ ) different from baseline (intragroup comparison). § Significantly ( $p < 0.05$ ) different from Cav-3 OE (intergroup comparison). † Significantly ( $p < 0.05$ ) different from IPC (intergroup comparison).

**Table 4-2: Morphology, echocardiography, and hemodynamics****Table 2. Morphology, echocardiography and hemodynamics**

	TGneg mice	Cav-3 OE mice
Heart Weight/Tibia Length (mg/mm)	6.3 ± 0.5	5.9 ± 0.4
Echocardiography		
AWd (mm)	0.79 ± 0.04	0.86 ± 0.01
LVIDd (mm)	3.62 ± 0.14	3.68 ± 0.11
PWd (mm)	0.86 ± 0.02	0.90 ± 0.01
AWs (mm)	1.24 ± 0.07	1.28 ± 0.07
LVIDs (mm)	2.17 ± 0.12	2.31 ± 0.12
PWs (mm)	1.32 ± 0.05	1.20 ± 0.05
FS (%)	39.9 ± 3.3	37.5 ± 2.3
Hemodynamics		
HR (beats/min)	431 ± 14	436 ± 16
MAP (mmHg)	72 ± 4	72 ± 2
RPP (beats · min <sup>-1</sup> · mmHg · 10 <sup>3</sup> )	31.2 ± 2.2	31.6 ± 1.6

Values are mean ± SEM. n = 9-10. Abbreviations are: TGneg, transgenic-negative; Cav-3 OE, caveolin-3 overexpression; AWd and AWs, anterior wall thickness in diastole and systole, respectively; LVIDd and LVIDs, left ventricular internal cavity diameter in diastole and systole, respectively; PWd and PWs, posterior wall thickness in diastole and systole, respectively; FS, fractional shortening; HR, heart rate; MAP, mean arterial pressure; RPP, rate-pressure product.

#### 4.6 References

1. Noble, R. 1943. The development of resistance by rats and guinea pigs to amounts of trauma usually fatal. *Am J Physiol* 38:346-351.
2. Murry, C.E., Jennings, R.B., and Reimer, K.A. 1986. Preconditioning with ischemia: a delay of lethal cell injury in ischemic myocardium. *Circulation* 74:1124-1136.
3. Hausenloy, D.J., Tsang, A., and Yellon, D.M. 2005. The reperfusion injury salvage kinase pathway: a common target for both ischemic preconditioning and postconditioning. *Trends Cardiovasc Med* 15:69-75.
4. Steinberg, S.F., and Brunton, L.L. 2001. Compartmentation of g protein-coupled signaling pathways in cardiac myocytes. *Annu Rev Pharmacol Toxicol* 41:751-773.
5. Williams, T.M., and Lisanti, M.P. 2004. The caveolin proteins. *Genome Biol* 5:214. PMID: PMC395759.
6. Palade, G. 1953. Fine structure of blood capillaries. *Journal of Applied Physics* 24:1424.
7. Yamada, E. 1955. The fine structure of the gall bladder epithelium of the mouse. *J Biophys Biochem Cytol* 1:445-458.
8. Pike, L.J. 2003. Lipid rafts: bringing order to chaos. *J Lipid Res* 44:655-667.
9. Rothberg, K.G., Heuser, J.E., Donzell, W.C., Ying, Y.S., Glenney, J.R., and Anderson, R.G. 1992. Caveolin, a protein component of caveolae membrane coats. *Cell* 68:673-682.
10. Song, K.S., Scherer, P.E., Tang, Z., Okamoto, T., Li, S., Chafel, M., Chu, C., Kohtz, D.S., and Lisanti, M.P. 1996. Expression of caveolin-3 in skeletal, cardiac, and smooth muscle cells. Caveolin-3 is a component of the sarcolemma and co-fractionates with dystrophin and dystrophin-associated glycoproteins. *Journal of Biological Chemistry* 271:15160-15165.
11. Feron, O., and Balligand, J.L. 2006. Caveolins and the regulation of endothelial nitric oxide synthase in the heart. *Cardiovasc Res* 69:788-797.
12. Patel, H.H., Head, B.P., Petersen, H.N., Niesman, I.R., Huang, D., Gross, G.J., Insel, P.A., and Roth, D.M. 2006. Protection of adult rat cardiac myocytes from ischemic cell death: role of caveolar microdomains and delta-opioid receptors. *Am J Physiol Heart Circ Physiol* 291:H344-350.

13. Horikawa, Y.T., Patel, H.H., Tsutsumi, Y.M., Jennings, M.M., Kidd, M.W., Hagiwara, Y., Ishikawa, Y., Insel, P.A., and Roth, D.M. 2008. Caveolin-3 expression and caveolae are required for isoflurane-induced cardiac protection from hypoxia and ischemia/reperfusion injury. *J Mol Cell Cardiol* 44:123-130.
14. Woodman, S.E., Park, D.S., Cohen, A.W., Cheung, M., Chandra, M., Shirani, J., Tang, B., Jelicks, L.A., Kitsis, R.N., Christ, G.J., et al. 2002. Caveolin-3 knock-out mice develop a progressive cardiomyopathy and show hyperactivation of the p42/44 MAP kinase cascade. *J Biol Chem* 277:38988-38997.
15. Head, B.P., Patel, H.H., Roth, D.M., Lai, N.C., Niesman, I.R., Farquhar, M.G., and Insel, P.A. 2005. G-protein coupled receptor signaling components localize in both sarcolemmal and intracellular caveolin-3-associated microdomains in adult cardiac myocytes. *J Biol Chem* 280:31036-31044.
16. Park, D.S., Cohen, A.W., Frank, P.G., Razani, B., Lee, H., Williams, T.M., Chandra, M., Shirani, J., Souza, A.P.D., Tang, B., et al. 2003. Caveolin-1 null (-/-) mice show dramatic reductions in life span. *Biochemistry* 42:15124-15131.
17. Feron, O., and Kelly, R.A. 2001. The Caveolar Paradox: Suppressing, Inducing, and Terminating eNOS Signaling. *Circ Res* 88:129-131.
18. Juhaszova, M., Zorov, D.B., Kim, S.H., Pepe, S., Fu, Q., Fishbein, K.W., Ziman, B.D., Wang, S., Ytrehus, K., Antos, C.L., et al. 2004. Glycogen synthase kinase-3 $\beta$  mediates convergence of protection signaling to inhibit the mitochondrial permeability transition pore. *J Clin Invest* 113:1535-1549. PMID: PMC419483.
19. Murry, C.E., Richard, V.J., Reimer, K.A., and Jennings, R.B. 1990. Ischemic preconditioning slows energy metabolism and delays ultrastructural damage during a sustained ischemic episode. *Circ Res* 66:913-931.
20. Aravamudan, B., Volonte, D., Ramani, R., Gursoy, E., Lisanti, M.P., London, B., and Galbiati, F. 2003. Transgenic overexpression of caveolin-3 in the heart induces a cardiomyopathic phenotype. *Hum. Mol. Genet.* 12:2777-2788.
21. Hausenloy, D.J., and Yellon, D.M. 2006. Survival kinases in ischemic preconditioning and postconditioning. *Cardiovasc Res* 70:240-253.
22. McNutt, N.S. 1975. Ultrastructure of the myocardial sarcolemma. *Circ Res* 37:1-13.

23. Ashraf, M., and Halverson, C.A. 1977. Structural changes in the freeze-fractured sarcolemma of ischemic myocardium. *Am J Pathol* 88:583-594.
24. Sybers, H.D., Maroko, P.R., Ashraf, M., Libby, P., and Braunwald, E. 1973. The effect of glucose-insulin-potassium on cardiac ultrastructure following acute experimental coronary occlusion. *Am J Pathol* 70:401-420.
25. Frank, J.S., Beydler, S., Kreman, M., and Rau, E.E. 1980. Structure of the freeze-fractured sarcolemma in the normal and anoxic rabbit myocardium. *Circ Res* 47:131-143.
26. Kordylewski, L., Goings, G.E., and Page, E. 1993. Rat atrial myocyte plasmalemmal caveolae in situ. Reversible experimental increases in caveolar size and in surface density of caveolar necks. *Circ Res* 73:135-146.
27. Krajewska, W.M., and Maslowska, I. 2004. Caveolins: structure and function in signal transduction. *Cell Mol Biol Lett* 9:195-220.
28. Matherne, G.P., Linden, J., Byford, A.M., Gauthier, N.S., and Headrick, J.P. 1997. Transgenic A1 adenosine receptor overexpression increases myocardial resistance to ischemia. *Proc Natl Acad Sci U S A* 94:6541-6546.
29. Rorabaugh, B.R., Ross, S.A., Gaivin, R.J., Papay, R.S., McCune, D.F., Simpson, P.C., and Perez, D.M. 2005. alpha1A- but not alpha1B-adrenergic receptors precondition the ischemic heart by a staurosporine-sensitive, chelerythrine-insensitive mechanism. *Cardiovasc Res* 65:436-445.
30. Ping, P., Song, C., Zhang, J., Guo, Y., Cao, X., Li, R.C., Wu, W., Vondriska, T.M., Pass, J.M., Tang, X.L., et al. 2002. Formation of protein kinase C(epsilon)-Lck signaling modules confers cardioprotection. *J Clin Invest* 109:499-507.
31. Wall, J.A., Wei, J., Ly, M., Belmont, P., Martindale, J.J., Tran, D., Sun, J., Chen, W.J., Yu, W., Oeller, P., et al. 2006. Alterations in oxidative phosphorylation complex proteins in the hearts of transgenic mice that overexpress the p38 MAP kinase activator, MAP kinase kinase 6. *Am J Physiol Heart Circ Physiol* 291:H2462-2472.
32. Brunner, F., Maier, R., Andrew, P., Wolkart, G., Zechner, R., and Mayer, B. 2003. Attenuation of myocardial ischemia/reperfusion injury in mice with myocyte-specific overexpression of endothelial nitric oxide synthase. *Cardiovasc Res* 57:55-62.
33. Jones, S.P., Greer, J.J., Kakkar, A.K., Ware, P.D., Turnage, R.H., Hicks, M., van Haperen, R., de Crom, R., Kawashima, S., Yokoyama, M., et al. 2004.

- Endothelial nitric oxide synthase overexpression attenuates myocardial reperfusion injury. *Am J Physiol Heart Circ Physiol* 286:H276-282.
34. Li, G., Chen, Y., Saari, J.T., and Kang, Y.J. 1997. Catalase-overexpressing transgenic mouse heart is resistant to ischemia-reperfusion injury. *Am J Physiol* 273:H1090-1095.
  35. Depre, C., Wang, L., Sui, X., Qiu, H., Hong, C., Hedhli, N., Ginion, A., Shah, A., Pelat, M., Bertrand, L., et al. 2006. H11 kinase prevents myocardial infarction by preemptive preconditioning of the heart. *Circ Res* 98:280-288.
  36. Lau, S., Patnaik, N., Sayen, R., and Mestril, R. 1997. Simultaneous overexpression of two stress proteins in rat cardiomyocytes and myogenic cells confers protection against ischemia-induced injury. *Circulation* 96:2287-2294.
  37. Ray, P.S., Martin, J.L., Swanson, E.A., Otani, H., Dillmann, W.H., and Das, D.K. 2001. Transgene overexpression of alphaB crystallin confers simultaneous protection against cardiomyocyte apoptosis and necrosis during myocardial ischemia and reperfusion. *FASEB J* 15:393-402.
  38. Gupta, S., and Knowlton, A.A. 2007. HSP60 trafficking in adult cardiac myocytes: role of the exosomal pathway. *Am J Physiol Heart Circ Physiol* 292:H3052-3056.
  39. Graf, G.A., Matveev, S.V., and Smart, E.J. 1999. Class B scavenger receptors, caveolae and cholesterol homeostasis. *Trends Cardiovasc Med* 9:221-225.
  40. Matveev, S., van der Westhuyzen, D.R., and Smart, E.J. 1999. Co-expression of scavenger receptor-BI and caveolin-1 is associated with enhanced selective cholesteryl ester uptake in THP-1 macrophages. *J Lipid Res* 40:1647-1654.
  41. Fecchi, K., Volonte, D., Hezel, M.P., Schmeck, K., and Galbiati, F. 2006. Spatial and temporal regulation of GLUT4 translocation by flotillin-1 and caveolin-3 in skeletal muscle cells. *FASEB J* 20:705-707.
  42. Liu, Y., Sato, T., O'Rourke, B., and Marban, E. 1998. Mitochondrial ATP-dependent potassium channels: novel effectors of cardioprotection? *Circulation* 97:2463-2469.
  43. Engelman, J.A., Chu, C., Lin, A., Jo, H., Ikezu, T., Okamoto, T., Kohtz, D.S., and Lisanti, M.P. 1998. Caveolin-mediated regulation of signaling along the p42/44 MAP kinase cascade in vivo. A role for the caveolin-scaffolding domain. *FEBS Lett* 428:205-211.

44. Feron, O., Dessy, C., Opel, D.J., Arstall, M.A., Kelly, R.A., and Michel, T. 1998. Modulation of the endothelial nitric-oxide synthase-caveolin interaction in cardiac myocytes. Implications for the autonomic regulation of heart rate. *Journal of Biological Chemistry* 273:30249-30254.
45. Raikar, L.S., Vallejo, J., Lloyd, P.G., and Hardin, C.D. 2006. Overexpression of caveolin-1 results in increased plasma membrane targeting of glycolytic enzymes: The structural basis for a membrane associated metabolic compartment. *J Cell Biochem* 98:861-871.
46. Young, L.H., Ikeda, Y., and Lefer, A.M. 2001. Caveolin-1 peptide exerts cardioprotective effects in myocardial ischemia-reperfusion via nitric oxide mechanism. *Am J Physiol Heart Circ Physiol* 280:H2489-H2495.
47. Ballard-Croft, C., Locklar, A.C., Kristo, G., and Lasley, R.D. 2006. Regional myocardial ischemia induced activation of MAPKs is associated with subcellular redistribution of caveolin and cholesterol. *Am J Physiol Heart Circ Physiol* 291:H658-667.
48. Koneru, S., Penumathsa, S.V., Thirunavukkarasu, M., Samuel, S.M., Zhan, L., Han, Z., Maulik, G., Das, D.K., and Maulik, N. 2007. Redox regulation of ischemic preconditioning is mediated by the differential activation of caveolins and their association with eNOS and GLUT-4. *Am J Physiol Heart Circ Physiol* 292:H2060-2072.
49. Murata, T., Lin, M.I., Huang, Y., Yu, J., Bauer, P.M., Giordano, F.J., and Sessa, W.C. 2007. Reexpression of caveolin-1 in endothelium rescues the vascular, cardiac, and pulmonary defects in global caveolin-1 knockout mice. *J Exp Med* 204:2373-2382.
50. Galbiati, F., Volonte, D., Chu, J.B., Li, M., Fine, S.W., Fu, M., Bermudez, J., Pedemonte, M., Weidenheim, K.M., Pestell, R.G., et al. 2000. Transgenic overexpression of caveolin-3 in skeletal muscle fibers induces a Duchenne-like muscular dystrophy phenotype. *PNAS* 97:9689-9694.

## **Chapter 5:**

**Cardiac-specific overexpression of caveolin-3 increases ANP production and attenuates cardiac hypertrophy**

## 5.1 Abstract

Atrial natriuretic peptide (ANP) is involved in controlling blood volume and pressure and can act directly on cardiac myocytes to inhibit cardiac hypertrophy. Clinical trials have suggested that ANP is a potential therapeutic in acute heart failure and myocardial infarction. ANP is stored and secreted from caveolae, cholesterol/sphingolipid-enriched invaginations of the plasma membrane that also contain caveolin proteins and natriuretic peptide receptors (NPR). We hypothesized that cardiac-specific overexpression of caveolin-3 (Cav-3 OE) would modulate ANP expression and attenuate cardiac hypertrophy. We found that adult cardiac myocytes incubated with increasing amounts of Cav-3 adenovirus show a dramatic increase in Cav-3 expression, ANP expression, and Akt phosphorylation. This increase in ANP expression was blocked with methyl- $\beta$ -cyclodextrin, which disrupts caveolae, and also by wortmannin, a PI3K inhibitor, although Cav-3 protein expression was unaltered. ANP mRNA was 7-fold greater in hearts from Cav-3 OE mice compared to the mice at baseline, although other fetal genes were unchanged. Circulating ANP levels were also increased in Cav-3 OE mice. If subjected to transverse aortic constriction, Cav-3 OE mice have reduced cardiac hypertrophy, maintained cardiac function, and decreased fibrosis compared to control mice. Cav-3 OE thus attenuates cardiac hypertrophy and increases ANP production, suggesting that a key mechanism by which Cav-3 OE mice are protected from pathological cardiac hypertrophy is via increased expression and release of ANP.

## 5.2 Introduction

Pathological changes in the heart are a major cause of morbidity and mortality in the Western world. One of these pathological changes is cardiac hypertrophy, commonly caused by stressors (e.g., myocardial infarction [MI], or hypertension) that create an increase demand on the heart. Cardiac hypertrophy is a leading risk factor for coronary artery disease and myocardial infarction, arrhythmias, and cardiac failure (1). Caveolae, microdomains of the sarcolemmal membrane that may influence such pathological events, are cholesterol- and sphingolipid- enriched invaginations of the plasma membrane(2, 3) that contain the structural proteins caveolins. There are three isoforms of caveolin (caveolin -1,-2,-3); caveolin-3 (Cav-3) is the dominant isoform found in cardiac myocytes (4).

Overexpression of Cav-3 in neonatal cardiac myocytes results in the inability of an adrenergic agonist (e.g., phenylephrine) and endothelin-1 to induce myocyte hypertrophy(5). Other studies have described that Cav-3 levels increase (6-8) with cardiac hypertrophy. Knockout of the Cav-3 gene results in cardiomyopathy and hyperactivation of Erk1/2(9). Non-specific, total body overexpression of Cav-3 has also been reported to cause cardiomyopathy (10). However, due to the fact that Cav-3 is not normally expressed in smooth muscle, vasculopathy may be the cause for that cardiomyopathy. Our previous studies have shown that caveolae and Cav-3 are necessary for cardiac protection(11). Furthermore, when Cav-3 is overexpressed in a cardiac myocyte-specific manner, protection from ischemia-reperfusion injury, which

shares numerous signaling pathways with hypertrophy, is evident(12). Taken together, these data suggest that selective overexpression of Cav-3 in the cardiac myocyte may have anti-cardiac hypertrophic effects.

The relationship between atrial natriuretic peptide (ANP) and caveolae/caveolins has been investigated for nearly two decades. ANP has diuretic, natriuretic, and vasodilatory effects, as well as autocrine effects on cardiac myocytes, inhibiting cardiac hypertrophy(13-15) ANP has been identified within caveolae closely associated with caveolin-3(16) and may be secreted via caveolae from cardiac myocytes(17). In the current study, we tested the hypothesis that cardiac myocyte-specific overexpression of Cav-3 results in an enhanced ability to cope with pathological cardiac hypertrophy via the increased production of ANP.

## **MATERIALS AND METHODS**

Please see *Chapter 2* for detailed materials and methods.

### **5.3 Results**

*Atrial natriuretic peptide (ANP) expression is caveolae-dependent.* Cardiac myocytes (CM) isolated from adult Sprague-Dawley rats were treated with increasing Caveolin-3 (Cav-3) adenovirus plaque forming units (PFU), ranging from 0-30x10<sup>7</sup> PFU, for 24 hr (Figure 5-1A). We found that as Cav-3 expression increased, ANP expression also increased in addition to phosphorylation of protein kinase B (Akt) and Erk. In order to determine whether Cav-3 expression or the formation of caveolae was causing the increase in ANP expression, we incubated CM with 500 nM methyl- $\beta$ -cyclodextrin

(M $\beta$ CD, an agent that disrupts caveolae) for 24 hr during the infection with the Cav-3 adenovirus. In the presence of M $\beta$ CD, no increase in ANP or pAkt expression was observed even though Cav-3 expression was substantially increased (Figure 5-1B).

*ANP expression is dependent on Akt phosphorylation.* CM were incubated with Cav-3 adenovirus for 24 hr in the presence of wortmannin, a PI3K inhibitor or DMSO (vehicle). Wortmannin inhibited Akt phosphorylation and ANP expression (Figure 5-2), thus implying that ANP expression is dependent on Akt signaling.

*Cardiac myocyte-specific overexpression of caveolin-3 (Cav-3 OE) increases caveolae number and ANP expression.* Left ventricular sections from Cav-3 OE mice revealed a dramatic increase in caveolae formation at the sarcolemmal membrane (Figure 5-3A;) a result consistent with previous reports regarding Cav-3 expression and caveolae formation (18). Furthermore, RNA isolated from left ventricular lysates revealed a nearly 7-fold increase in ANP expression compared to non-transgenic mice (Control), although no differences were observed in several other fetal genes, suggesting that Cav-3 OE mice are not in a hypertrophic state (Figure 5-3B). CM isolated from Cav-3 OE mice treated with actinomycin D (5  $\mu$ g/mL) for up to 2 hr had no significant decrease in ANP expression (Figure 5-3C). ANP protein expression (in left ventricular lysates) and secretion (plasma samples) were increased in Cav-3 OE mice. (Figure 5-3, D and E) although those mice had no significant change in mean arterial pressure (MAP). (Figure 5-3F). Studies with rat CM indicated that Cav-3 expression did not inhibit Erk phosphorylation (Figure 5-1A) but by contrast, CM isolated from

Cav-3 OE mice were resistant to Erk phosphorylation following adrenergic stimulation with phenylephrine (PE; 2 $\mu$ M) for 15 min (PE:  $0.391 \pm 0.06$  vs. Vehicle:  $0.438 \pm 0.06$ , N=4,  $P>0.05$ ). By contrast, PE stimulation substantially increased Erk phosphorylation in control myocytes (PE:  $0.860 \pm 0.03$  vs. Vehicle:  $0.639 \pm 0.02$ , N=4,  $*P<0.05$ ) (Supplementary Figure 5-1A and B).

*Caveolin-3 co-localizes with ANP and inhibits nuclear factor of activated T-cells (NFATc3) translocation into the nucleus, but increases pAkt translocation.* CM from control and Cav-3 OE mice were isolated and stained with antibodies to ANP and Cav-3. In control myocytes ANP was mainly localized near the nucleus and ~25% of ANP colocalized with Cav-3 (Figure 5-4, A, B, and C;  $P<0.001$ ). Cav-3 OE myocytes not only had increased Cav-3 expression, but also increased ANP expression, in particular around the nucleus and localized within the sarcolemma. By contrast with the results observed for control myocytes, nearly 90% of ANP was found to co-localize with Cav-3 in the Cav-3 OE myocytes (Figure 5-4, A, B, and C;  $P<0.001$ ). In order to determine whether the increase in ANP had effect on hypertrophic signaling, nuclear and cytoplasmic fractions were isolated from left ventricular lysates. Cav-3 OE lysates had a significantly greater ratio between cytoplasmic and nuclear NFATc3 (Figure 5-4, D and E,  $P<0.05$ ), suggesting an inhibition of hypertrophic signaling. Moreover, nuclear expression of pAkt was greater in Cav-3 OE mice (Figure 5-4, F and G,  $P<0.05$ ).

*Caveolin-3 overexpression prevents pressure-induced cardiac hypertrophy and fibrosis.* Control and Cav-3 OE mice underwent 4 weeks of transverse aortic constriction (TAC), which is a model of pressure-induced hypertrophy (19). A Log-rank test on a Kaplan-Meier survival curve revealed a significant decrease in deaths associated with TAC in Cav-3 OE mice (Figure 5-5A). Furthermore, control mice had an increase in concentric hypertrophy, nearly doubling in size in response to TAC, whereas Cav-3 OE mice had a blunted response to TAC (Figure 5-5B). Furthermore, Left ventricle (LV) to body weight (BW) and tibia length (TL) ratios revealed nearly a doubling in control mice ( $P<0.001$ ) but Cav-3 OE mice had a blunted response to TAC (Figure 5-5C  $P<0.01$ ). Wheat germ agglutinin staining of left ventricular cross-sections indicated myocyte hypertrophy and blunting of hypertrophy by Cav-3 OE: Control TAC myocytes were nearly 60% larger in surface area compared to Cav-3 OE myocytes subjected to TAC (Figure 5-4D;  $P<0.001$ ). Echocardiography revealed that in response to TAC, control mice had significant growth in both the septum and the posterior wall of the LV, however, in the Cav-3 OE mice only the posterior LV wall increased (Supplementary Table 5-1) following TAC. Assessment of apoptosis by immunofluorescent TUNEL stain revealed no significant changes in apoptosis (Data not shown). Fibrosis associated with pressure-induced cardiac remodeling was also attenuated in Cav-3 OE mice: Control mice had greater perivascular and interstitial fibrosis whereas Cav-3 OE mice did not (Figure 5-5E). RNA was isolated 48 hr post-TAC from control and Cav-3 OE mice to determine expression levels of hypertrophic genes. At that time, Cav-3 OE mice had much higher levels of expression of ANP mRNA (Figure 5-6A) but lower expression of  $\alpha$ sk-actin and  $\beta$ MHC mRNA,

suggesting an inhibition of hypertrophy. Furthermore, unlike control mice subjected to 48 hr of TAC, Cav-3 OE mice did not display activation of  $\alpha$ -sk-actin (Figure 5-6, B and C). Cav-3 protein expression increased 2-fold in both control and Cav-3 OE mice following 48 hr of TAC ( $P<0.01$  and  $P<0.001$ , respectively) although near normal levels were observed 4 wk after TAC (Supplementary Figure 5-2, A and B).

#### *Caveolin-3 overexpression maintains cardiac function*

Cardiac function was monitored via echocardiography, carotid catheterization, and wet lung weights. Serial echocardiography revealed that control mice had a significant decrease in ejection fraction and %fractional shortening following 4 wk of TAC (Figure 5-7, A and B;  $P<0.05$ ), whereas Cav-3 OE mice had no significant change in either measure of cardiac function. After 48 hr of TAC, a subset of control and Cav-3 OE mice received bilateral carotid catheterization to monitor the pressure gradient across the stenosis. All gradients were approximately 80 mmHg (data not shown). Carotid catheterization revealed no significant differences in heart rate or mean arterial pressure in control vs. Cav-3 OE mice prior to or after TAC (Supplementary Table 5-2). However, control mice revealed a significant decrease in left ventricular systolic function ( $dP/dt_{\max}$ ) following TAC (Figure 5-7C;  $P<0.01$ ), whereas Cav-3 OE mice had no such change;  $dP/dt_{\max}$  was significantly greater in Cav-3 OE mice than control mice following TAC (Figure 5-7C;  $P<0.05$ ). Overall, the hemodynamic data suggest that Cav-3 OE mice maintain greater contractility even in the presence of increased afterload. Furthermore, left ventricular relaxation ( $dP/dt_{\min}$ ) was significantly decreased (Figure 5-7D;  $P<0.05$ ) in control mice following 4 wk of TAC, a result

consistent with increased fibrosis and detrimental cardiac remodeling; by contrast, Cav-3 OE mice had a blunted fibrotic response. Wet lung weight (Lung) to BW and TL ratios were significantly increased in control, but not Cav-3 OE, mice following TAC ( $P<0.05$ ), suggesting that the control mice had fluid accumulation within their lungs due to decreased cardiac function whereas Cav-3 OE did not (Figure 5-7 E)

#### 5.4 Discussion

Our results show that cardiac-specific overexpression of Cav-3 is able to blunt pressure-induced pathological hypertrophy by increasing ANP expression and may not completely be due to inhibition of pErk. Furthermore, the increase in ANP expression may be due to the hyper phosphorylation of Akt observed in Cav-3 OE mice, suggesting a novel insight into long term ANP delivery and therapy.

Koga et al,(5) described that Cav-3 overexpression could inhibit Erk phosphorylation. The authors hypothesized that the scaffolding domain of caveolin bound Erk and thus overexpressed caveolin-3 inhibits Erk phosphorylation. Subsequently, Kikuchi et al,(6) described that caveolae and Cav-3 increased following phenylephrine treatment and abdominal banding, a result suggesting that Cav-3 expression might compensate for the increase in afterload by generating more caveolae and perhaps concentrating kinases involved in signaling. By contrast, our data suggest that Cav-3 expression does not directly correlate with Erk inhibition. Although we were able to recapitulate Koga's findings in CM isolated from Cav-3 OE mice (Supplementary Figure 5-1), increasing Cav-3 expression in rat CM did not inhibit Erk phosphorylation (Figure 5-1A), suggesting that Erk phosphorylation may

be an indicator of hypertrophy rather than mechanism for observed responses.

Furthermore, 48 hr of TAC banding dramatically increased expression of Cav-3 and Erk phosphorylation in control mice (Supplementary Figure 5-2), thus implying that a mechanism other than Erk inhibition mediates the anti-hypertrophic effects of Cav-3.

Tsujita et al(20) have noted that localization of the serine/threonine kinase Akt to the nucleus can prevent cardiac hypertrophy. The authors found that nuclear Akt was able to induce ANP expression, prevent pathological hypertrophy and maintain cardiac function following TAC. The increase in ANP that occurs with cardiac hypertrophy may compensate for the increase in afterload via its diuretic, natriuretic, and vasodilating actions as well as its ability to inhibit aldosterone synthesis and renin secretion (13-15). ANP has been utilized as a treatment to reduce post myocardial infarction remodeling(21) and to improve stroke volume index in patients with heart failure.(22) However, due to its relatively short half-life and instability ANP has been difficult to use as a drug.

Increasing Cav-3 expression in CMs increased pAkt and ANP expression. These increases, however, seemed to be much more dependent on the formation of caveolae and the localization of Cav-3 in caveolae rather than on total Cav-3 expression since the M $\beta$ CD treatment–promoted decrease in caveolae, and not Cav-3, expression significantly lowered pAkt and ANP expression levels (Figure 5-1B). Furthermore, treatment with wortmannin inhibited both pAkt and ANP expression, suggesting that pAkt may contribute to the induction in ANP expression (20). Our findings suggest that caveolae store ANP and protect it from degradation and in addition, facilitate the temporal and spatial organization of PI3K and pAkt, thereby

allowing signaling to occur that contributes to the upregulation of ANP expression. Similar to previous data obtained with atrial myocytes (23-25) we observed that control CM show perinuclear localization of ANP whereas Cav-3 OE CM had much more ANP in the cytoplasm and colocalized with Cav-3 (Figure 5-3, A, B, and C). We speculate that this increase in extra-nuclear ANP may prevent the dephosphorylation of NFATc3, thereby resulting in less translocation into the nucleus and ultimately in an inhibition of cardiac hypertrophy(26). Furthermore, Cav-3 OE mice had much more pAkt expression within the nucleus, suggesting a potential mechanism for the increased ANP expression in Cav-3 OE mice.

The co-localization of ANP with caveolae and caveolins was suggested 20 years ago but little further work has investigated these relationships (27),(16, 17). We have recently shown that myocyte-specific caveolin-3 overexpression can mimic ischemia-induced preconditioning and can protect the heart from ischemic injury via an increase in pAkt signaling, effects that were blocked with 5-hydroxydecanoate, a mitochondrial  $K_{ATP}$  channel inhibitor (18). Similarly, isolated rat hearts pre-treated with ANP display cardio-protective effects that are blocked with 5-hydroxydecanoate (28). Caveolin-3 knockout mice display uninhibited hypertrophic signaling(9), an effect akin to that observed with mice that have a knockout of natriuretic peptide receptor-A , the major signaling receptor for ANP in cardiac myocytes(29). In addition, our results in which Cav-3 OE mice are resistant to pressure-induced hypertrophy can potentially be attributed to the increase in pAkt signaling and subsequent increase in ANP expression, which has been described to be not only anti-hypertrophic(30), but also anti-fibrotic(31) and inotropic(22),

Increased ANP levels are generally thought to reflect cardiac dysfunction and have been utilized to identify cardiac hypertrophy (32). However, in the current study and unlike other hypertrophic models and hypertrophic “markers”, Cav-3 OE mice have increased ANP levels but not increases in other hypertrophic markers when compared to control mice. This suggests that Cav-3 OE has a unique ability to specifically alter ANP levels without inducing the complete fetal gene response, a result akin to the ability of nuclear localization of pAkt to prevent hypertrophy(20). Kikuchi et al, noted that treatment with hypertrophic agonists increases Cav-3 protein and caveolae formation but could not determine if this was an effect secondary to increased cardiac hypertrophy(6). The current results help answer this question: overexpressing caveolae and caveolin-3 do not seem to exacerbate cardiac hypertrophy, but instead prevent hypertrophy, thus suggesting a protective rather than a secondary role.

In conclusion, the data shown here indicate that a plasma membrane structural protein, Cav-3, has the unique ability to increase caveolae formation and to induce a “protective phenotype” that is characterized by increased ANP transcription, translation, and secretion, thus leading to decreased cardiac remodeling. The present data thus suggest a relationship between Cav-3 and ANP expression and identify a novel mechanism and therapeutic rationale for the use of ANP in heart failure.

## **5.5 Acknowledgements**

We would like to thank Dr. Diane Huang (Veterans Affairs San Diego Healthcare Systems) for ACM isolation of Control and Cav-3 OE mice.

This work was supported by American Heart Association Predoctoral Fellowship 06150217Y (Y. Horikawa), Hypertension Training Grant NIH/NHLBI 5 T32 HL007261 (Y. Horikawa), American Heart Association Beginning Grant in Aid 0765076Y (Dr Tsutsumi), American Heart Association Scientist Development Grant 0630039N (Dr Patel), NIH 1PO1 HL66941 (Drs Insel and Roth), Merit Award from the Department of Veterans Affairs (Dr Roth), and NIH RO1 HL081400 (Dr Roth).

Chapter 5, in full, is being prepared for publication. The dissertation author was the primary investigator and author for this manuscript.

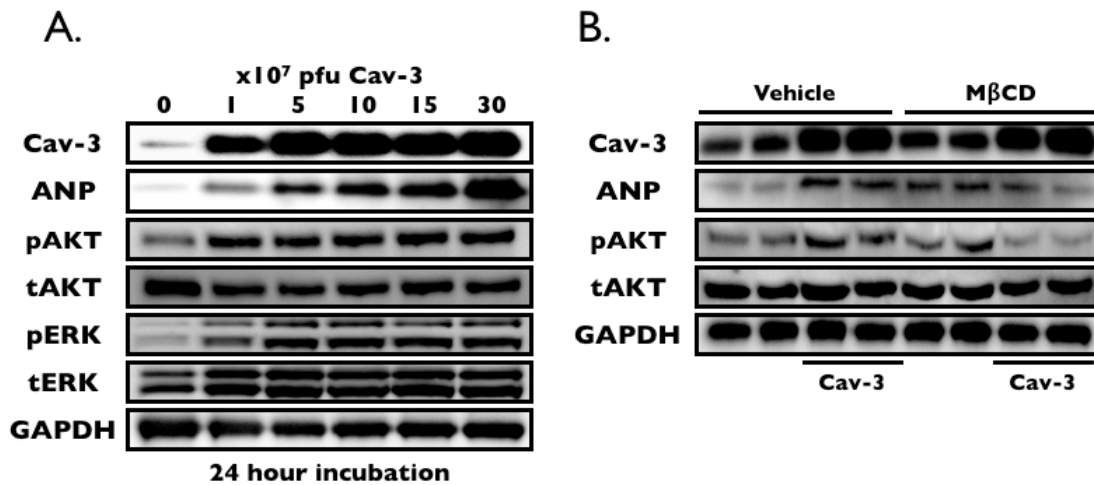


**Figure 5-1:** Caveolin-3 (Cav-3) and caveolae alter atrial natriuretic peptide (ANP) expression and protein kinase B phosphorylation (pAkt). **(A)** Adult cardiac myocytes (CM) isolated from Sprague-Dawley rats were infected with increasing plaque-forming units (pfu) of adenovirus expressing Cav-3. ANP expression and AKT phosphorylation increased in parallel with the increase in Cav-3 expression. Erk phosphorylation also increased in Cav-3 overexpressing CM. **(B)** Rat CM were treated with vehicle or methyl- $\beta$ -cyclodextrin (M $\beta$ CD, removes caveolae) during virus infection for 24 hr. Although Cav-3 expression was increased in M $\beta$ CD-treated CM, a decrease in ANP expression and AKT phosphorylation was observed.

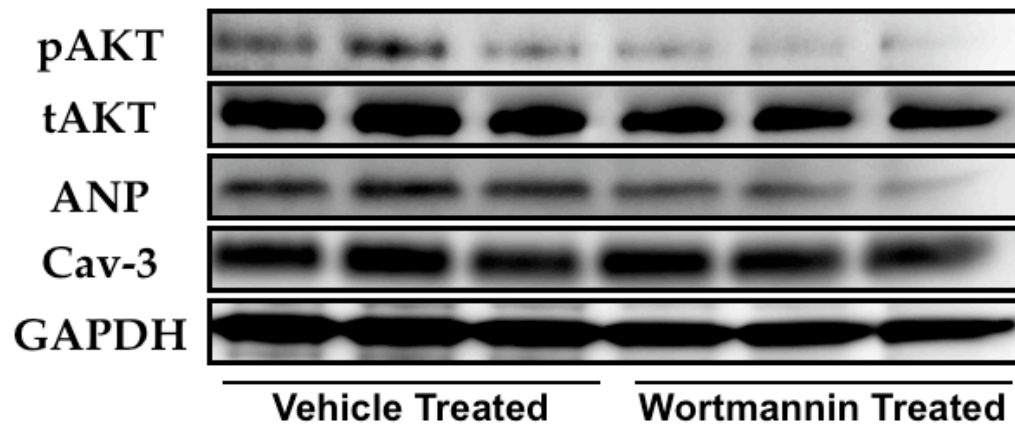


**Figure 5-2:** Akt phosphorylation and ANP expression are prevented by wortmannin. CM were incubated with  $1.0 \times 10^7$  PFU Cav-3 adenovirus in the presence of DMSO (vehicle) or wortmannin (PI3K inhibitor) for 24 hr. Wortmannin inhibited Akt phosphorylation and ANP expression.

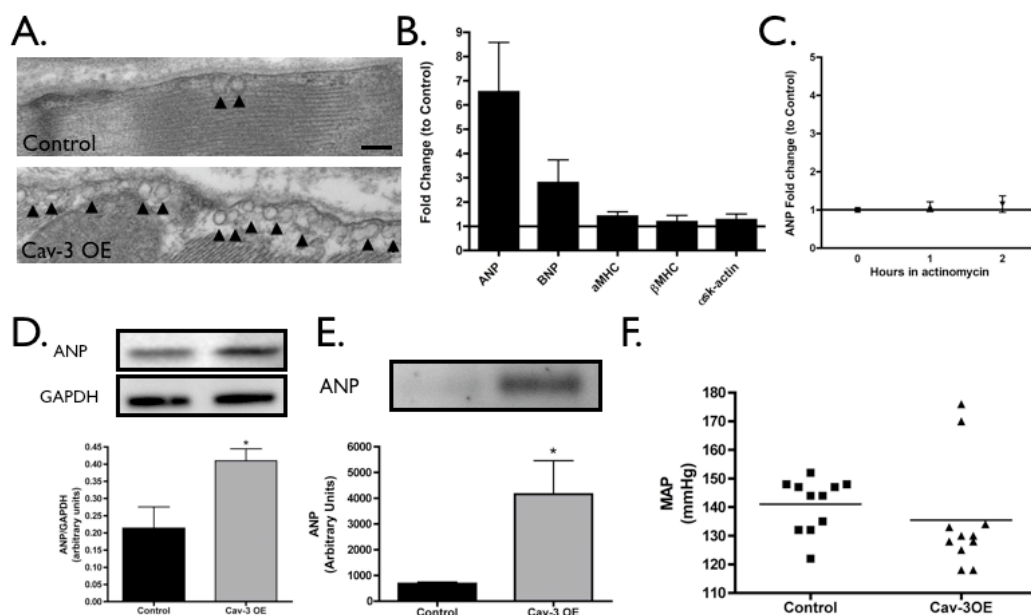


**Figure 5-3:** Cardiac myocyte-specific caveolin-3 overexpressing (Cav-3 OE) mice have increased caveolae and ANP. **(A)** Electron microscopy of the left ventricle revealed a dramatic increase in caveolae formation at the plasma membrane. Scale bar = 0.10  $\mu$ m; N=2. **(B)** Real-time polymerase chain reaction (RT-PCR) revealed a nearly 7-fold increase in ANP (Cav-3 OE) compared to transgene negative (Control) mice at baseline, whereas the other “fetal genes” remained at similar levels to control. N=5-6. **(C)** CM isolated from Cav-3 OE mice were treated with Actinomycin D (5 $\mu$ g/mL) for 0-2 hr. No change in ANP expression was observed when compared to non-treated Cav-3 OE myocytes. N=4. **(D)** and **(E)** ANP protein was significantly increased in Cav-3 OE left ventricular lysates and plasma. \*  $P<0.05$ ; N=4. **(F)** Awake, non anesthetized blood pressures were monitored. Cav-3 OE mice had a non-statistically significant trend toward lower mean arterial pressure (MAP) compared to control mice.

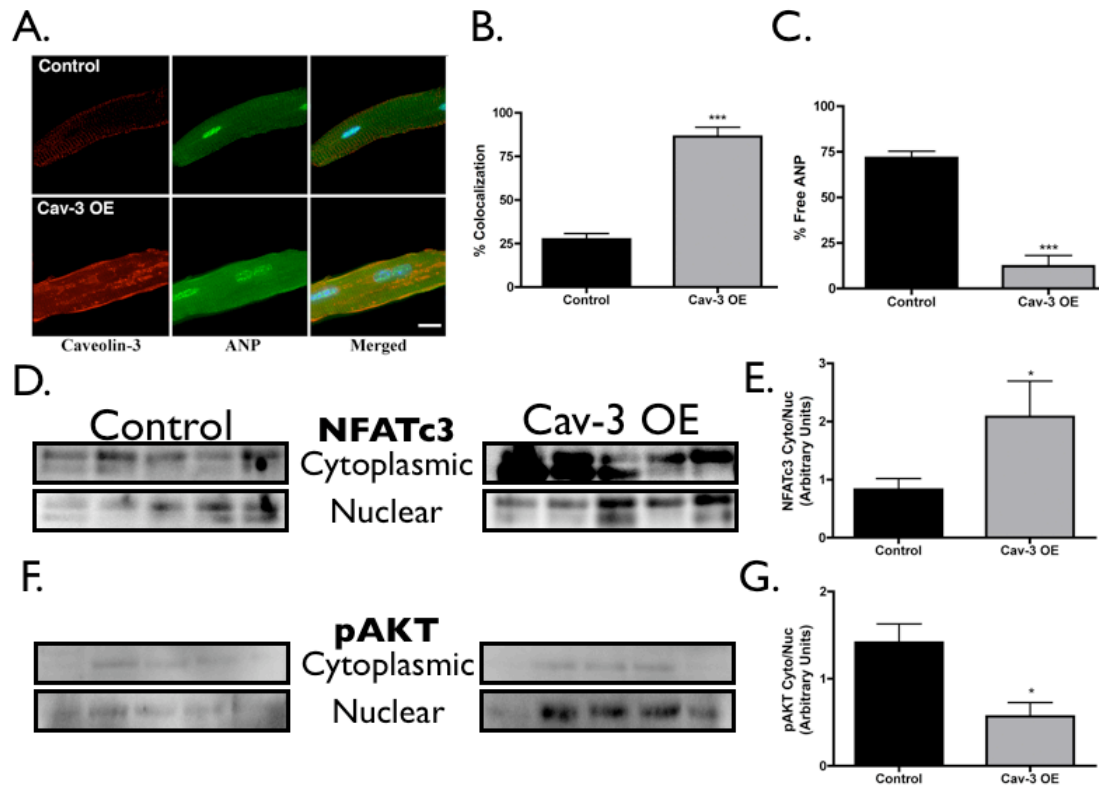


**Figure 5-4:** ANP co-localizes with Cav-3 and inhibits nuclear factor of T-cells (NFATc3). (A), (B), and (C) CM from Cav-3 OE mice were probed with ANP and Cav-3 antibody. In control CM, ANP predominantly localized to the nucleus, whereas, Cav-3 OE CM had significantly more ANP colocalized with Cav-3. Furthermore, the control mice had a larger percent of ANP not localized near Cav-3 \*\*\*  $P < 0.001$ ,  $N=4$ . (D) and (E) Nuclear and cytoplasmic fractions from control and Cav-3 OE ventricular lysates were isolated and then probed for NFATc3. Cav-3 OE mice had a significantly higher ratio of NFATc3 in the cytoplasm compared to control mice. \*  $P < 0.05$ ,  $N=5$ . (F) and (G) Nuclear and cytoplasmic fractions from control and Cav-3 OE ventricular lysates were isolated and then probed for pAkt. Cav-3 OE mice had a significantly lower ratio of pAkt in the cytoplasm compared to control mice. \*  $P < 0.05$ ,  $N=5$

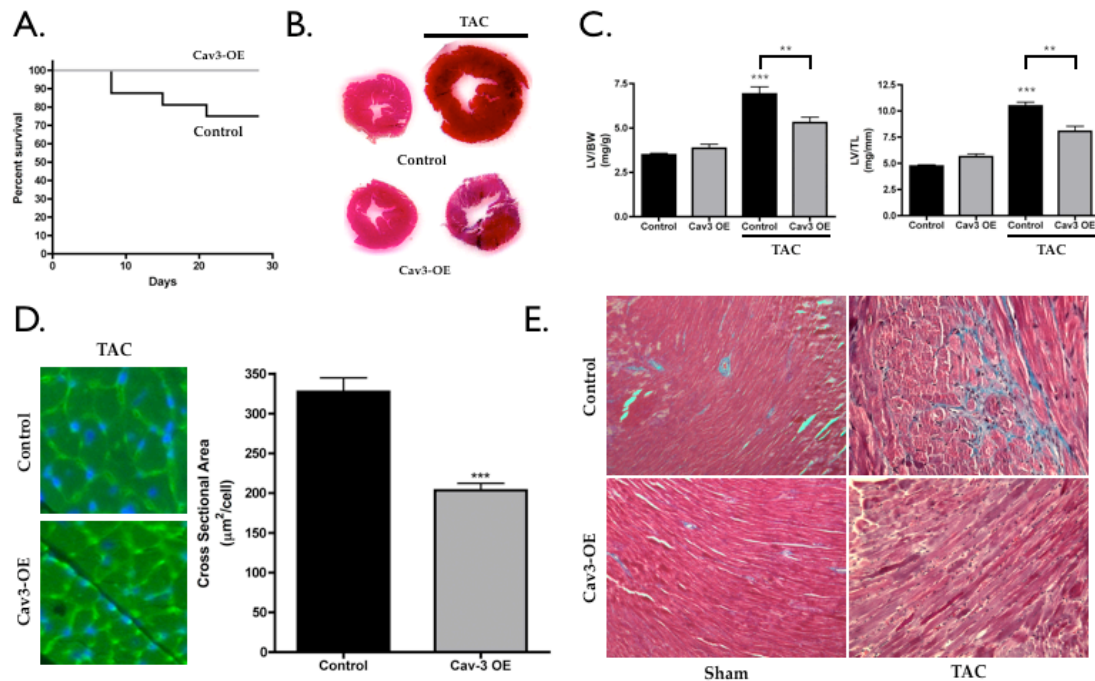


**Figure 5-5:** Cav-3 overexpression inhibits pressure induced cardiac hypertrophy and fibrosis. **(A)** Kaplan-Meier curves show a significant survival effect in Cav-3 OE mice compared to Control mice during TAC.  $P < 0.05$ .  $N = 12-16$ . **(B)** Unlike control hearts exposed to transverse aortic constriction (TAC) Cav-3 OE hearts had significantly less concentric hypertrophy. **(C)** Left ventricle (LV) to body weight (BW) and tibia length (TL) ratios revealed a significant increase in control mice following TAC, whereas Cav-3 OE mice were significantly blunted. \*\*\*  $P < 0.001$ , \*\*  $p < 0.01$ ,  $N = 8-16$ . **(D)** A nearly 60% decrease in cross sectional area was observed in Cav-3 OE myocytes following TAC via wheat germ agglutinin staining. \*\*\*  $P < 0.001$ ,  $N = 7$ . **(E)** TAC induced interstitial and perivascular fibrosis in sections from control mice, whereas this was dramatically decreased in sections from Cav-3 OE mice.

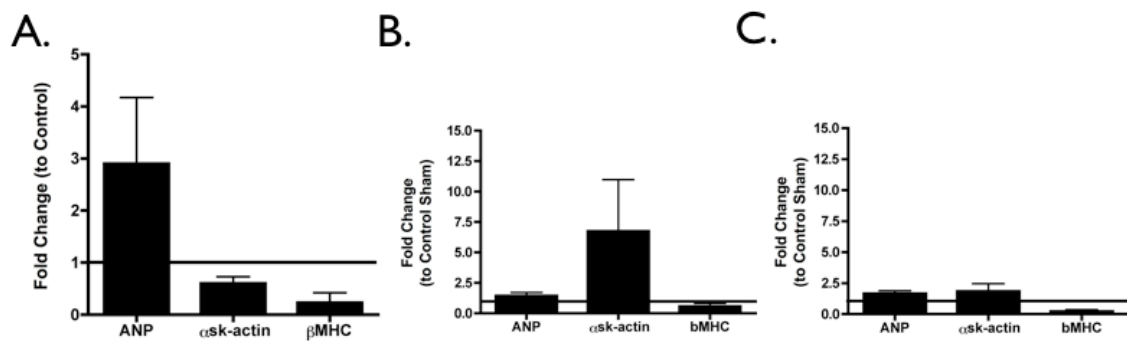


**Figure 5-6:** Real-time polymerase chain reaction following 48 hr of TAC. **(A)** 48 hr after TAC Cav-3 OE mice have nearly a 3-fold increase in ANP expression level whereas  $\alpha$ -skeletal actin ( $\alpha$ -sk-actin) and  $\beta$ -myosin heavy chain ( $\beta$ MHC) are dramatically less than in control mice. N=5. **(B)** 48 hr after TAC, control mice have nearly a 7-fold increase in  $\alpha$ -sk-actin, suggesting activation of the fetal genes, compared to control sham mice whereas, **(C)** Cav-3 OE mice have no increases in the fetal genes compared to Cav-3 OE sham, suggesting a blunting in hypertrophy in Cav-3 OE mice.

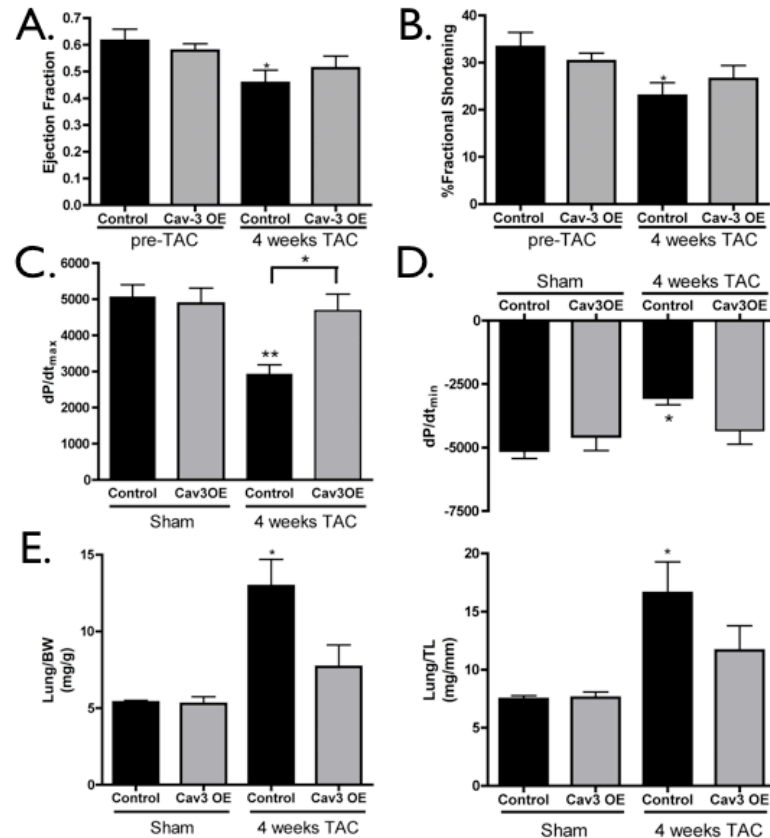
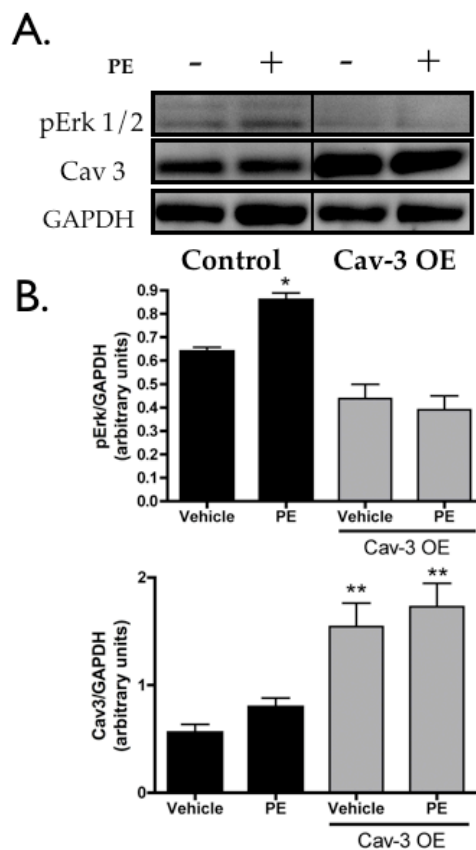
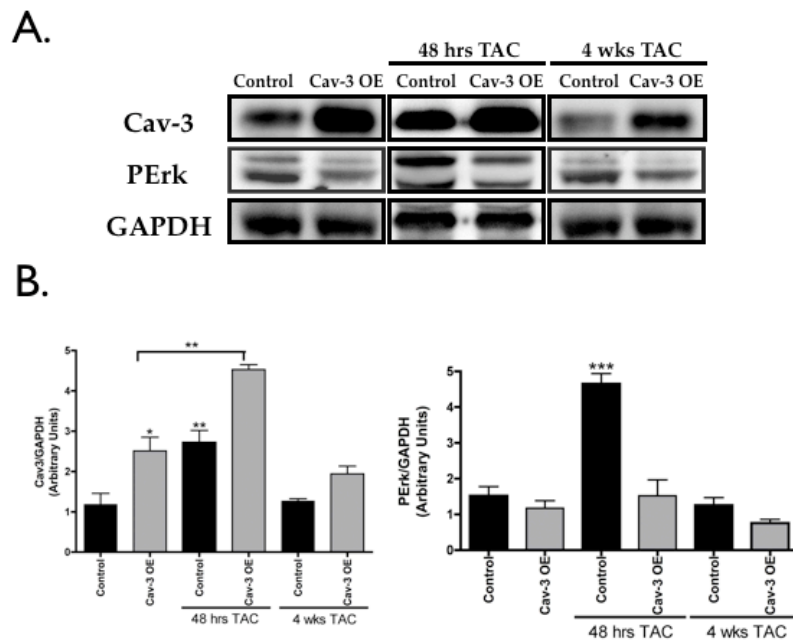


**Figure 5-7:** Caveolin-3 overexpression maintains cardiac function after TAC. (A) and (B) Sequential echocardiography of Control and Cav-3 OE mice revealed a significant decrease in Control mice after TAC in both ejection fraction and %fractional shortening. No detrimental functional changes were observed in Cav-3 OE mice. \* $P < 0.05$  vs. Control.  $N = 8$ . (C) and (D) Carotid catheterization revealed significant loss in left ventricular systolic function ( $dp/dt_{max}$ ) in control mice, whereas Cav-3 OE mice were able to maintain function. These changes were also observed in left ventricular relaxation ( $dp/dt_{min}$ ). \*\*  $P < 0.01$  vs. Control, \* $P < 0.05$ .  $N = 8$ . (E) Wet lung weight (Lung) to BW and TL revealed a significant increase in control mice following TAC. \*  $P < 0.05$  vs. Control.  $N = 5-8$ .



**Supplementary Figure 5-1:** Cav-3 overexpression inhibits phenylephrine (PE) induced Erk phosphorylation. (A) and (B) CM isolated from Control and Cav-3 OE mice were incubated in phenylephrine (PE; 2 $\mu$ M) for 15 minutes. PE significantly increased Erk phosphorylation in Control CM, but had no effect on Cav-3 OE CM.

\* $P < 0.05$ . \*\* $P < 0.01$  vs. Vehicle,  $N = 4$ .



**Supplementary Figure 5-2:** Cav-3 and pErk levels increase with TAC. (A) and (B) 48 hrs after TAC a significant increase in Cav-3 and pErk is observed in control mice, however, at 4 wk both of these changes return back to normal levels. \*  $P < 0.05$  vs. Control, \*\*  $P < 0.01$  vs. Control or Cav-3 OE, \*\*\*  $P < 0.001$  vs. Control. N=4.

**Table 5-1:** Echocardiography measurements

	Control		Cav-3 OE	
	Sham	TAC	Sham	TAC
<b>N</b>	8	8	8	11
<b>IVSd (mm)</b>	0.91 ± 0.05	1.34 ± 0.05***	0.88 ± 0.05	1.10 ± 0.05††§
<b>LVIDd (mm)</b>	4.07 ± 0.09	4.21 ± 0.06	3.85 ± 0.08	4.09 ± 0.17
<b>LVPWd (mm)</b>	0.79 ± 0.05	1.25 ± 0.07***	0.80 ± 0.04	1.13 ± 0.07§
<b>IVSs (mm)</b>	1.27 ± 0.10	1.69 ± 0.08*	1.20 ± 0.08	1.46 ± 0.07
<b>LVIDs (mm)</b>	2.91 ± 0.12	3.27 ± 0.12	2.67 ± 0.14	3.07 ± 0.24
<b>LVPWs (mm)</b>	1.11 ± 0.11	1.53 ± 0.07*	1.17 ± 0.07	1.41 ± 0.09

**Supplementary Table 1**

Echocardiography measurements. \*\*\*  $P < 0.001$  and \*  $P < 0.05$  vs. Sham Control. §  $P < 0.05$  and §§  $P < 0.01$  vs. Sham Cav-3 OE. ††  $P < 0.01$  vs. Control TAC.

Table 5-2: Hemodynamic data

	Control		Cav-3 OE	
	Sham	TAC	Sham	TAC
<b>N</b>	6	6	8	8
<b>Heart Rate (bpm)</b>	442 ± 32	486 ± 22	509 ± 28	485 ± 25
<b>MAP (mmHg)</b>	53.6 ± 2.5	59.8 ± 5.5	72.1 ± 7.1	69.0 ± 5.3

**Supplementary Table 2**  
Hemodynamic Data.

## 5.6 References

1. Heineke, J., and Molkenkin, J.D. 2006. Regulation of cardiac hypertrophy by intracellular signalling pathways. *Nat Rev Mol Cell Biol* 7:589-600.
2. Palade, G. 1953. Fine structure of blood capillaries. *Journal of Applied Physics* 24:1424.
3. Yamada, E. 1955. The fine structure of the gall bladder epithelium of the mouse. *J Biophys Biochem Cytol* 1:445-458.
4. Song, K.S., Li, S., Okamoto, T., Quilliam, L.A., Sargiacomo, M., and Lisanti, M.P. 1996. Co-purification and direct interaction of Ras with caveolin, an integral membrane protein of caveolae microdomains. Detergent-free purification of caveolae microdomains. *J Biol Chem* 271:9690-9697.
5. Koga, A., Oka, N., Kikuchi, T., Miyazaki, H., Kato, S., and Imaizumi, T. 2003. Adenovirus-Mediated Overexpression of Caveolin-3 Inhibits Rat Cardiomyocyte Hypertrophy. *Hypertension* 42:213-219.
6. Kikuchi, T., Oka, N., Koga, A., Miyazaki, H., Ohmura, H., and Imaizumi, T. 2005. Behavior of caveolae and caveolin-3 during the development of myocyte hypertrophy. *J Cardiovasc Pharmacol* 45:204-210.
7. De Souza, A.P., Cohen, A.W., Park, D.S., Woodman, S.E., Tang, B., Gutstein, D.E., Factor, S.M., Tanowitz, H.B., Lisanti, M.P., and Jelicks, L.A. 2005. MR imaging of caveolin gene-specific alterations in right ventricular wall thickness. *Magn Reson Imaging* 23:61-68.
8. Ohsawa, Y., Toko, H., Katsura, M., Morimoto, K., Yamada, H., Ichikawa, Y., Murakami, T., Ohkuma, S., Komuro, I., and Sunada, Y. 2004. Overexpression of P104L mutant caveolin-3 in mice develops hypertrophic cardiomyopathy with enhanced contractility in association with increased endothelial nitric oxide synthase activity. *Hum Mol Genet* 13:151-157.
9. Woodman, S.E., Park, D.S., Cohen, A.W., Cheung, M., Chandra, M., Shirani, J., Tang, B., Jelicks, L.A., Kitsis, R.N., Christ, G.J., et al. 2002. Caveolin-3 knock-out mice develop a progressive cardiomyopathy and show hyperactivation of the p42/44 MAP kinase cascade. *J Biol Chem* 277:38988-38997.
10. Aravamudan, B., Volonte, D., Ramani, R., Gursoy, E., Lisanti, M.P., London, B., and Galbiati, F. 2003. Transgenic overexpression of caveolin-3 in the heart induces a cardiomyopathic phenotype. *Hum. Mol. Genet.* 12:2777-2788.

11. Horikawa, Y.T., Patel, H.H., Tsutsumi, Y.M., Jennings, M.M., Kidd, M.W., Hagiwara, Y., Ishikawa, Y., Insel, P.A., and Roth, D.M. 2008. Caveolin-3 expression and caveolae are required for isoflurane-induced cardiac protection from hypoxia and ischemia/reperfusion injury. *J Mol Cell Cardiol* 44:123-130.
12. Head, B.P., Patel, H.H., Tsutsumi, Y.M., Hu, Y., Mejia, T., Mora, R.C., Insel, P.A., Roth, D.M., Drummond, J.C., and Patel, P.M. 2008. Caveolin-1 expression is essential for N-methyl-D-aspartate receptor-mediated Src and extracellular signal-regulated kinase 1/2 activation and protection of primary neurons from ischemic cell death. *FASEB J* 22:828-840.
13. Nishikimi, T., Maeda, N., and Matsuoka, H. 2006. The role of natriuretic peptides in cardioprotection. *Cardiovasc Res* 69:318-328.
14. Rubattu, S., Sciarretta, S., Valenti, V., Stanzione, R., and Volpe, M. 2008. Natriuretic peptides: an update on bioactivity, potential therapeutic use, and implication in cardiovascular diseases. *Am J Hypertens* 21:733-741.
15. Lee, C.Y., and Burnett, J.C., Jr. 2007. Natriuretic peptides and therapeutic applications. *Heart Fail Rev* 12:131-142.
16. Doyle, D.D., Ambler, S.K., Upshaw-Earley, J., Bastawrous, A., Goings, G.E., and Page, E. 1997. Type B atrial natriuretic peptide receptor in cardiac myocyte caveolae. *Circulation Research* 81:86-91.
17. Newman, T.M., Severs, N.J., and Skepper, J.N. 1991. The pathway of atrial natriuretic peptide release--from cell to plasma. *Cardioscience* 2:263-272.
18. Tsutsumi, Y.M., Horikawa, Y.T., Jennings, M.M., Kidd, M.W., Niesman, I.R., Yokoyama, U., Head, B.P., Hagiwara, Y., Ishikawa, Y., Miyanohara, A., et al. 2008. Cardiac-specific overexpression of caveolin-3 induces endogenous cardiac protection by mimicking ischemic preconditioning. *Circulation* 118:1979-1988.
19. Rockman, H.A., Ross, R.S., Harris, A.N., Knowlton, K.U., Steinhilber, M.E., Field, L.J., Ross, J., Jr., and Chien, K.R. 1991. Segregation of atrial-specific and inducible expression of an atrial natriuretic factor transgene in an in vivo murine model of cardiac hypertrophy. *Proc Natl Acad Sci U S A* 88:8277-8281.
20. Tsujita, Y., Muraski, J., Shiraishi, I., Kato, T., Kajstura, J., Anversa, P., and Sussman, M.A. 2006. Nuclear targeting of Akt antagonizes aspects of cardiomyocyte hypertrophy. *Proc Natl Acad Sci U S A* 103:11946-11951.

21. Kuga, H., Ogawa, K., Oida, A., Taguchi, I., Nakatsugawa, M., Hoshi, T., Sugimura, H., Abe, S., and Kaneko, N. 2003. Administration of atrial natriuretic peptide attenuates reperfusion phenomena and preserves left ventricular regional wall motion after direct coronary angioplasty for acute myocardial infarction. *Circ J* 67:443-448.
22. Saito, Y., Nakao, K., Nishimura, K., Sugawara, A., Okumura, K., Obata, K., Sonoda, R., Ban, T., Yasue, H., and Imura, H. 1987. Clinical application of atrial natriuretic polypeptide in patients with congestive heart failure: beneficial effects on left ventricular function. *Circulation* 76:115-124.
23. Yamada, H., Saito, Y., Mukoyama, M., Nakao, K., Yasue, H., Ban, T., Imura, H., and Sano, Y. 1988. Immunohistochemical localization of atrial natriuretic polypeptide (ANP) in human atrial and ventricular myocytes. *Histochemistry* 89:411-413.
24. Nagata, M., Hiroe, M., Yu, Z.X., Sekiguchi, M., and Hirose, K. 1988. Immunohistochemical localization of alpha human atrial natriuretic peptide in human atrium obtained from endomyocardial biopsy and cardiac surgery. *Heart Vessels* 4:112-115.
25. Hira, G.K., Sarada, I.R., Wong, S.T., Pang, S.C., and Flynn, T.G. 1993. Immunoactive iso-ANP/BNP in plasma, tissues and atrial granules of the rat. *Regul Pept* 44:1-9.
26. Wilkins, B.J., De Windt, L.J., Bueno, O.F., Braz, J.C., Glascock, B.J., Kimball, T.F., and Molkentin, J.D. 2002. Targeted disruption of NFATc3, but not NFATc4, reveals an intrinsic defect in calcineurin-mediated cardiac hypertrophic growth. *Mol Cell Biol* 22:7603-7613.
27. Page, E., Upshaw-Earley, J., and Goings, G.E. 1994. Localization of atrial natriuretic peptide in caveolae of in situ atrial myocytes. *Circulation Research* 75:949-954.
28. Okawa, H., Horimoto, H., Mieno, S., Nomura, Y., Yoshida, M., and Shinjiro, S. 2003. Preischemic infusion of alpha-human atrial natriuretic peptide elicits myoprotective effects against ischemia reperfusion in isolated rat hearts. *Mol Cell Biochem* 248:171-177.
29. Oliver, P.M., Fox, J.E., Kim, R., Rockman, H.A., Kim, H.S., Reddick, R.L., Pandey, K.N., Milgram, S.L., Smithies, O., and Maeda, N. 1997. Hypertension, cardiac hypertrophy, and sudden death in mice lacking natriuretic peptide receptor A. *Proc Natl Acad Sci U S A* 94:14730-14735.

30. Horio, T., Nishikimi, T., Yoshihara, F., Matsuo, H., Takishita, S., and Kangawa, K. 2000. Inhibitory regulation of hypertrophy by endogenous atrial natriuretic peptide in cultured cardiac myocytes. *Hypertension* 35:19-24.
31. Maki, T., Horio, T., Yoshihara, F., Suga, S., Takeo, S., Matsuo, H., and Kangawa, K. 2000. Effect of neutral endopeptidase inhibitor on endogenous atrial natriuretic peptide as a paracrine factor in cultured cardiac fibroblasts. *Br J Pharmacol* 131:1204-1210.
32. Schwartz, K., Boheler, K.R., de la Bastie, D., Lompre, A.M., and Mercadier, J.J. 1992. Switches in cardiac muscle gene expression as a result of pressure and volume overload. *Am J Physiol* 262:R364-369.

**Chapter 6:**  
**Discussion and Conclusions**

## 6.1 Major Findings of the Dissertation

The major objective of this dissertation was to identify the importance of a plasma membrane structural protein, Cav-3 and its impact on cardiac failure by understanding its role in both cardiac protection against ischemia/reperfusion injury and cardiac hypertrophy. This dissertation tested the hypothesis that Cav-3 is vital for the protection against heart failure and that the increase in Cav-3 can induce preconditioning and inhibit hypertrophy possibly by the increased expression of ANP.

*Chapter 3* identified the importance of Cav-3 and caveolae in isoflurane-induced preconditioning. We found that caveolae and Cav-3 were essential for isoflurane-induced preconditioning in both *in vitro* and *in vivo* hypoxia/ischemia reperfusion models. Brief exposure to isoflurane was able to induce significant cardiac protection against a lethal hypoxia/reperfusion injury in adult rat cardiac myocytes. However, pharmacological removal of caveolae and Cav-3 from the plasma membrane completely inhibited preconditioning. These findings were confirmed *in vivo* in Cav-3 knockout mice (Cav-3 KO). Although control mice were able to be preconditioned with isoflurane and were significantly protected against ischemia/reperfusion injury, Cav-3 KO mice had no apparent protection and demonstrated cardiac injury (as detected by troponin I release). These results suggest that Cav-3 is vital to preconditioning and that cardiac specific overexpression of Cav-3 may result in a “protected phenotype.”

*Chapter 4* addressed cardiac protection resulting from cardiac-specific Cav-3 overexpression. A cardiac-specific Cav-3 overexpressing transgenic mouse (Cav-3 OE) was developed in order to investigate the role of Cav-3 in the heart. We found

that Cav-3 OE mice were protected from ischemia/reperfusion injury and did not require a preconditioning stimulus. Furthermore, this protection appeared to result from Akt signaling, which was basally upregulated in Cav-3 OE mice while nitric oxide synthase expression and activity were not different in Cav-3 OE mice. Non-preconditioned hearts from Cav-3 OE mice resembled a preconditioned heart both structurally (via electron microscopy) and in terms of Akt phosphorylation. These results suggest that Cav-3 expression is able to modulate Akt phosphorylation and produce protection against lethal ischemic injury.

*Chapter 5* incorporated the results from *Chapter 3* and *4* and investigated the role of Cav-3 in transverse aortic constriction (TAC) model of cardiac hypertrophy. We found that an increase of Cav-3 resulted in an increase in Akt phosphorylation and ANP expression that coincided with Cav-3 expression. These changes were directly related to caveolae formation in that pharmacological disruption of caveolae inhibited changes in both Akt and ANP. Furthermore, Cav-3 OE mice not only had an increase in Cav-3 expression but also Akt phosphorylation and ANP expression. As a result, Cav-3 OE mice were protected against pressure-induced cardiac hypertrophy and maintained cardiac function and showed reduced fibrosis in response to TAC. These results suggest that Cav-3 expression can directly alter Akt phosphorylation and subsequent ANP expression which is known to have anti-hypertrophic properties.

Taken together, these results suggest that Cav-3 may be vital to the prevention and perhaps the treatment of heart failure. The results thus show that a structural protein can regulate cardiac protection and cardiac hypertrophy. These results

suggest a very unique mechanism and potential therapeutic for increasing ANP expression for the treatment of heart failure.

## **6.2 Discussion of Major Dissertation Issues**

### *Global Cav-3 OE vs. cardiac specific Cav-3 OE*

Prior to this dissertation mice that globally overexpressed Cav-3 had been developed (1). Interestingly those mice developed significant cardiomyopathy, flagrant fibrosis, and pronounced cardiac dysfunction even without any type of hypertrophic or heart failure stimulus. Furthermore, the investigators showed dramatic changes in NOS activity and the dystrophin glycoprotein complex. However, unlike our cardiac-specific Cav-3 overexpressing mice, the prior-studied mice overexpressed Cav-3 in all organ tissues including the vasculature. Interestingly, we found that human embryonic kidney cells-293 (HEK-293) when treated with Cav-3 a significant amount of cell death was observed within 48 hours (Figure 6-1). These results suggest that overexpressing Cav-3 in non-myocyte cells may have detrimental effects that perhaps ultimately cause cardiac dysfunction and death.

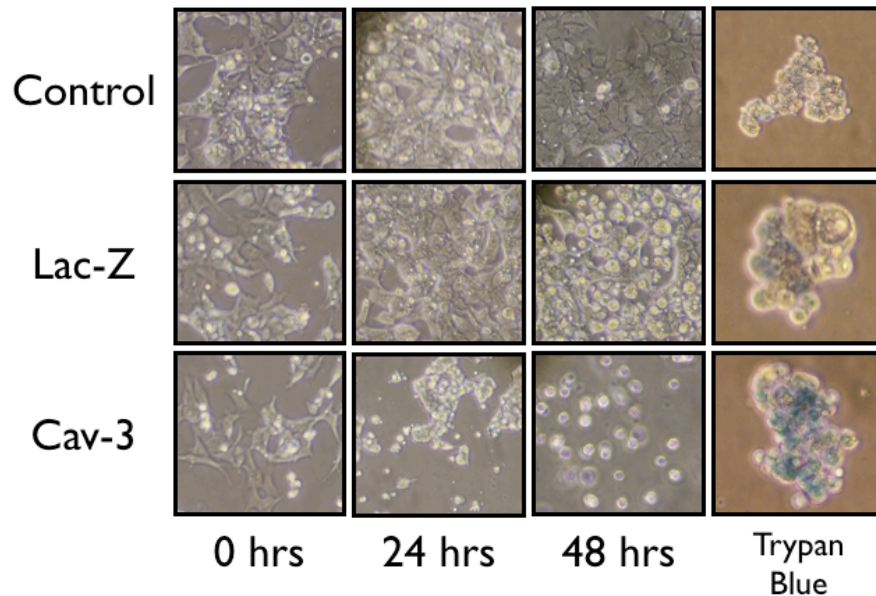


**Figure 6-1:** HEK-293 cells expressing Lac-Z or Cav-3. Cav-3 overexpression induced dramatic cellular death over 48 hours.

*ANP as a marker for heart failure vs. a treatment*

Traditionally, it is believed that ANP is secreted in response to wall stretch in cardiac chambers (in particular the atria), which is elevated during cardiac hypertrophy and heart failure(2-4). Furthermore, numerous studies have correlated ANP expression levels to clinical outcome and survivability(5). Due to its numerous protective cardiac effects, ANP has been investigated as a potential treatment in heart failure. ANP not only has vasodilatory and natriuretic properties but also anti-fibrotic (6) and anti-hypertrophic (7) properties via the natriuretic peptide receptor-A, and -B (NPR-A, NPR-B, respectively) (2). Clinically, ANP has improved clinical outcome in 82% of patients who had acute heart failure (8). Unfortunately, the half-life of ANP is 2-5 min in humans(9) and as a result it requires continuous infusion in order to be effective clinically. Interestingly, Cav-3 OE mice basally have an increased level of

ANP, although the other hypertrophic genes do not seem to be elevated. Thus, in effect, mice that overexpress Cav-3 could be a model for a constant vascular delivery of ANP.

### 6.3 Future directions

The main purpose of this dissertation was to investigate the role of Cav-3 and caveolae in heart failure. Caveolae are microdomains that are known to interact with numerous signaling molecules vital to cardiac protection and remodeling; these include G-proteins, G-protein coupled receptors (GPCR), and epidermal growth factor receptor (EGFR). As a result, future investigations will look into other signaling pathways that may be modulated by Cav-3, such as the role Cav-3 in the transactivation of EGFR by GPCRs.

Transactivation of EGFR by GPCRs has recently been suggested to be another mechanism involved in cardiac hypertrophy(10). Preliminary results in Cav-3 OE mice suggest that Erk phosphorylation differs when a GPCR transactivates (via the hypertrophic ligand, phenylephrine: PE) EGFR vs. direct activation of EGFR (via EGF). We found that Erk phosphorylation was inhibited in Cav-3 OE in the presence of transactivation whereas an increase in phosphorylation was observed when EGFR was directly activated with EGF (Figure 6-2).

Recent data has suggested that EGFR transactivation may not be G-protein regulated and instead may be predominantly a  $\beta$ -arrestin effect(11). However, our data suggests that this may not be completely true and that the different G-proteins may have different roles involved in EGFR transactivation. Further studies involving G-

proteins and caveolins are necessary to understand this relationship, but preliminary investigations have suggested that G<sub>q</sub> protein activation may be able to activate downstream MMPs and EGFR signaling, thus bypassing  $\beta$ -arrestin signaling altogether. Taken together, the data suggests that Cav-3 may also play a regulatory role in other signaling mechanisms involved in cardiac hypertrophy.

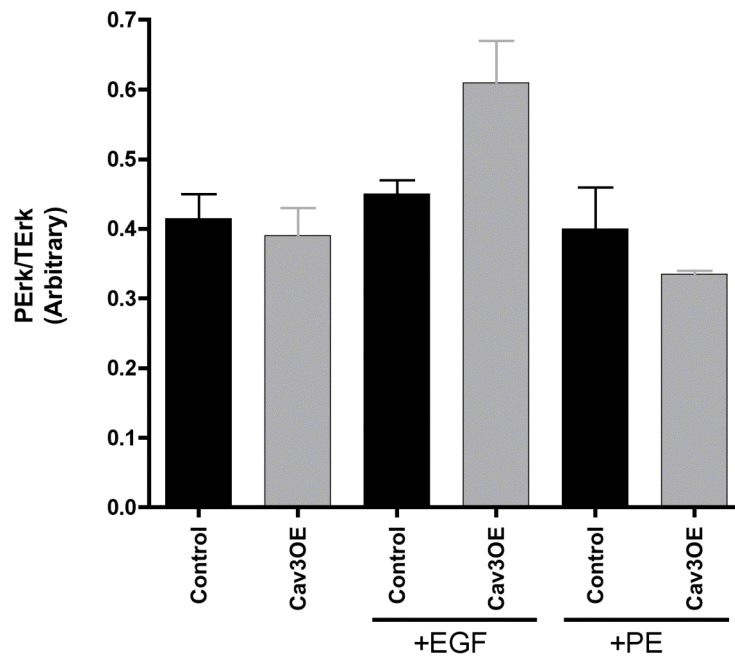


**Figure 6-2:** Erk phosphorylation increases in Cav-3 OE when induced with epidermal growth factor, whereas PE induction results in a decrease in Erk phosphorylation.

#### 6.4 Conclusions

In conclusion, our data suggests that Cav-3 is vital and essential to cardiac protection and that overexpression in the heart can lead to protective effects against both ischemic damage and hypertrophy. This dissertation identifies a unique mechanism by which Cav-3 protein can increase caveolae at the plasma membrane,

which, in turn, resulted in increased nuclear translocation of Akt and increased ANP expression. Thus, increasing Cav-3 may be a unique mechanism to exploit the therapeutic properties of ANP in the treatment of heart failure.

## 6.5 References

1. Aravamudan, B., Volonte, D., Ramani, R., GURSOY, E., Lisanti, M.P., London, B., and Galbiati, F. 2003. Transgenic overexpression of caveolin-3 in the heart induces a cardiomyopathic phenotype. *Hum. Mol. Genet.* 12:2777-2788.
2. Rubattu, S., Sciarretta, S., Valenti, V., Stanzione, R., and Volpe, M. 2008. Natriuretic peptides: an update on bioactivity, potential therapeutic use, and implication in cardiovascular diseases. *Am J Hypertens* 21:733-741.
3. Nishikimi, T., Maeda, N., and Matsuoka, H. 2006. The role of natriuretic peptides in cardioprotection. *Cardiovasc Res* 69:318-328.
4. Saito, Y., Nakao, K., Arai, H., Sugawara, A., Morii, N., Yamada, T., Itoh, H., Shiono, S., Mukoyama, M., Obata, K., et al. 1987. Atrial natriuretic polypeptide (ANP) in human ventricle. Increased gene expression of ANP in dilated cardiomyopathy. *Biochem Biophys Res Commun* 148:211-217.
5. Falcao, L.M., Pinto, F., Ravara, L., and van Zwieten, P.A. 2004. BNP and ANP as diagnostic and predictive markers in heart failure with left ventricular systolic dysfunction. *J Renin Angiotensin Aldosterone Syst* 5:121-129.
6. Maki, T., Horio, T., Yoshihara, F., Suga, S., Takeo, S., Matsuo, H., and Kangawa, K. 2000. Effect of neutral endopeptidase inhibitor on endogenous atrial natriuretic peptide as a paracrine factor in cultured cardiac fibroblasts. *Br J Pharmacol* 131:1204-1210.
7. Horio, T., Nishikimi, T., Yoshihara, F., Matsuo, H., Takishita, S., and Kangawa, K. 2000. Inhibitory regulation of hypertrophy by endogenous atrial natriuretic peptide in cultured cardiac myocytes. *Hypertension* 35:19-24.
8. Suwa, M., Seino, Y., Nomachi, Y., Matsuki, S., and Funahashi, K. 2005. Multicenter prospective investigation on efficacy and safety of carperitide for acute heart failure in the 'real world' of therapy. *Circ J* 69:283-290.
9. Rosenzweig, A., and Seidman, C.E. 1991. Atrial natriuretic factor and related peptide hormones. *Annu Rev Biochem* 60:229-255.
10. Asakura, M., Kitakaze, M., Takashima, S., Liao, Y., Ishikura, F., Yoshinaka, T., Ohmoto, H., Node, K., Yoshino, K., Ishiguro, H., et al. 2002. Cardiac hypertrophy is inhibited by antagonism of ADAM12 processing of HB-EGF: metalloproteinase inhibitors as a new therapy. *Nat Med* 8:35-40.

11. Noma, T., Lemaire, A., Naga Prasad, S.V., Barki-Harrington, L., Tilley, D.G., Chen, J., Le Corvoisier, P., Violin, J.D., Wei, H., Lefkowitz, R.J., et al. 2007. Beta-arrestin-mediated beta1-adrenergic receptor transactivation of the EGFR confers cardioprotection. *J Clin Invest* 117:2445-2458.